The Thesis Committee for Hratch Antoine Agopian
Certifies that this is the approved version of the following Thesis:

Impact of Permeation and Gelling Times on the Strength of N-Sodium Silicate Grouted Sands

APPROVED BY
SUPERVISION COMMITTEE:
Chadi El Mohtar, Supervisor
Robert B. Gilbert

Impact of Permeation and Gelling Times on the Strength of N-Sodium Silicate Grouted Sands

By

Hratch Antoine Agopian

Thesis

Presented to the Faculty of the Graduate School of
The University of Texas at Austin
in Partial Fulfillment
of the Requirements
for the Degree of

Master of Science in Engineering

The University of Texas at Austin
August 2019

Dedication

To my parents, Vasken Agopian and Anni Deir Ghazarian, my sister, Nathalie Maria Agopian, my current advisor Dr. Chadi El Mohtar, my previous advisor Dr. Grace Abou Jaoude-Estephan, and my friends.

Impact of Permeation and Gelling Times on the Strength of N-Sodium Silicate Grouted Sands

by

Hratch Antoine Agopian, MSE
The University of Texas at Austin, 2019
Supervision: Chadi El Mohtar

Grouting is a technique used frequently to alter in-situ engineering soil parameters, mainly strength, deformability, and permeability. Chemical grouting in particular refers to injection of one or multiple fluids in grouting holes, with the aim of permeating the volume desired before the grout sets. Engineers require crucial parameters pre-, during, and post-gelation to quantify the economics and the efficacy of the treatment. The field of chemical grouting is highly reliant on laboratory and field pilot tests, due to the complexity of its mechanisms and processes. This study aims at understanding the behavior of Ottawa sand grouted using N-sodium silicate grout neutralized by dibasic ester.

Sodium silicate grouting is one of the oldest methods in chemical grouting; its survival in the field is largely due to its economics. This type of grout is among the least expensive in its family and pertains desirable properties such as flexibility in controlling gelling time, and ease of penetration in finer soils. Sodium silicate is also environmentally friendly, a quality much desired in this modern era. This research aims at finding the impact of the gelation time, relative to grout permeation time, on the properties of the grouted sand. The rheological properties of various mixes were first tested using a

rheometer to identify the impact of the different mix components on the viscosity and set time. The various components of the grout mix were altered to determine the optimal mix. Select mixes were then subjected to a series of two syneresis tests on the gel itself and the grouted mass. The former showed a 70% loss in mass of the gel over the first year compared to non-measurable changes in volume in the latter. Grouted mass syneresis testing also showed that the lost mass is controlled by the exposed surface area, rather than total mass or volume. It was also concluded that constant mixing of the grout during the permeation phase is crucial in obtaining optimal results. A series of unconfined compressive strength tests revealed that sodium silicate grouts experience sedimentation and filtration during and post the grouting process (and prior to gelling). In an effort to show and overcome the effect of sedimentation, laboratory tests were conducted where the start of grouting was delayed such that the permeation was concluded at the onset of its gelation. The permeated samples with delayed start exhibited a higher strength than those permeated without a delay at a similar permeated number of pore volumes. The difference in strength decreased as the number of permeated pore volumes increased (and thus the time delay becomes smaller). A similar trend was seen in the moduli of the two series of tests with different gelling times. Additionally, a decrease in strength was observed within the grouted mass as we move away from the injection point; this variation in strength is mostly associated with filtration. Tests on 6” specimens with delayed permeation (reduced impact from sedimentation) showed a linear increase in the strength of the samples as the number of permeated pore volumes increased.

Table of Contents

List of Tables

List of Figures

CHAPTER 1. INTRODUCTION

1.1 Overview

Grouting is not a new "transforming" technology. Early applications of grouting bedrock underlying dams dated to as early as the 1800s (Warner, 2004). The solutions were constituted of aqueous suspensions, with consideration to maximum particle size versus discontinuity/fissure width. However, it was quickly understood that particulate grouts are of limited success upon permeating soils (Warner, 2004). Particulate grouts are limited by filtration; a phenomenon that occurs due to the clogging of the pores in the soil as more and more of the suspension solution is penetrated. Filtration will limit the radius of the treatment, the smaller the voids in the soil the less effective each grout hole will be. This shifted the grouting community to focus on chemical grouts; aqueous solutions that are meant to penetrate the soil and gel at a later stage. Chemical grouts, however, do not provide high strength properties as Portland cement grouts but are very effective in terms of dealing with permeability problems.

A demand for lower viscosity grout that gels or hardens upon placement arouse, and in 1987, Jeziorski developed a phenomenal solution via sodium-silicate combined with an organic setting agent in a one-shot rapid injection process (Warner, 2004). Again, problems arose because of the almost instantaneous gelling of the grout, limiting penetration distance as well as clogging the grouting equipment. It was quickly understood that some time to start of gelation is required, and this time must be both manageable and practical.

Another solution was sought after by a Dutch engineer; Hugo Joosten, with his famous two-shot Joosten process in 1925. The first stage included the injection of "water-glass" better known as sodium silicate upon the ground, followed by a second stage of strong brine injection to result in an almost instantaneous gelation (LittleJohn, 1985). Calcium chloride was the common inorganic setting reagent that neutralized the sodium and precipitated the silica. The Joosten process was used until the late 1960s and idealized as one of the first successful processes in the world of grouting, initiating its modern era (Karol, 2003). Ever since, grouting has been in high demand as a ground remediation/control mechanism in geotechnical engineering in addition to gaining popularity in other fields like mining engineering and petroleum engineering. Numerous improvements were introduced to the field of grouting over the years, and today, there exists many different mixes, each tailored to suit a specific problem.

1.2 Theses Organization

This thesis consists of five chapters. Below is a brief description of each chapter:

- Chapter 1 is the introduction to the topic of chemical grouting and a brief history of its applications. This chapter also includes the organization of the thesis itself.
- Chapter 2 is a brief literature review of work performed by other authors in the past.
- Chapter 3 includes a description of the materials used in this thesis, and the procedure and methodology adopted in obtaining the desired results.
- Chapter 4 shows the results obtained from the various tests performed in this thesis and analyses the results. This chapter includes, respectively, results from rheology testing, syneresis testing, and strength testing.
- Chapter 5 summarizes the analysis and presents the main findings of this thesis. This chapter also includes recommendations for future work.
- Chapter 6 covers the appendices.

1.3 Objectives

This study aims at understanding the behavior of Ottawa sand grouted using N-sodium silicate grout neutralized by dibasic ester. The detailed objectives are:

- Characterize pre-, during, & post-gelation grout properties.
- Characterize Ottawa sand.
- Test the performance of different mixes with different setting times on the unconfined compressive behavior of the grouted masses.
- Understand flow characteristics of the various grouts during permeation.
- Understand and quantify the extent of grout sedimentation after permeation on the unconfined compressive behavior of the grouted masses.
- Understand grout syneresis behavior and influential parameters.

1.4 Motivation

This Master's thesis under the title "Impact of Permeation & Gelling Times on the Strength of N-Sodium Silicate Grouted Sands" was supervised by Professor Chadi El Mohtar and done by Hratch Antoine Agopian with the aim to conclude the Master's Degree in Civil Engineering with emphasis on Geotechnical Engineering at the University of Texas at Austin throughout the academic years 2017-2019.

Grouting is an old yet much used technique to treat in-situ soils. This field is highly reliant on its practitioners, due to the complexity of its mechanisms and processes. Field pilot tests and laboratory tests are crucial in every situation of designing a grouting project. Moreover, companies who practice grouting have internal techniques and ways of lowering the cost of a particular project due to their experience in the field which makes it hard for newcomers to enter this field.

This thesis aims at helping practitioners make better decisions involving the design of a grouting project. It also serves to help newcomers to the field get acquainted with its ways. Furthermore, this thesis aims at understanding some complex mechanisms involved in its many processes highlighting crucial influential parameters. The need to make grouting techniques public drives the authors of this thesis to publish their findings.

CHAPTER 2. LITERATURE REVIEW

Grouting is a process by which pores, fissures, and voids in natural or synthetic materials are filled, as to alter their physical properties. The Grouting Committee, part of The Geotechnical Engineering Division of the American Society of Civil Engineers, defines grout as follows: "in soil and rock grouting, a material is injected into a soil or rock formation to change the physical characteristics of the formation" (Karol, 2003).

Chemical grouting more specifically, refers to the use of grout as a fluid, with or without colloidal suspensions, but no suspended solid particles (LittleJohn, 1985). Chemical grouts are characterized by having higher penetrability than particulate grouts, viscosity of the grout mix being the critical parameter determining groutability and penetration distance (Karol, 2003). Silicate based chemical grouts are the most widely used due to their low cost; various compositions alter penetrability and gelation time, regulating soil strength and permeability in their wake. Silicate based chemical grouts have also gained popularity in the chemical grouting industry due to their non-toxic nature; in an era of ever-increasing ecofriendly resolutions (Guyer, 2015). This section aims at addressing past research concerning the properties and effects of sodium silicate grouts.

2.1 Chemistry & Manufacturing Processes

Sodium silicate is a chemical product consisting of silica, sodium oxide, and water (Xue, 2018) and is considered an alkali silicate due to the presence of sodium atoms. The compound is of tetrahedral structure, with the presence silicic chains on a tridimensional network having a solid macroscopic structure with silica as a basic atom (Federal Highway Administration, 1977). The most basic products often used in chemical grouting are alkali silicates, sodium silicate being the predominant form in all ground chemical grouting work (Federal Highway Administration, 1977). Sodium silicate is prepared commercially using the following chemical reaction termed complete fusion (Xue, 2018; Federal Highway Administration, 1977):

$$nSiO_2 + Na_2CO_3 \rightarrow nSiO_2.Na_2O + CO_2 \quad at\ 1400\,℃$$

The sodium silicate is formed in an autoclave with water under controlled high pressure and temperature conditions generating colloidal solutions very sensitive to temperature changes (LittleJohn et al.., 1997; PQ Corporation, 2004). The colloidal nature of the product is confirmed by the Tyndall effect; the Tyndall effect being defined as the scattering of light as a light beam passes through a colloid. The solutions are

characterized by the alkali/silica ratio of 1 to 4, a parameter which greatly influences the properties and use of the final product. However, ratios close to 2 are deemed detergent action silicates and are used in other industrial applications, whereas ratios of 3 to 4 are deemed adhesive action silicates suitable for grouting applications (Federal Highway Administration, 1977).

Another commercial manufacturing process is also used; the hydrothermal process (Xue, 2018). This process also involves an autoclave under high pressure and temperature conditions and the reaction occurs as follows (PQ Corporation, 2004):

$$NaOH + SiO_2 \rightarrow (SiO_2)_x.(Na_2O) + H_2O$$

However, this method cannot yield alkali/silica ratios of higher than 2.5, and is used to produce sodium silicates for other industrial applications. Additionally, the pH value of sodium silicates is in the range of 11 to 13 with the lower values obtained with increasing silica content (Hurley, n.d.).

2.2 Viscosity of the Grout

Viscosity of the grout is one the key factors determining its successful penetration into the soil matrix. As such, viscosity; defined as the behavior of the fluid's resistance to flow and given the unit cP, is often used to determine the groutability of soils (Guyer, 2015). Chemical grouts, and specifically silicate-based grouts, are characterized by their low viscosity, addressing its application in even finer soils (Guyer, 2015). Given the large variety of mixes and base materials commercially available, silicate-based chemical grout viscosities often fall in the 1.5-80 cP range, with the lower end much desired in finer soils (Krumrine and Boyce, 1985).

Viscosity of the grout is a time dependent parameter, some chemical grouts having an ever-increasing viscosity with time pending gelation, others indicating minimal change in viscosity with an abrupt change close or at gelation (Ortiz, 2015; Powers et al., 2007); the former being less desired since it limits penetration time and thus distance (Powers et al., 2007; PQ Corporation, 2003). This phenomenon is shown in Figure 2-1.

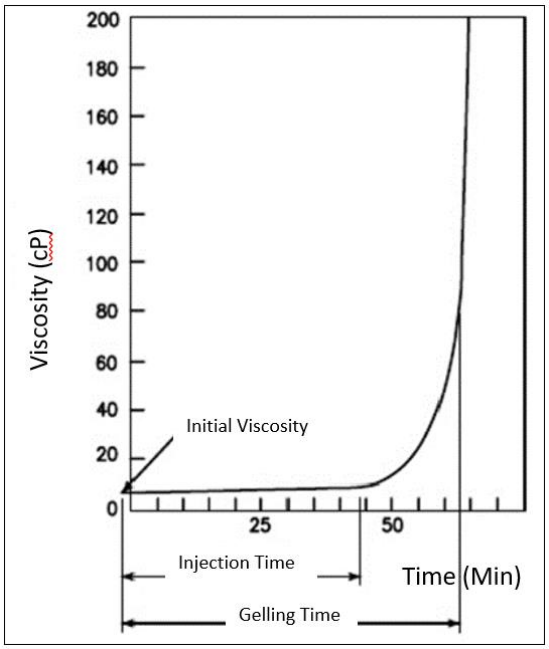

Figure 2-1: Viscosity Change with Time (Adapted from Powers et al., 2007)

Silicate-based grout viscosity is also a function of silicon dioxide to sodium oxide ratio. An extensive study by LittleJohn et al… (1997) and a further corroboration by Karol (2003) concluded that sodium oxide influences gel strength; with higher levels resulting in stronger gels, and that as the above defined weight ratio increases, so does the viscosity of the mix. Plots generated by both authors show this phenomenon and are shown in Figure 2-2 & Figure 2-3. Silicate-based grouts are thus diluted to maintain enough solids content for treatment purposes while having low enough viscosities as to permeate the desired volume.

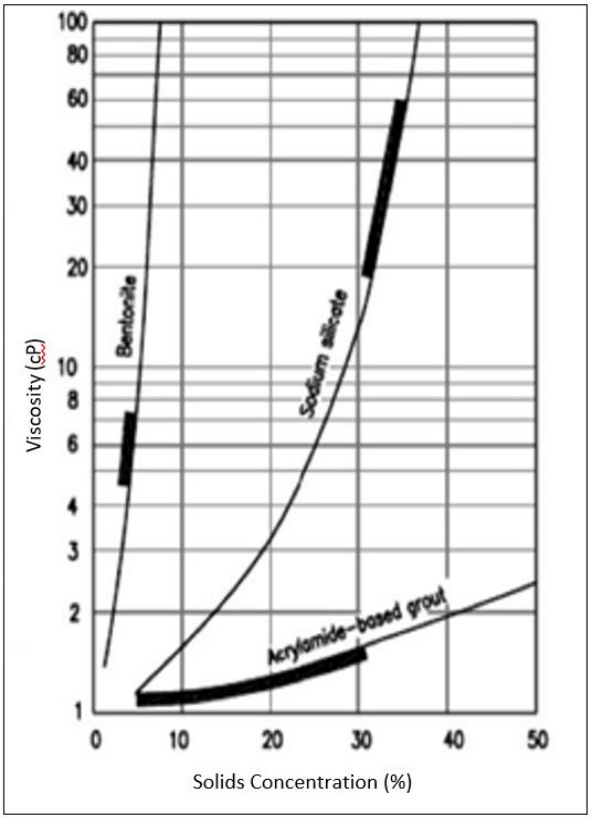

Figure 2-2: Viscosity Change with Concentration of Solids in the Mix (Adopted from Karol, 2003)

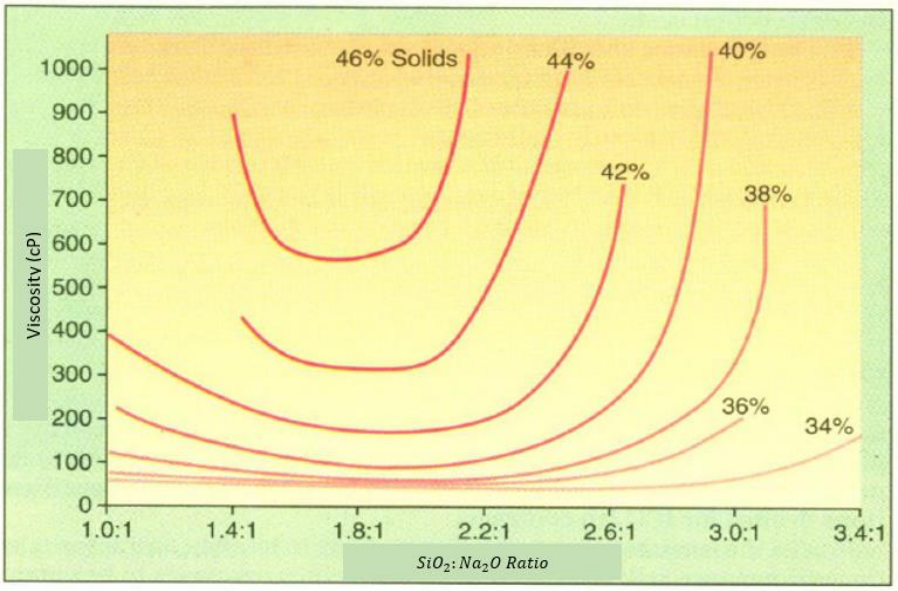

Figure 2-3: Viscosity-Weight Ratio Relationship for Crystal Sodium Silicate Solutions (Adopted from LittleJohn et al., 1997)

Furthermore, grout viscosity is highly influenced by medium temperature. A decrease in grout viscosity is expected with the increase in medium temperature, highlighted in Figure 2-4 & Figure 2-5 (Powers et al., 2007; LittleJohn et al., 1997).

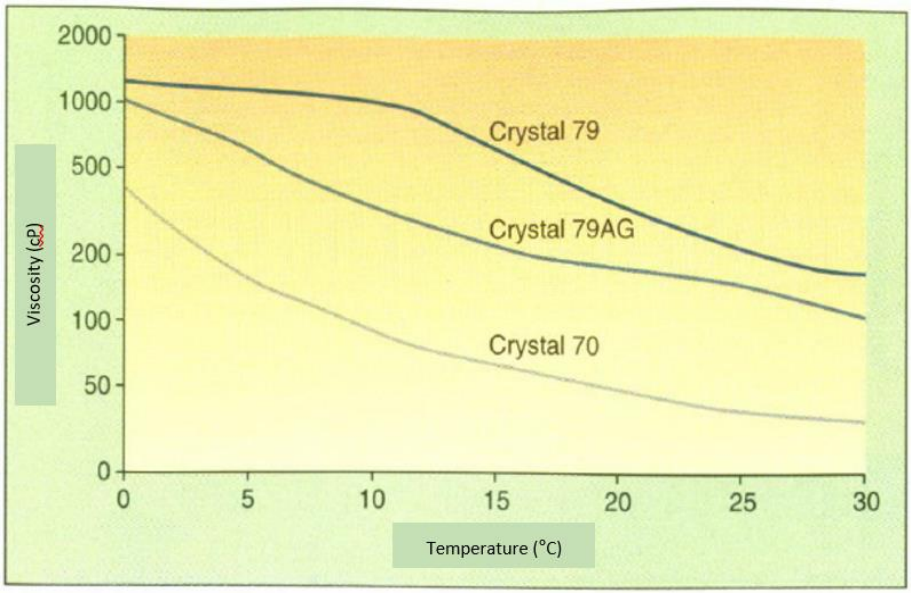

Figure 2-4: Viscosity-Temperature Curves for Crystal Sodium Silicate Solutions with 3.3 Weight Ratio (Adopted from LittleJohn et al., 1997)

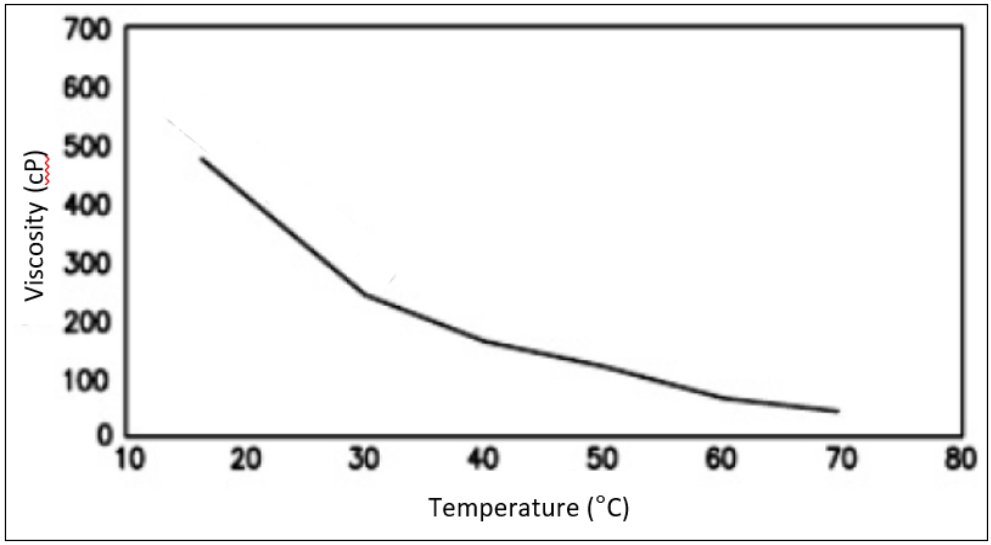

Figure 2-5: Viscosity of N-Sodium Silicate with Temperature (Adopted from Powers et al.., 2007)

2.3 Gelation or Setting Time

According to LittleJohn et al., (1985), setting time is defined as the time required for the grout to gel counted from the moment of mixing. The extent and rate of silicate gelation varies as a function of silicate concentration, pH value, ionic strength, and temperature (Krumine & Boyce, 1985). The process by which a grout gels in the soil matrix is attributed to polymerization or precipitation, where organic and inorganic reactants are used to neutralize the silica respectively. The most common organic setting reagents include ethyl acetate, triacetin, and dibasic ester while the most common inorganic setting reagents include carbon dioxide, calcium chloride, calcium hydroxide, and calcium oxide (PQ Corporation, 2003).

Organic setting reagents achieve silica precipitation by pH modification; understood to be below a pH of 10 (PQ Corporation, 2004). In addition, organic setting reagents are advantageous in the sense that they offer flexible gelling time but at the cost of a relatively weaker strength, as compared to inorganic setting reagents (Krumine & Boyce, 1985). A slow hydrolysis process is triggered as an organic setting agent is added to the silicate solution; active components of the mix are transformed to carboxylic acid (LittleJohn et al., 1997). Inorganic additives such as $CaCl_2$ can be added to accelerate gelation time (Krumine & Boyce, 1985). This hydrolysis process is described in detail by Krumine & Boyce (1985) and restated here:

$$RCHO + OH^- \rightarrow RCO_2^- + H^+$$

$$R(CO)NH_2 + OH^- \rightarrow RCO_2^- + NH_3$$

$$RCO_2R^1 + OH^- \rightarrow RCO_2^- + R^1OH$$

The acid will utilize the alkali component of silicate after the hydrolysis process; the alkali component will maintain a pH value at which the silica component is dissolved. Polymerization or gel formation will occur as the alkalinity is neutralized by the acid reducing silica solubility in its wake in a condensation process (Krumine & Boyce, 1985) as shown below:

$$\equiv SiOH \leftrightarrow^{Ka} \equiv SiO^- + H^+$$

$$\equiv SiO^- + \equiv SiOH \rightarrow \equiv Si - O - Si \equiv + OH^-$$

The degree of neutralization given by the following equation is important as several properties of the treated soil depend upon it (LittleJohn et al., 1997):

$$Degree\ of\ Neutralization = \frac{V_H\ x\ SG_H\ x\ 6200}{V_S\ x\ SG_S\ x\ N_A\ x\ M_H}$$

Where: - V_H is the volume of hardener in liters

- SG_H is the specific gravity of the hardener
- V_S is the volume of silicate in liters
- SG_S is the specific gravity of the silicate
- N_A is the weight percentage of alkali (Na_2O) in silicate
- M_H is the molecular weight if the hardener

In his study, LittleJohn et al… (1997) concluded that the greater the level of silicate in the grout, the stronger the treated ground will be. Low silicate levels (20-30% by volumetric ratio to the grout) are believed to be suitable only for waterproofing purposes whereas higher silicate levels (60-70%) result in high strength gels suitable for long term strengthening purposes.

Inorganic setting reagents on the other hand are used to form the gel through precipitation. Dissolved polyvalent cations react with the silicate to produce a silicate gel by the metal ion reaction (Wang, 2017; PQ Corporation, 2004). However, this reaction is rapid, as the inorganic setting reagent reacts almost instantaneously with the silicate, precipitating the silicate and forming the gel (Xue, 2018).

As explained in a paper published by LittleJohn et al., (1997), several parameters affect gelation time; namely nature and concentration of the silicate, type and concentration of hardener used, nature of the soil, and temperature of the grout and the soil.

2.4 Groutability

A groutable soil is one which will, under practical pressure limitations, accept injection of a given chemical grout at a sufficient flow rate to render the project economically and practically feasible (Baker, 1983). As such, an extensive ground investigation is needed to determine the much-required ground parameters. If the reduction in permeability of the grouted mass is the target, site characterization should include permeability and porosity data, along with hydraulic gradients and chemical properties of the ground water, and if strengthening of the ground is desired, more information is necessary in the form of shear strength tests on undisturbed samples or in-situ strength tests in the form of penetrometer or dilatometer tests (LittleJohn, 1985).

Chemical grouting is often the recommended solution for sandy deposits awaiting treatment. Larger grains such as gravels are better treated with the less costly cement grout solutions, while smaller grains such as silts and clays cannot be permeated

effectively with even the most diluted form of silicate-based grouts. As such, silicate-based chemical grouts are best used for sandy deposits with less than 25% silts and clays (Baker, 1983). Penetration distance is the cost-effective parameter to be addressed, and is a function of grout viscosity, initial ground permeability, medium particle size distribution, and injection pressure (Guyer, 2015; Ortiz, 2015). As the penetration distance decreases, the number of grouting holes must increase to treat the same ground, thus increasing the cost of the treatment due to the larger quantity of holes to be drilled (Powers et al., 2007). In a report addressed to the US Department of Transportation, Baker (1983) established guidelines as to determine the groutability of deposits based on particle size distribution shown in Figure 2-6.

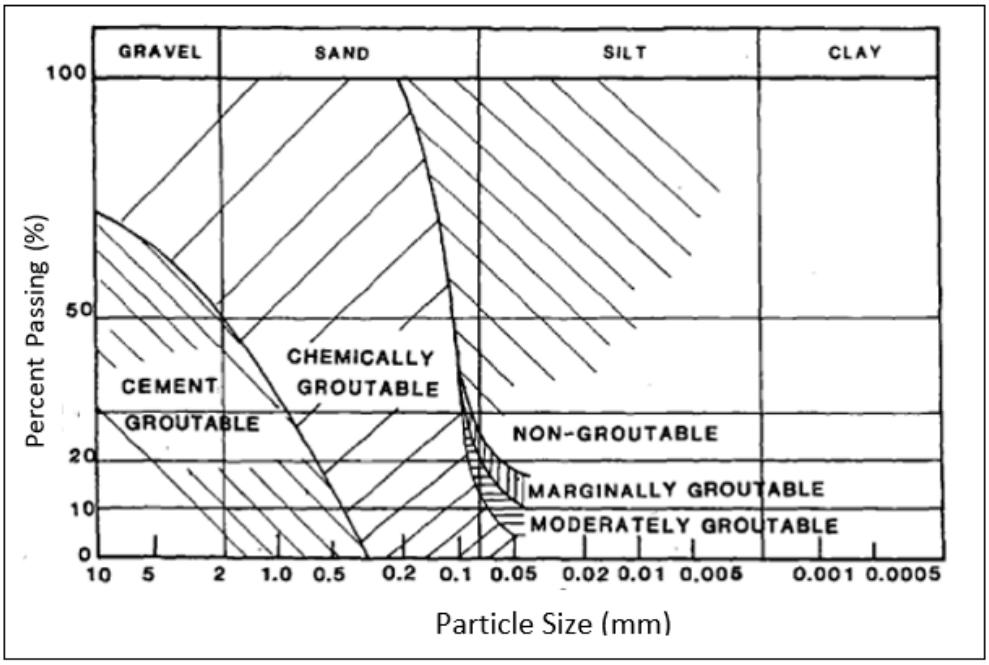

Figure 2-6: Grain Size Distribution for Chemically Groutable Soils (Adopted from Baker, 1983)

Furthermore, Baker (1983) has a set of recommendations for the range of groutable soils based on permeability and based on percent finer than sieve number 200 as shown in Table 2-1.

Table 2-1 Groutability Based on Soil Permeability (Adopted from Baker, 1983)

Soil Permeability (cm/sec)	Groutability	Percent Passing Sieve #200 (%)	Groutability
10^{-1}-10^{-3}	Easily Groutable	<12	Groutable
10^{-3}-10^{-4}	Moderately Groutable	12-20	Moderately Groutable
10^{-4}-10^{-5}	Marginally Groutable (Not Practical)	20-25	Marginally Groutable (Not Practical)
$>10^{-5}$	Ungroutable	>25	Ungroutable

2.5 Strength & Stiffness of Grouted Masses

Chemical grouting is often used to increase the strength of the soil, along with its initial stiffness. This increase in strength is attributed to the individual soil particles being glued together by the chemical adherence property; an internal force restraint phenomenon (Schiffman & Wilson, 1956). Many researchers, namely Diefenthal et al., (1979) and LittleJohn (1985) among others, have reached to a conclusion that the gel matrix adds cohesion to the strength of the soil, but the internal friction angle of the material remains unchanged. The Mohr-Coulomb failure criterion is deemed valid for sodium silicate grouted sands (Diefenthal et al.., 1979; Dano et al.., 2004). This warrants its characterization by the less costly unconfined compression test (Christopher et al., 1989). Furthermore, chemical grouts are considered viscoelastic; their strength significantly changes with the rate of loading. Thus, strain rate must be standardized to acquire comparable strengths (LittleJohn, 1985). Figure 2-7 shows the unchanged friction angle of the soil matrix with and without grout, along with the increasing strength result with increasing strain rate.

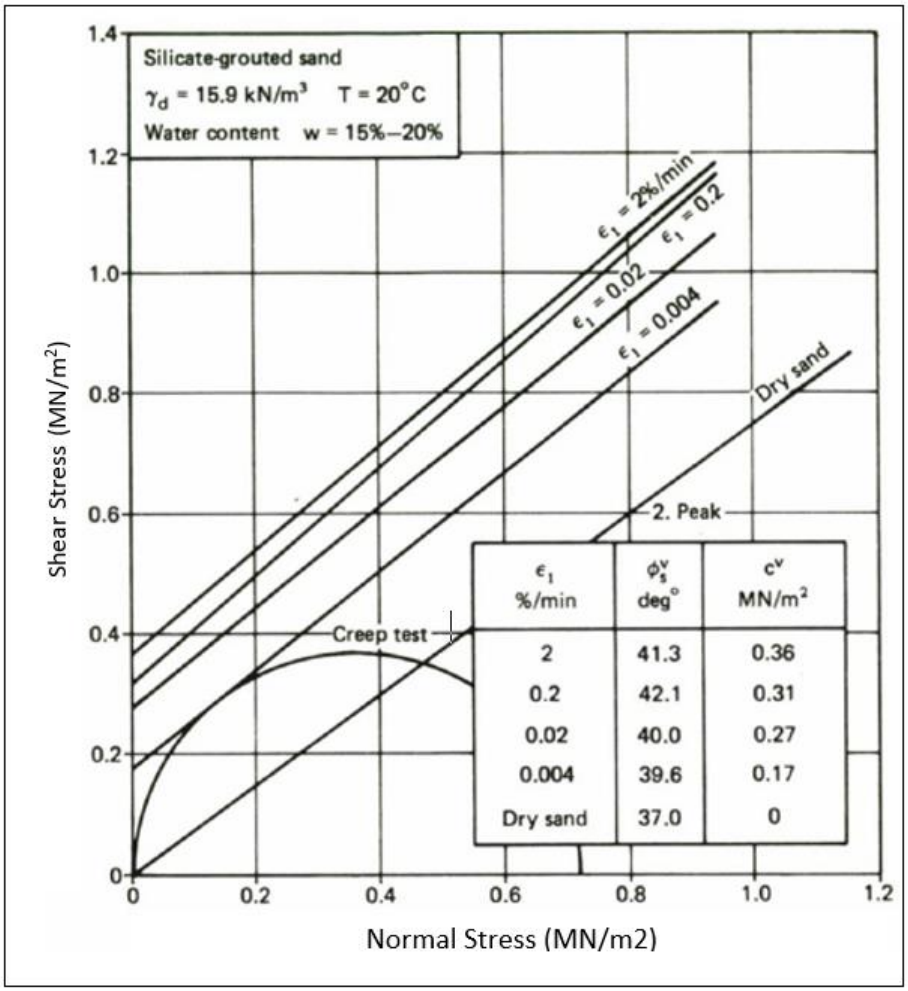

Figure 2-7: Grout Influence on Strength Parameters with Influence of Strain Rate (Adopted from LittleJohn, 1985)

2.6 Permeability of Grouted Masses

Another application where chemical grouting has gained popularity is reducing the permeability of the ground. This reduction in permeability is mainly due to the fact that the interconnected voids in the sand mass itself are filled up with the chemical grout and gelled to seal. Reports of a reduction in permeability of three to six orders of magnitude have been generated by many researchers (Krumine & Boyce, 1985; LittleJohn, 1985).

With such a function in mind, chemical grouts have been used in water cutoff projects frequently (LittleJohn, 1983). In his paper, LittleJohn (1983) shows the efficacy of

chemical grouts in reducing the permeability of a sand and gravel mass from $2.5x10^{-4}$ to $2.3x10^{-6}$ in the famous Aswan Dam project in Egypt.

Many factors affect the performance of chemical grouts along its lifetime; syneresis of the grout is one that has a detrimental effect on its water cutoff function. As the grout ages, the gel loses some of its volume unplugging some of the channels which were once plugged, and thus an increase in permeability of the ground is expected. This increase in permeability is expected to be one to two orders of magnitude higher than that of the initially treated soil (May et al., 1986).

Hydraulic gradient is another main factor affecting the performance of the chemically treated ground; it also affects the permeation of the grout to reach its intended destination in the first place. It is trivial to conclude that higher hydraulic gradients will have a higher detrimental effect on the grouted mass. The grout thus must be designed to resist the hydraulic gradient, recommended range for the design hydraulic gradient is three to five (LittleJohn, 1985). The following equation is presented by LittleJohn (1985):

$$i = \frac{4\tau_f}{d\,\delta_w}$$

Where:

- τ_f is the shear strength of the set gel
- d is the effective diameter of the average pore
- δ_w is the unit weight of water

The chemical composition of the flowing liquid also affects the performance of the grouted mass. In a study completed by May et al. (1986), it was concluded that sodium silicate had the most chemical resistance amongst four grouts when tested with 12 different liquids (acrylate, Portland cement, and urethane).

CHAPTER 3. MATERIALS AND METHODOLOGY

In this section, an elaborate account of materials used, and testing procedures is discussed.

3.1 Materials

3.1.1 GROUT COMPONENTS

N-Sodium silicate, tap water, dibasic ester, white vinegar, and Tergitol NP-9 were used in generating the different grout mixes used in this thesis.

Sodium silicate solution is a versatile inorganic chemical made by combining sand and soda ash (sodium carbonate) at high temperature. Adjusting the ratio of sand to soda ash yields a variety of products with unique functionality used in many industrial and consumer product applications.

The specific type of sodium silicate used in this series of experiments is PQ Corporation's N Sodium Silicate solution. Material properties are summarized in Table 3-1 below:

Table 3-1: N-Sodium Silicate Manufacturer's Properties

Property	Unit	Value
Alkali Silica Ratio	-	2.6-3.2
pH	-	11-12
Boiling Point	°C	100
Freezing Point	°C	N/A
Melting Point	°C	N/A
Density	Be	42

Tap water was used from the laboratory hose and the white vinegar used was Hill Country Fare distilled white vinegar with 5% acidity. Brenntag Dibasic Ester solution and Brenntag Surfactant NP-9 was used in this thesis.

3.1.2 SAND

Ottawa ASTM C778 graded sand was used in the series of experiments in this thesis. The sand has the following properties highlighted in Table 3-2.

Table 3-2: ASTM 778 Sand Properties

Property	Unit	Value
G_s	-	2.65
e_{min}	-	0.48
e_{max}	-	0.76
D_{10}	mm	0.2
D_{30}	mm	0.32
D_{60}	mm	0.4
C_u	-	1.94
C_c	-	1.28
USCS Classification	-	SP

3.2 Specimen Preparation & Data Acquisition Techniques

3.2.1 GROUT MIXES

Six grout mixes were evaluated in this study; Table 3-3 lists their volumetric compositions. The grout was prepared as follows:

1. In a first beaker, add sodium silicate and tap water.
2. In a second beaker, add Tergitol NP-9, Dibasic Ester, and white vinegar, respectively.
3. Mix both solutions thoroughly before they are to be combined, then mix the combined mix for 30 seconds before permeation.

Table 3-3: Mix Proportions

Mix Fractions by Volume					
Mix	N-Sodium Silicate (%)	Tap Water (%)	Dibasic Ester (%)	Tergitol N-9 (%)	Vinegar (%)
A	50.00	43.73	6.14	0.14	0.00
AA	50.00	31.23	6.14	0.14	12.50
C	50.00	22.35	15.00	0.15	12.50
D	50.00	20.00	17.50	0.00	12.50
SM	50.00	31.23	4.00	0.14	14.64
Trial 1	50.00	35.73	6.14	0.14	8.00

3.2.2 RHEOLOGY

The advanced rheometer Physica MCR 301 by Anton Paar was used with cone and plate configuration and with the hood on to preserve the mixture moisture. A small amount of grout was injected using a syringe from the mother batch onto the plate, and the top conical plate was lowered to 0.093 mm squeezing the excess grout. This excess was carefully removed and replaced with tap water in the small groove around the plate to ensure saturated conditions and the hood lowered to seal. This process took 3 to 4 minutes after the batch was mixed and took 7 hours to complete the series of tests. The testing series included:

- A linear shear rate ramp 0-200 1/s with the acquisition data every 1 second for 200 points.
- A resting period of 5 seconds before the next test.
- A linear amplitude shear strain sweep at 0.0001-100% with a frequency of oscillation of 1 Hertz and the acquisition of data every 1 second for 290 points.
- A resting period of 5 seconds before the next test.
- A constant amplitude shear strain of 0.01% with a frequency of oscillation of 1 Hertz and the acquisition of data every 15 seconds for 1500 points.
- A linear amplitude shear strain sweep ranging from 0.01% to 50% with a frequency of oscillation of 1 Hertz and the acquisition of data every 5 second for 500 points.

In this way, pre- & post-gelation properties were obtained, and time to gelation was precisely pinpointed.

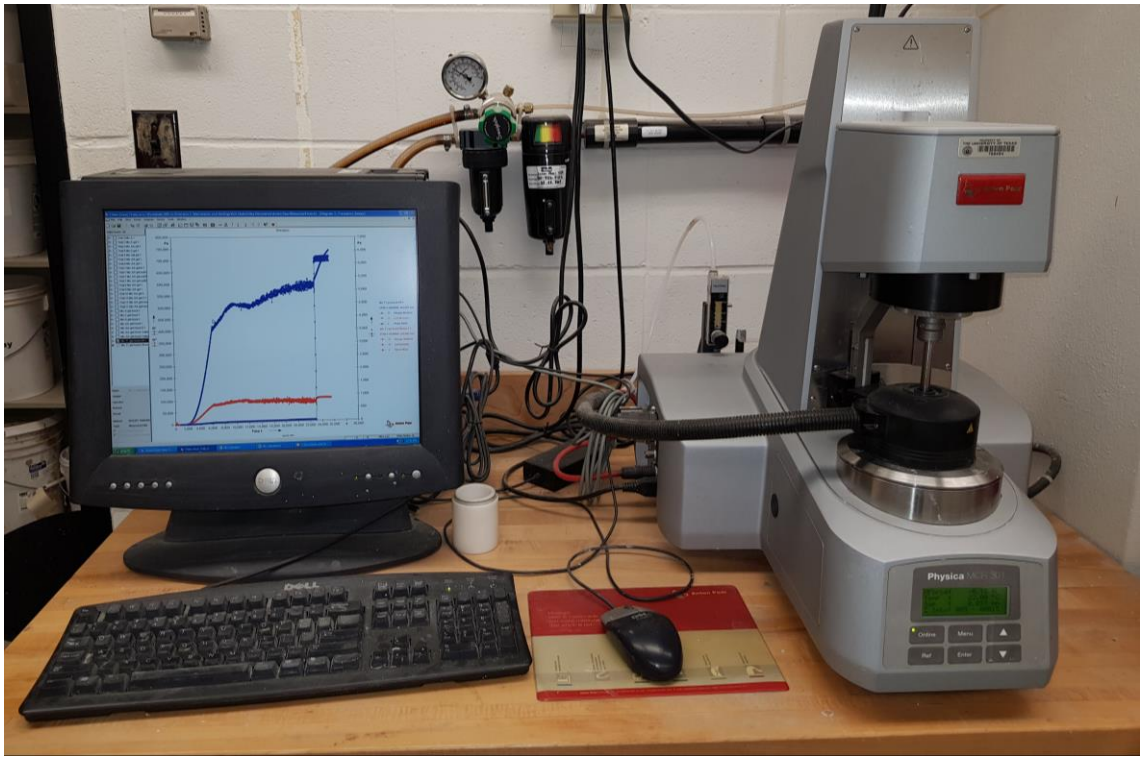

Figure 3-1: Rheometer Setup

Figure 3-2: Rheometer Cone & Plate Configuration

3.2.3 SAND COLUMN PREPARATION & PERMEATION

Three column heights were used in the series of experiments presented: 6”, 12”, & 24”. The columns were prepared as follows:

1. A permeation cell is constructed such that one, two, or four 6” split molds will hold the samples. The cell is constructed using Plexiglass split molds with a wall thickness of 1” and an inner diameter of 2.8”. Rubber gaskets are used between every component of the setup. An additional 2” from the top and bottom of the samples is constructed using 2” Plexiglass tubes of the same diameter to fill coarse and fine gravel:
    a. A sieve if placed over the nozzle where the fluid is permeated to prevent the material from flowing back into the lines.
    b. About an inch of coarse gravel is placed followed by about another inch of fine gravel. These materials act as fluid diffusers; allowing uniform permeation of the samples.
    c. 6” split molds are filled with sand by the dry pluviation method; the drop height is kept constant at about an inch during the process to ensure a similar relative density across the whole sample. One, two, or four split molds were used to build 6”, 12”, & 24” specimen.
    d. An inch of fine gravel followed by another inch of course gravel is added at the top for similar reasons as previously mentioned.
    e. The mass of sand intake and two measurements of height before and after placement of the sand column were also measured.
2. Sample is subjected to water permeation; records are kept for the time it takes to permeate one pore volume of water through the sample. The sample is then permeated with two more additional pore volumes of water to ensure full saturation. A displacement pump is used with a constant push volume of 100 mL/min.
3. Sample is subjected to a number of pore volumes of the desired grout.
4. The sample is then stored in the permeation cell for at least a day, some samples are extracted after a day and stored in plastic wrap, while others are left in the permeation cell till strength test date. Samples used for syneresis testing are stored in plastic wrap and extracted at day one. Samples built to heights greater than 6” are cut to 6” before storing using a medium tooth saw.

Note: Grout mix is constantly stirred using a shear mixer during permeation to ensure grout homogeneity.

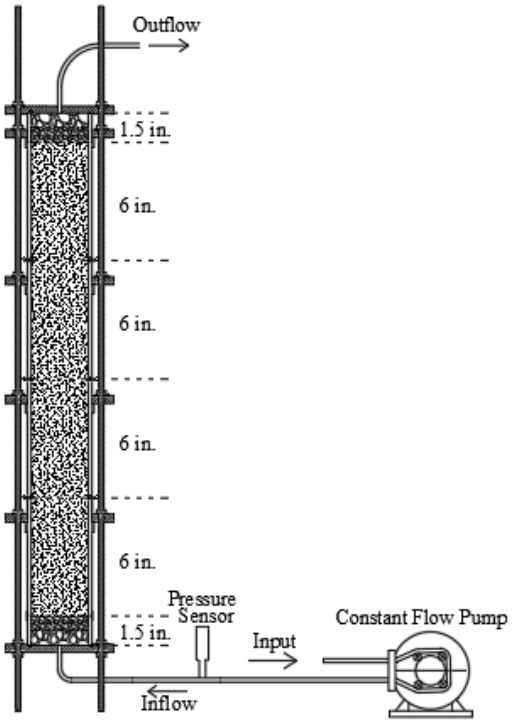

Figure 3-3: Permeation Setup Sketch

3.2.4 STRENGTH TESTING

Unconfined compression testing was performed on saw-cut samples of the grouted sand using GEOJAC automated load actuator from GEOTAC. The procedure is as follows:

1. The permeation cell is disassembled carefully.
2. The sample is extracted from the split mold.
3. The sample ends are marked along with the sample name.
4. The sample ends are trimmed using a saw, making sure to level the ends.
5. The sample is then weighed, then five height measurements are taken (four corners and the middle) and three diameter measurements are taken (at third points).
6. The sample is then placed in an unconfined compression setup which has a calibrated LVDT and load transducer.
7. The sample is sheared at a constant rate of 1%/min of its height, with records kept of load and position.

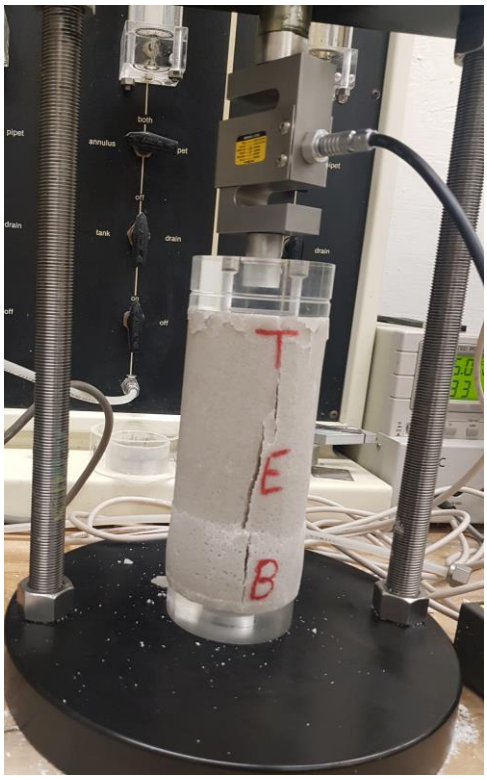

Figure 3-4: Unconfined Compression Setup

Figure 3-5: Samples Before Testing

Figure 3-6: Samples After Testing

3.2.5 SYNERESIS TESTING

Two series of syneresis tests were performed, namely gel syneresis and grouted mass syneresis.

For gel syneresis, grout mixes where poured in volumetric tubes and beakers for volumetric and mass measurements at various time intervals.

Syneresis tests were also performed on samples of the grouted mass. The procedure is as follows:

1. The permeation cell is disassembled carefully.
2. The sample is extracted from the split mold.
3. The sample ends are marked along with the sample name.
4. The sample ends are trimmed using a saw, making sure to level the ends.
5. The sample is then weighed, then five height measurements are taken (four corners and the middle) and three diameter measurements are taken (at third points).
6. The sample is then wrapped airtight and stored (as in Figure 3-7).
7. The sample is then frequently measured as in step 5 and stored as in step 6.

Figure 3-7: Samples Storing

CHAPTER 4. RESULTS AND ANALYSIS

In this section, the results of the experimental program will be presented and analyzed. First, the results from rheology tests will be discussed and analyzed; rheology testing allows for a preliminary assessment of the ideal grout mix to be used in the later stages of this thesis. Syneresis results will then be presented and analyzed, followed by the bulk of this thesis; strength testing.

4.1 Rheology

Rheology is the study of flow of matter and deformation. With the information obtained by running the series of tests shown next, we can compare the performance of the different mixes. As per the guidelines shown in the "Materials and Methodology" section, a series of tests were run on mixes A, AA, C, D, SM, and T1. The first set of tests was run without the hood, and it was quickly understood that the hood is required to prevent moisture migration. The results are shown in the two sections to follow.

Three different tests are run on each mix. The goal of the first test is to obtain the viscosity of the mix pre-gelation; this parameter is paramount in the permeation process. The more viscous the grout the higher pressure generated due to higher losses when permeating the soil column. The second test is run to pinpoint the onset and end of the gelation process; this is of more accurate account than the 45-degree test used in the field. The last test is run to obtain an account of the strength of the gel itself post-gelation. With this information at hand, we can compare the different mixes and alter their constituents to create the most efficient mix before we permeate the many columns and determine grouted mass parameters.

Three distinct measurements were taken for each mix when tested for their rheology as previously mentioned; pre-gelation high shear rate viscosity, start and end of gelation by various indicators, and post-gelation strength-strain. The discussion to follow aims to clarify the tests undertaken in each of the three sections of the testing program before presenting them in the sections to follow.

The viscosity of the grout at various shear rates was tested for pre-gelation. In this test, a shear rate ramp of 0-200 Hz was used, and the shear stress measured. Then the dynamic viscosity of the mix at various shear rates is calculated as:

$$\eta = \frac{\tau}{\dot{\gamma}}$$

It is important to note that viscosity depends on temperature, pressure, time, and shear rate. In our test, temperature was set at 22 degrees Celsius, the pressure is that of atmospheric pressure, and the gel has no time-dependent effects.

After determining the viscosity-shear rate relationship of the mix, the mix is set to rest for 5 seconds then thoroughly mixed for about 5 minutes and reset to rest for 5 seconds. At this point, different components of the grout have been mixed for about 11 to 13 minutes, and a constant low amplitude test of 1 Hz frequency is applied and the results acquired every 15 seconds.

Measuring storage and loss moduli will help pinpoint the start and end of gelation; as well as measurements of phase angle. The three parameters will herein be explained mathematically:

To characterize visco-elastic behavior, the gel is sinusoidally deformed at a specific strain (0.01%) and frequency (1 Hz), and the resulting stress recorded. For a linear visco-elastic material, the stress will vary sinusoidally with the strain. An ideal elastic material will have both the stress and the strain in phase (phase angle of zero degrees), whereas an ideal viscous material will have the stress and strain out of phase (phase angle of 90 degrees). Figure 4-1 helps better visualize the process:

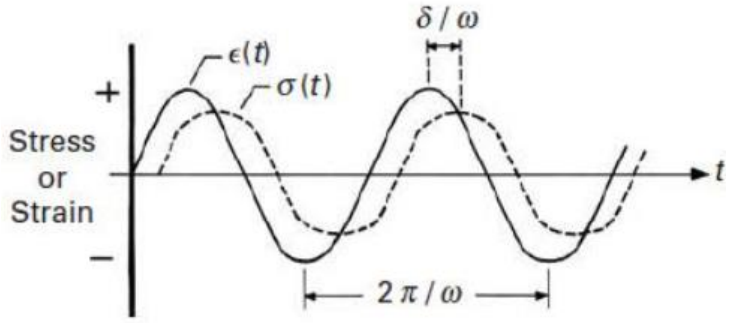

Figure 4-1: General Viscoelastic Response

Strain lags behind stress, and the following two equations are set:

$$e = e_0 \sin(\omega t)$$

$$\sigma = \sigma_0 \sin(\omega t + \delta)$$

Where ω is the is the frequency and δ is the phase lag.

Thus, the stress can be written as:

$$\sigma = \sigma_0 \cos(\delta) \sin(\omega t) + \sigma_0 \sin(\delta) \cos(\omega t)$$

For visco-elastic material the stress has two components; $\sigma_0 \cos(\delta)$ in phase with strain, and $\sigma_0 \sin(\delta)$ out of phase with strain.

Thus, the storage and loss moduli can be inferred as:

$$G' = \frac{\sigma_0 \cos(\delta)}{e_0} \qquad G'' = \frac{\sigma_0 \sin(\delta)}{e_0}$$

In simple words, the storage modulus is an account of how much of the strain is recoverable versus the loss modulus which is an account of how much of the strain is lost due to mechanical dissipation of energy.

A phasor diagram in Figure 4-2 as shown below indicates that both moduli can define a complex modulus, G^*, as follows:

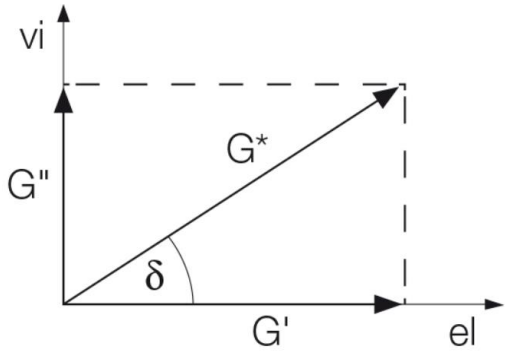

Figure 4-2: Complex Modulus

If,

$$e = e_0 \exp(i\omega t)$$

$$\sigma = \sigma_0 \exp(i(\omega t + \delta))$$

Thus,

$$G^* = \frac{\sigma}{e} = \frac{\sigma_0}{e_0} \exp(i\delta) = \frac{\sigma_0}{e_0} (\cos\delta + i \sin\delta) = G' + iG''$$

Lastly, after the gel has hardened, an amplitude sweep of 0.01% to 50% strain is applied at a frequency of 1 Hz, and the shear stress measured to determine post-gelation strength.

4.1.1 TESTING WITHOUT HOOD

As per the guidelines shown in the "Materials and Methodology" section, Mix A was first tested. The results of the series of tests on this grout is shown below.

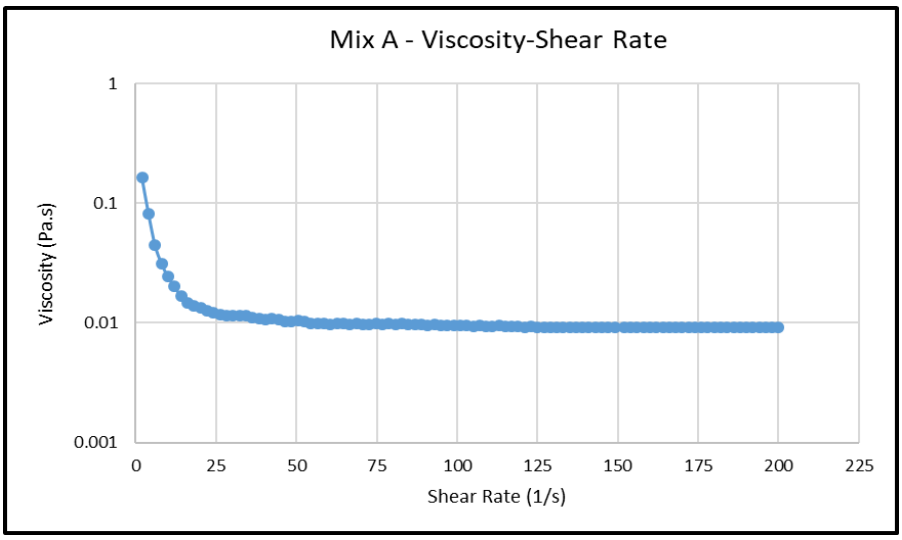

Figure 4-3: Mix A Pre-Gelation Viscosity-Shear Rate

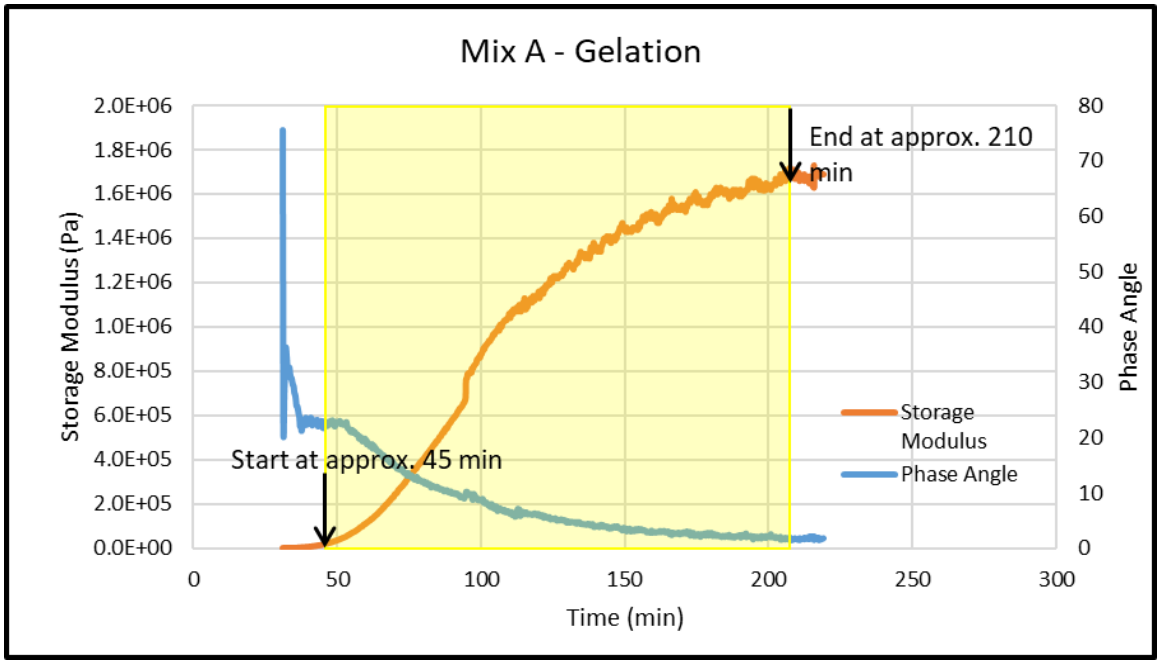

Figure 4-4: Mix A Gelation Assessment

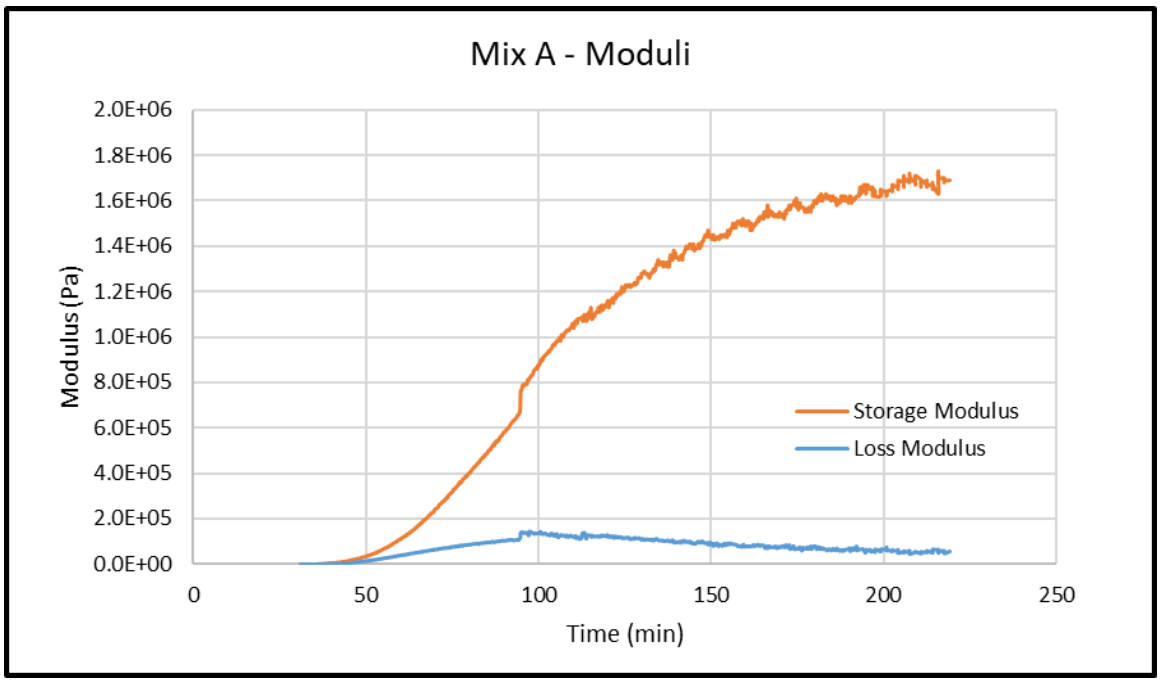

Figure 4-5: Mix A Moduli

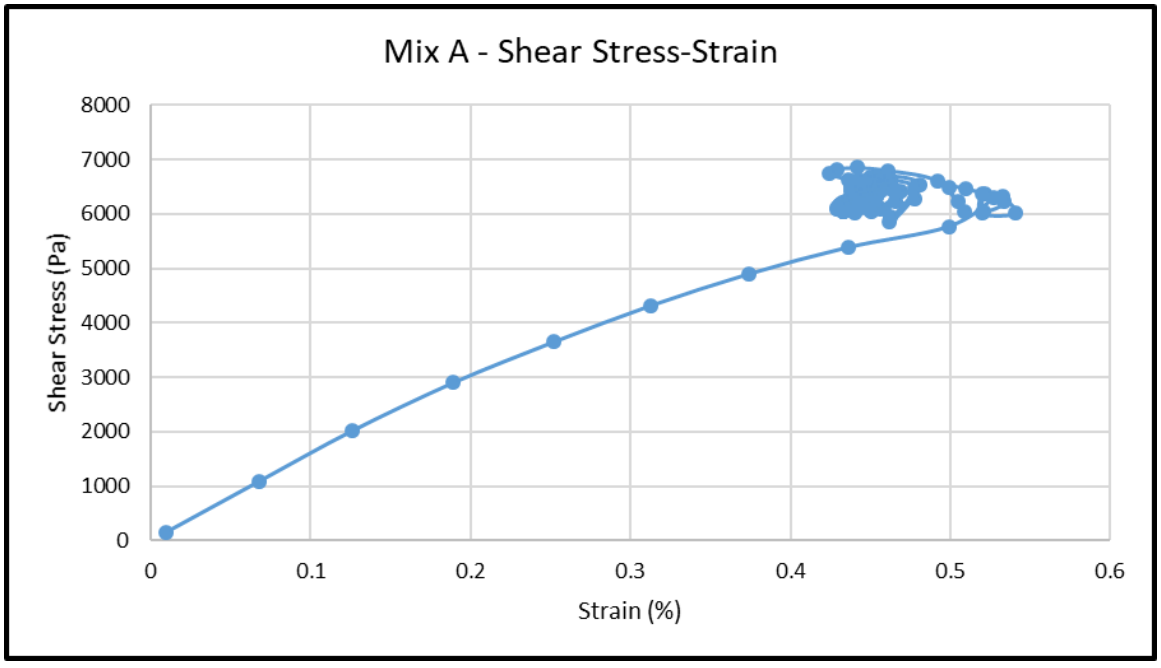

Figure 4-6: Mix A Post-Gelation Strength

The results for Mix D are shown below.

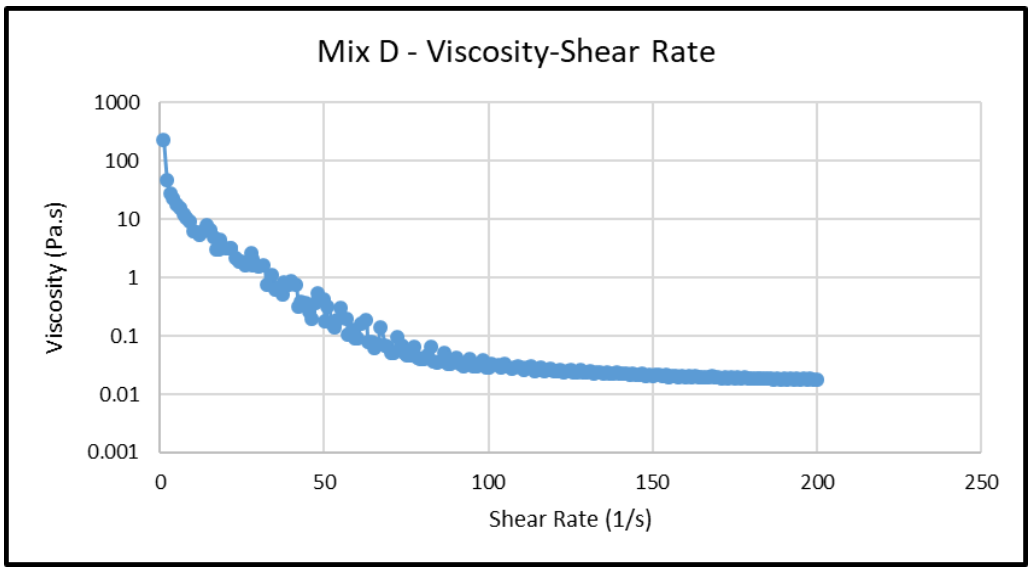

Figure 4-7: Mix D Pre-Gelation Viscosity-Shear Rate

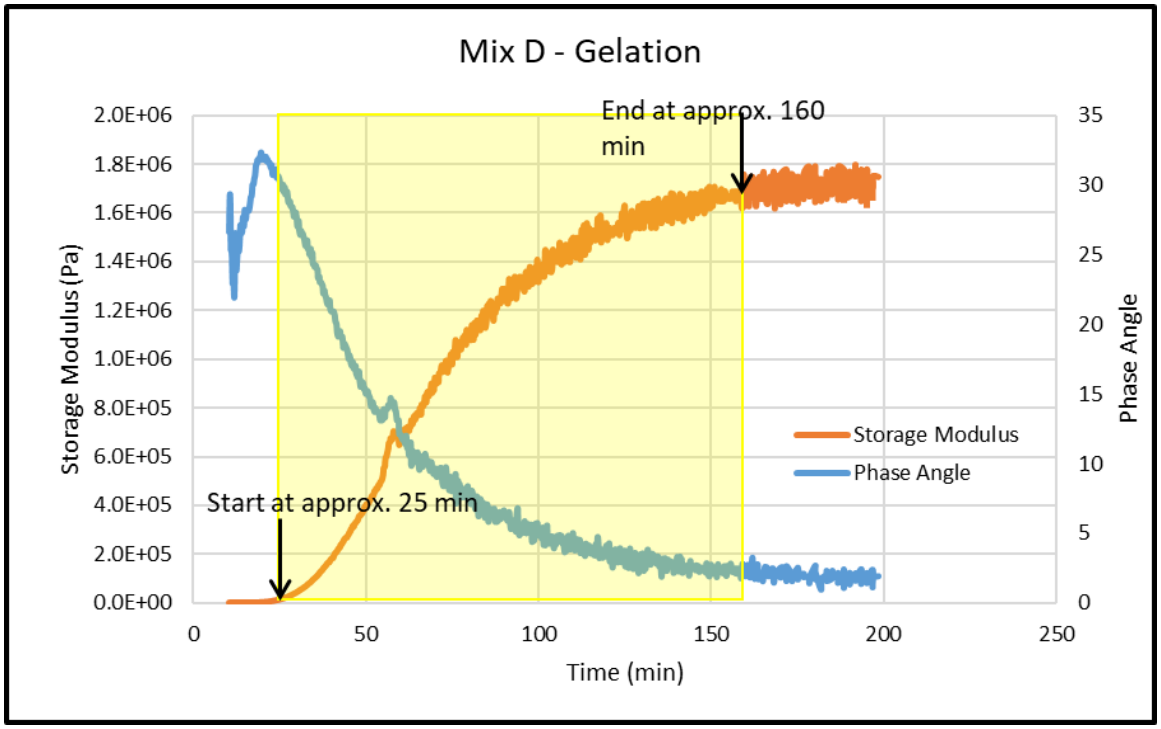

Figure 4-8: Mix D Gelation Assessment

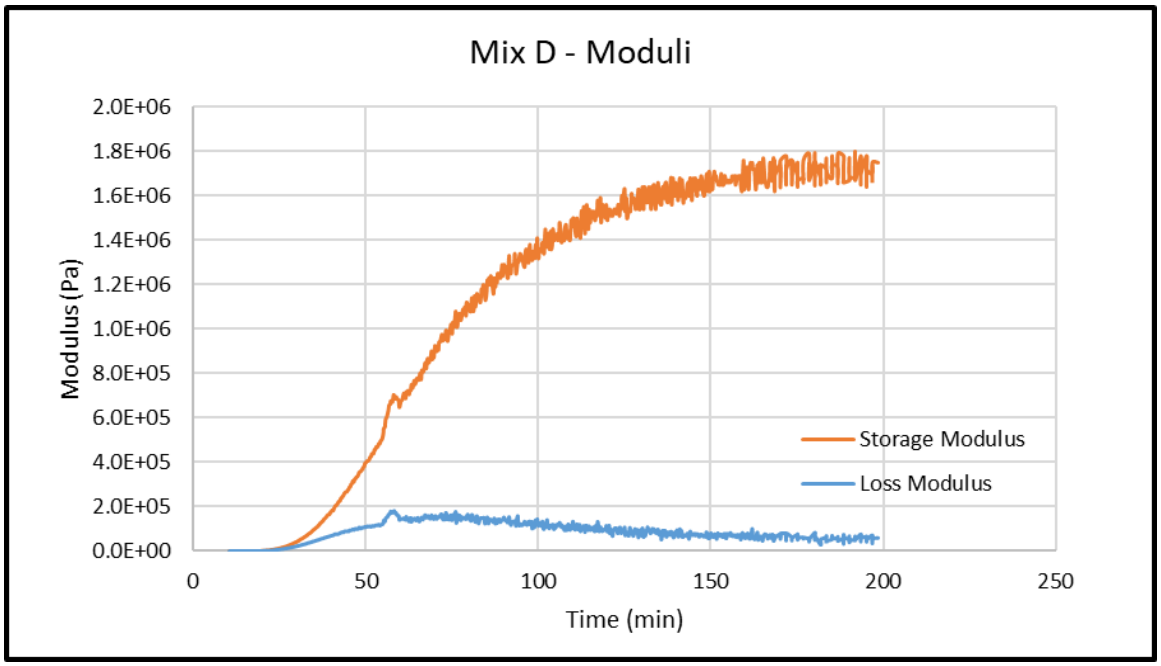

Figure 4-9: Mix D Moduli

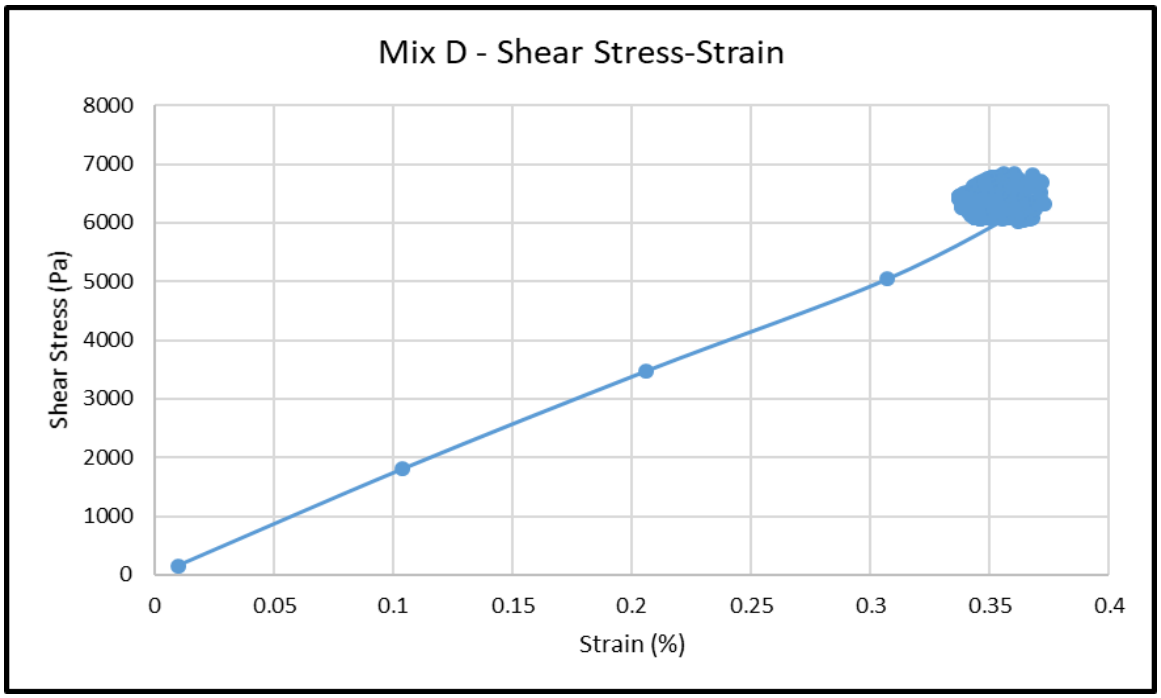

Figure 4-10: Mix D Post-Gelation Strength

The results for Mix SM are shown below.

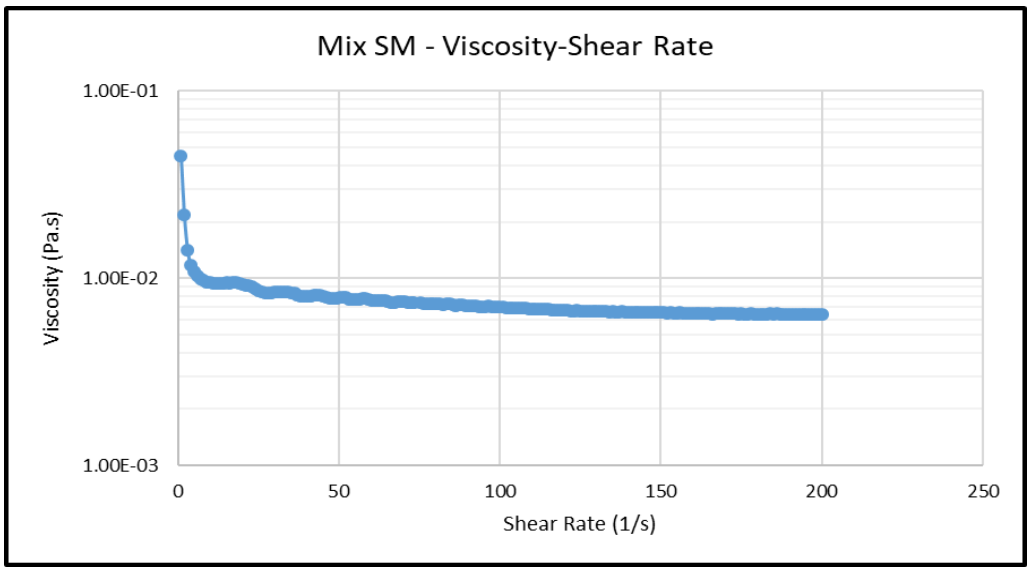

Figure 4-11: Mix SM Pre-Gelation Viscosity-Shear Rate

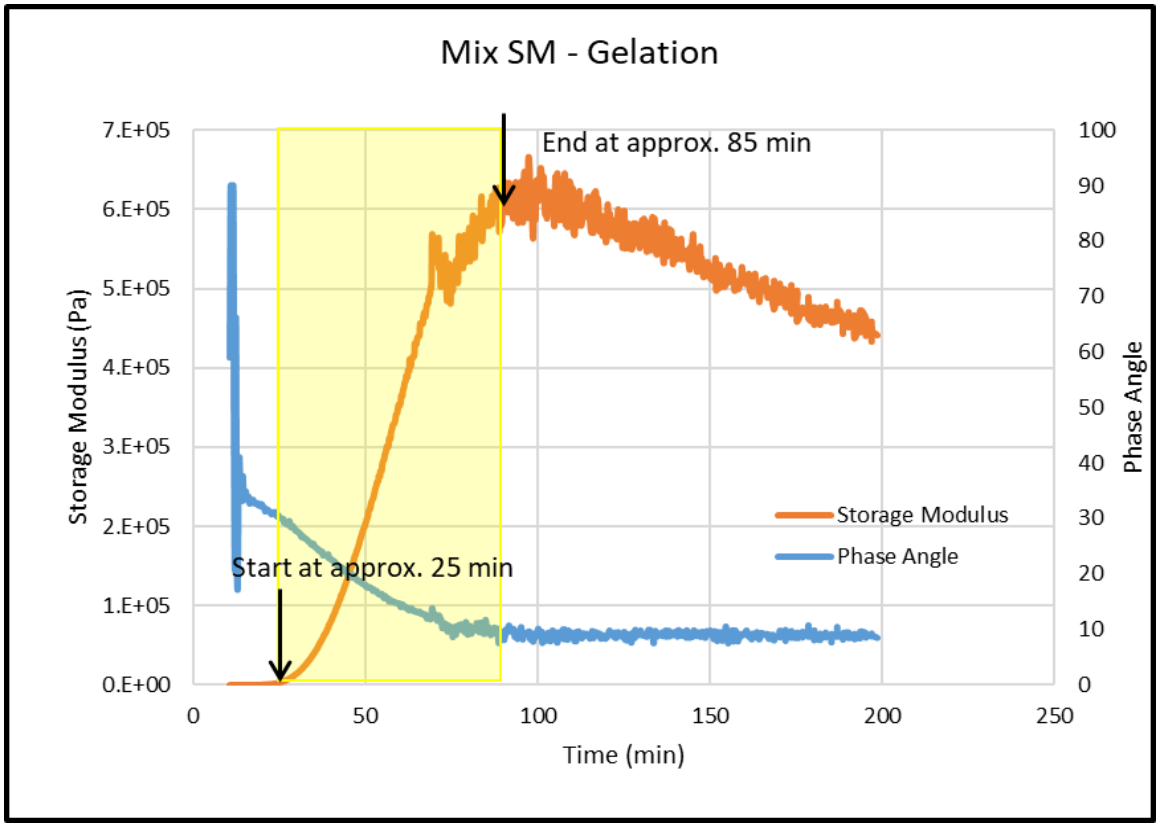

Figure 4-12: Mix SM Gelation Assessment

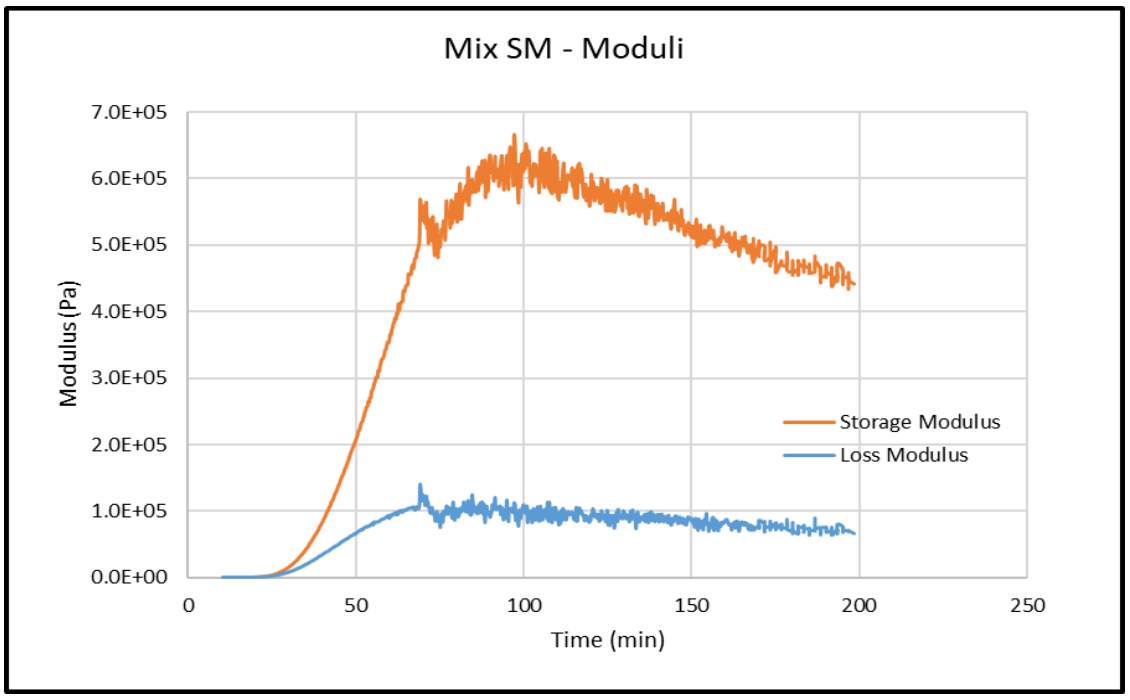

Figure 4-13: Mix SM Moduli

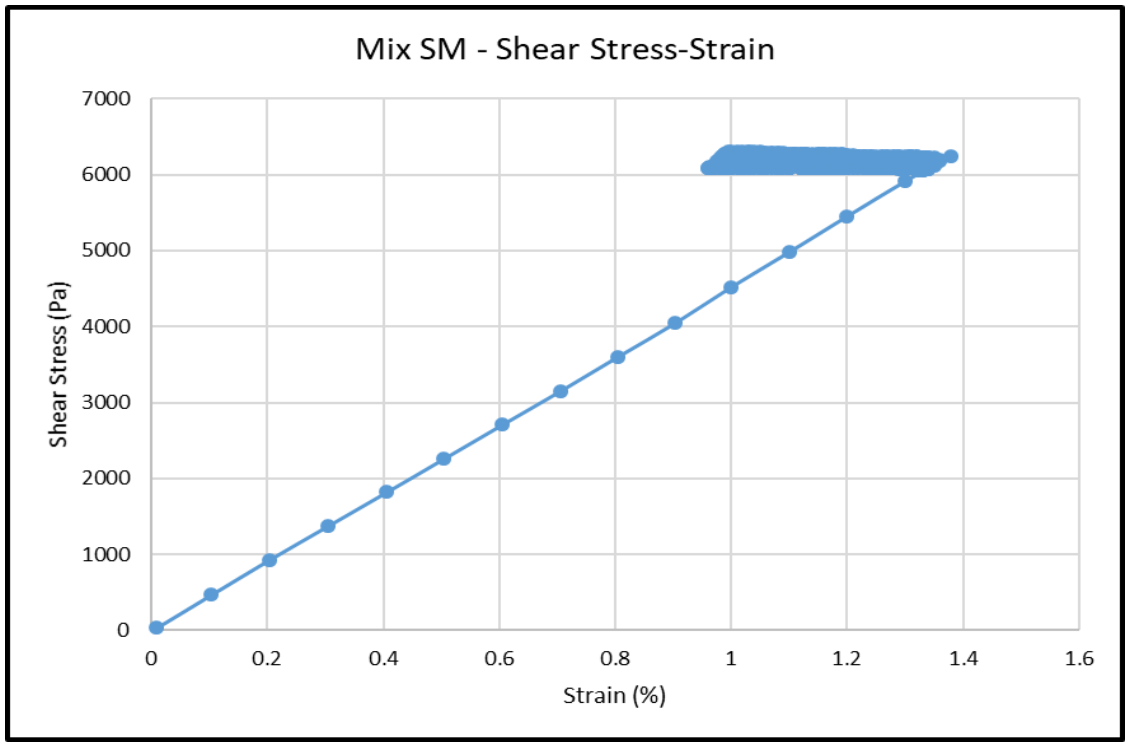

Figure 4-14: Mix SM Post-Gelation Strength

The results for Mix AA are shown below.

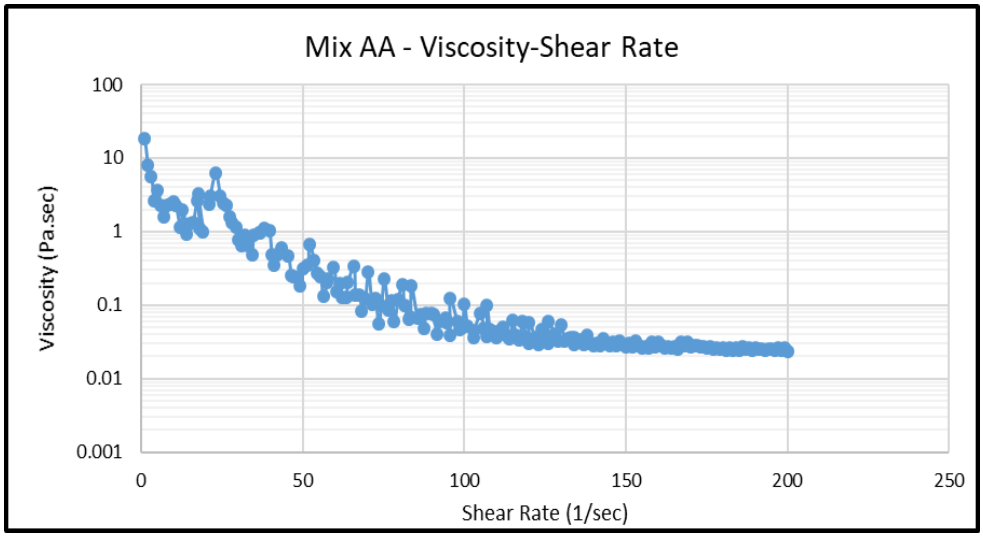

Figure 4-15:Mix AA Pre-Gelation Viscosity-Shear Rate

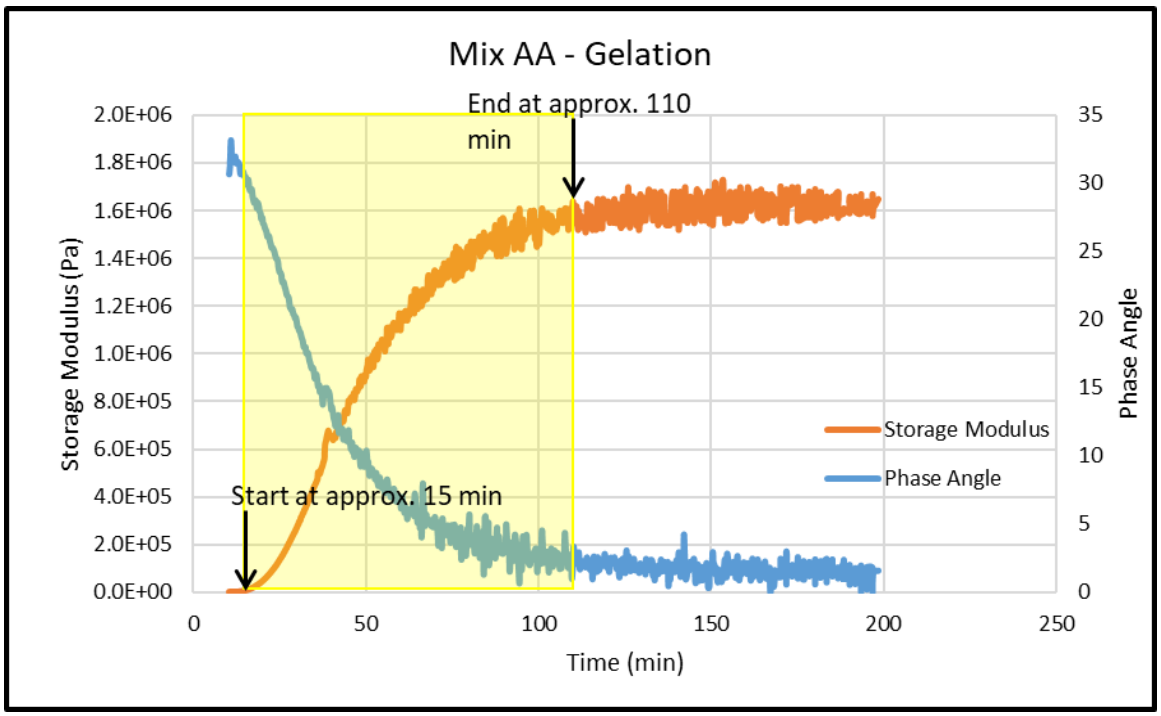

Figure 4-16: Mix AA Gelation Assessment

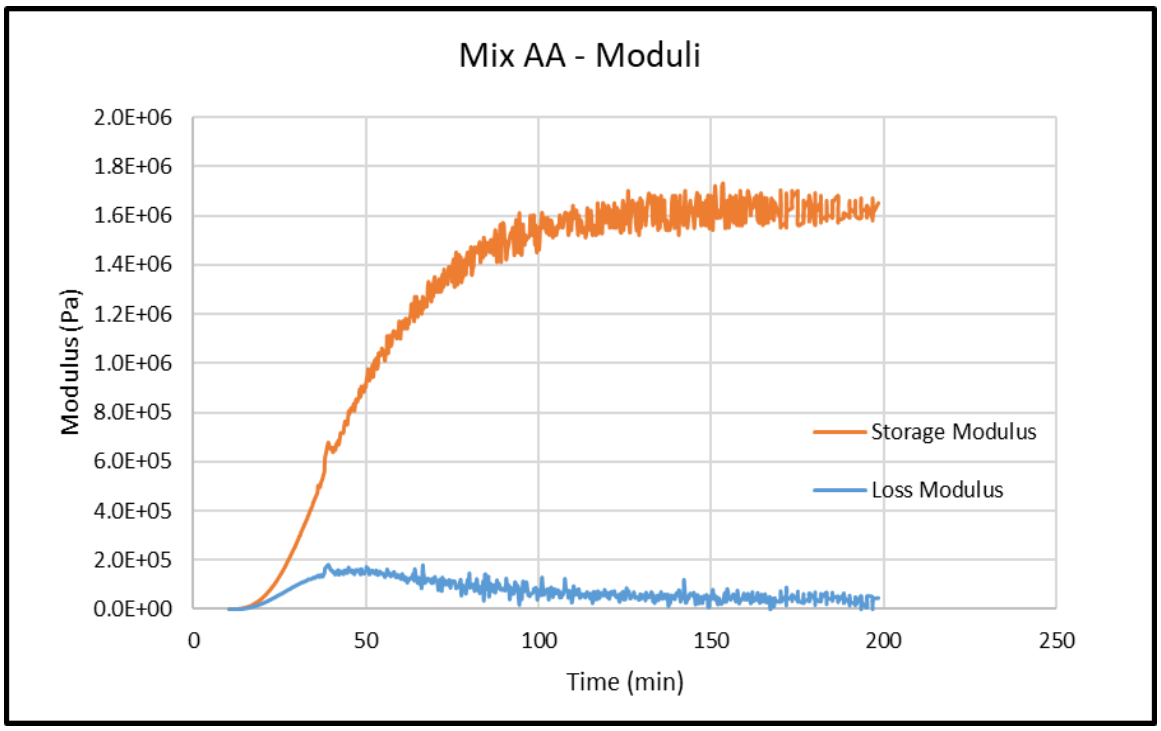

Figure 4-17: Mix AA Moduli

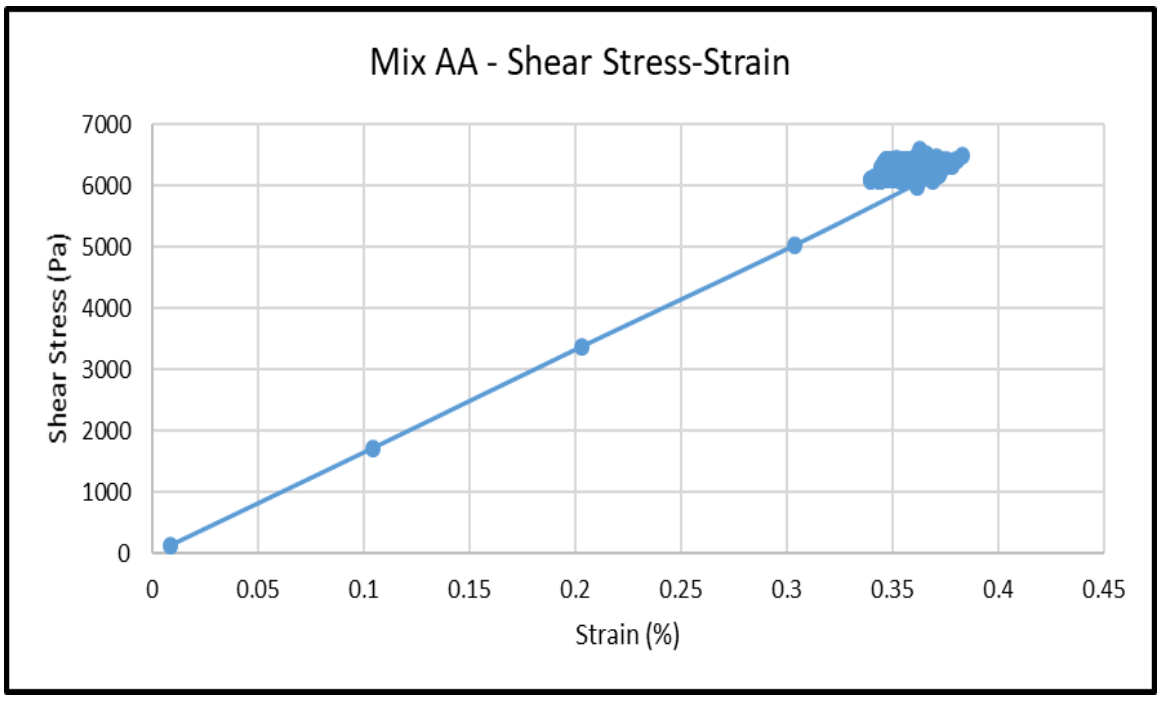

Figure 4-18: Mix AA Post-Gelation Strength

The table below summarizes the results of the four tests run on the four different mixes.

Table 4-1: Rheology Testing without Hood Summary

Mix	A	D	SM	AA
Viscosity at High Shear Rate (Pa.s)	0.0092	0.0179	0.0064	0.0234
Gelation Start (min)	45	25	25	15
Gelation End (min)	210	160	85	110
Storage Modulus (MPa)	1730	1800	664	1730
Loss Modulus (MPa)	143	179	141	179

Mix A is our base mix upon which the performance of the other mixes is compared to.

Mix AA was prepared with the substitution of a portion of the water in the mix with vinegar (pH modifier) in an effort to control the gelation time. The mix started to gel earlier and attained terminal strength faster than the base mix. However, as the data suggests, the gel is more viscous than the base mix but its post-gelation stress-strain curve indicates a stiffer gel.

Mix SM was then prepared by lowering the proportion of dibasic ester in the mix and substituting it with vinegar, as shown in the "Materials and Methodology" section. The mix had a lower viscosity than the base mix, a controlled and short gelling time, but at the cost of a large decrease in storage modulus. This is corroborated by the post-gelation performance being very ductile as compared to the base mix and thus this mix was dismissed.

Mix D was then prepared and tested by keeping the proportion of vinegar constant and substituting some of the water with the dibasic ester. The result was a longer gelation time with little effect on both moduli. This mix was dismissed since more than triple the dibasic ester was used with little added value and it was soon understood that mix AA is the ideal mix at hand.

However, each test takes about 7 hours to complete, and thus moisture migration was a large issue. To yield results with better accuracy, the tests were redone with the installation of a hood on the rheometer to control the humidity of the system. The section to follow addresses this issue and compares the results of both tests.

4.1.2 TESTING WITH HOOD

As per the guidelines shown in the "Materials and Methodology" section, Mix A was first tested. The results of the series of tests on this grout is shown below.

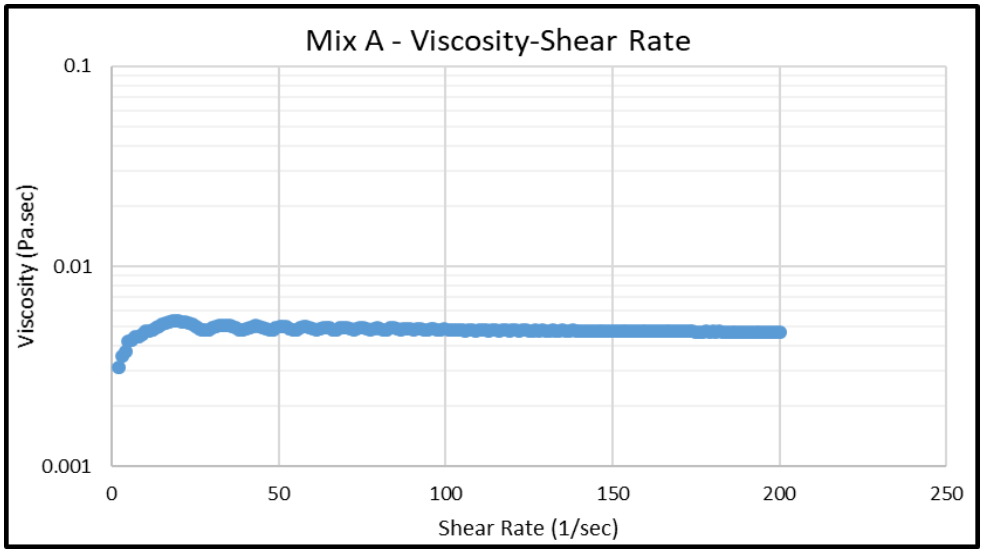

Figure 4-19: Mix A Pre-Gelation Viscosity-Shear Rate

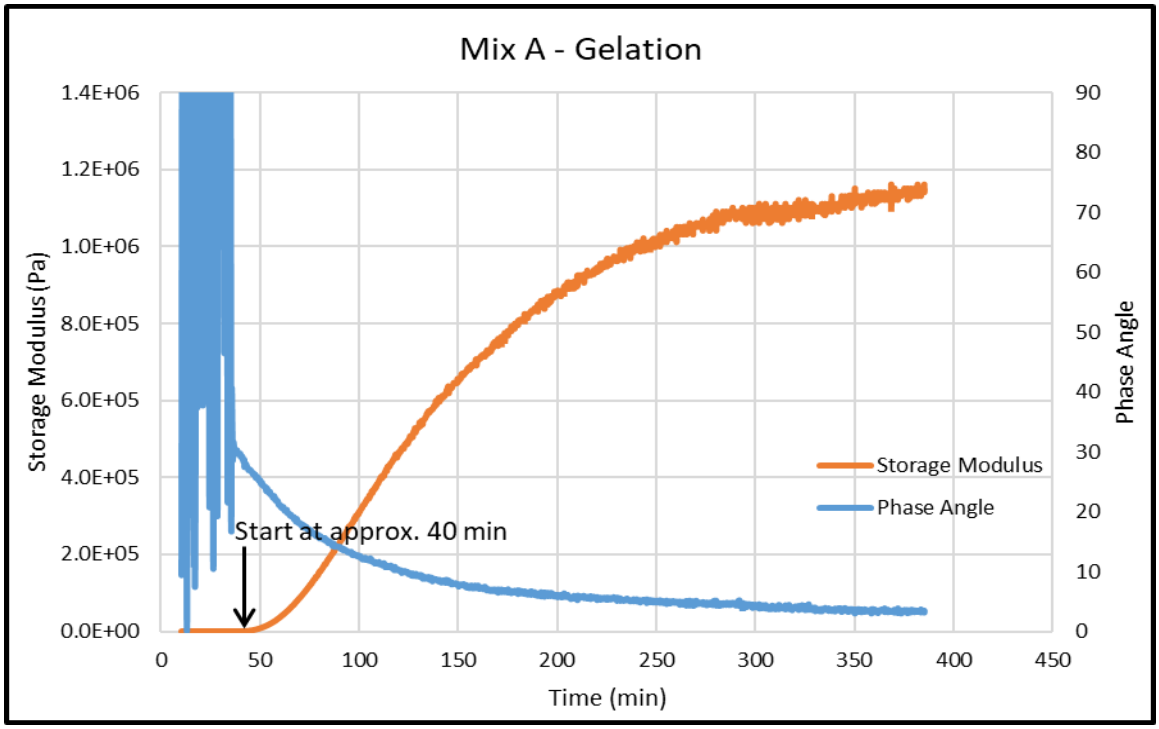

Figure 4-20: Mix A Gelation Assessment

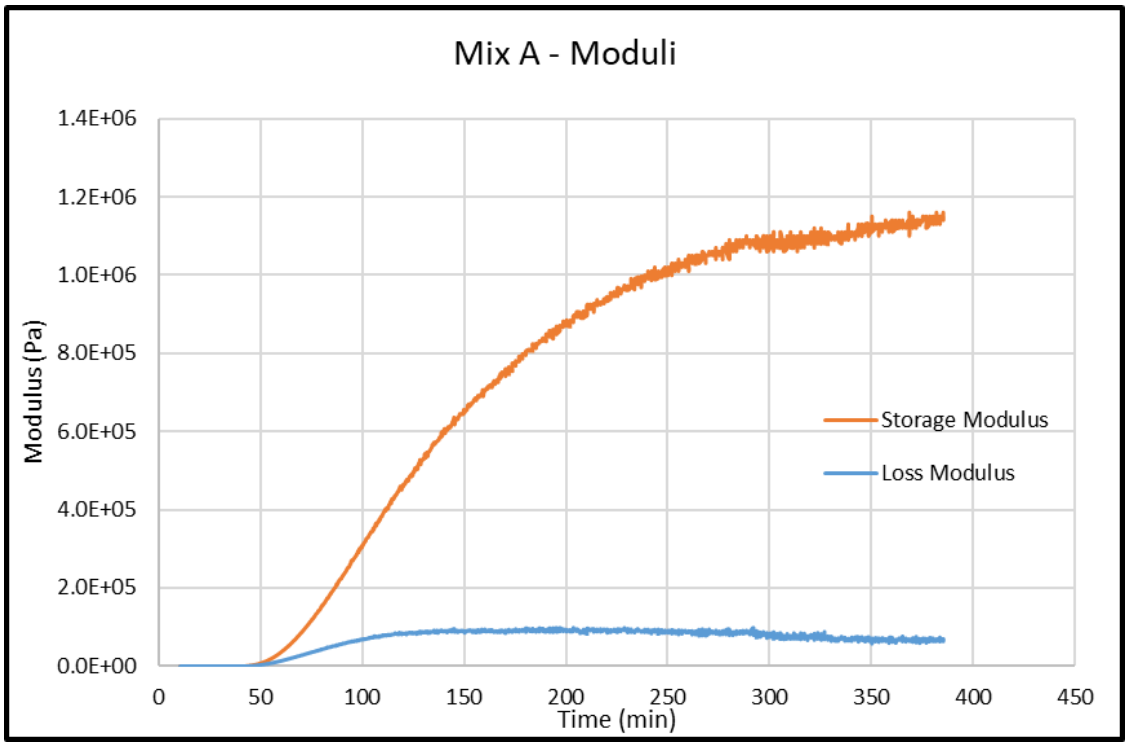

Figure 4-21: Mix A Moduli

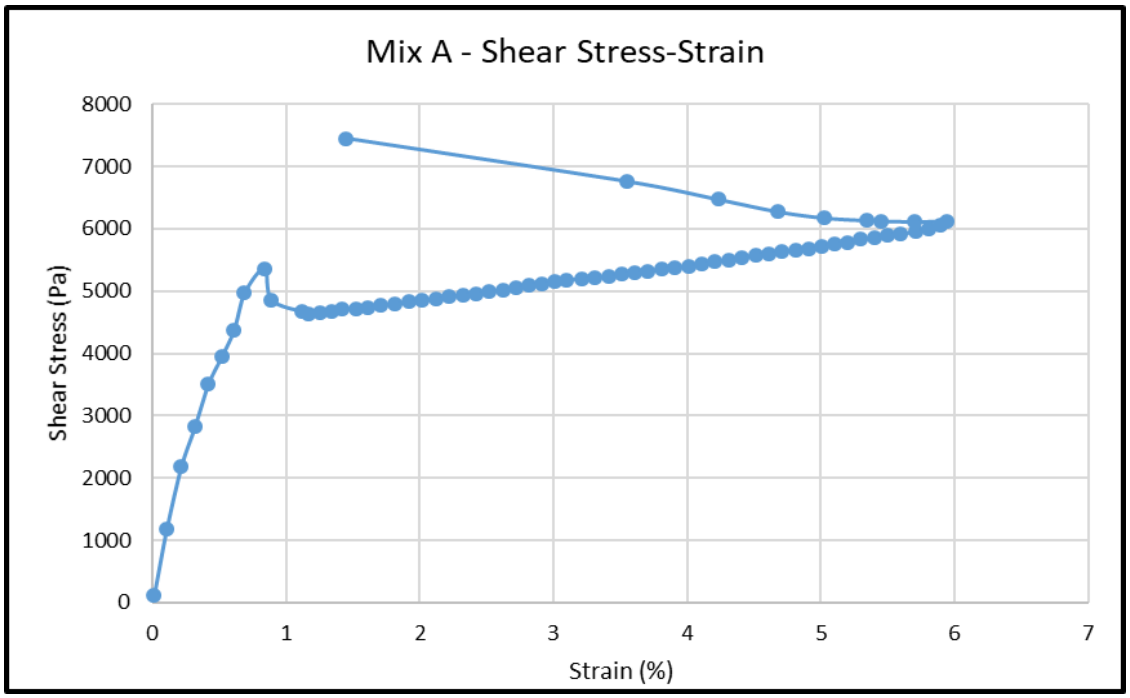

Figure 4-22: Mix A Post-Gelation Strength

The results for Mix C are shown below.

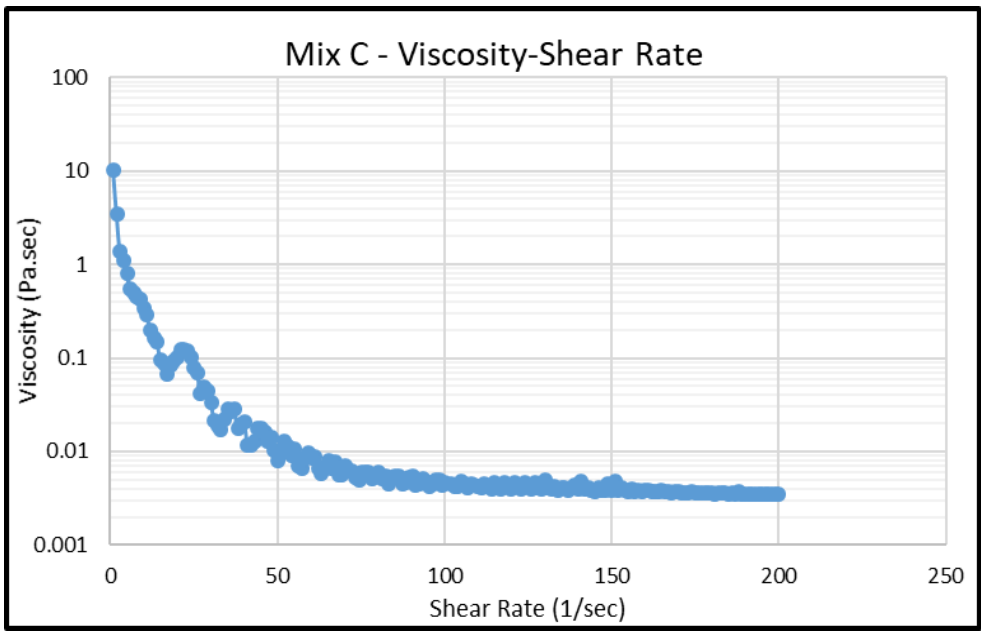

Figure 4-23: Mix C Pre-Gelation Viscosity-Shear Rate

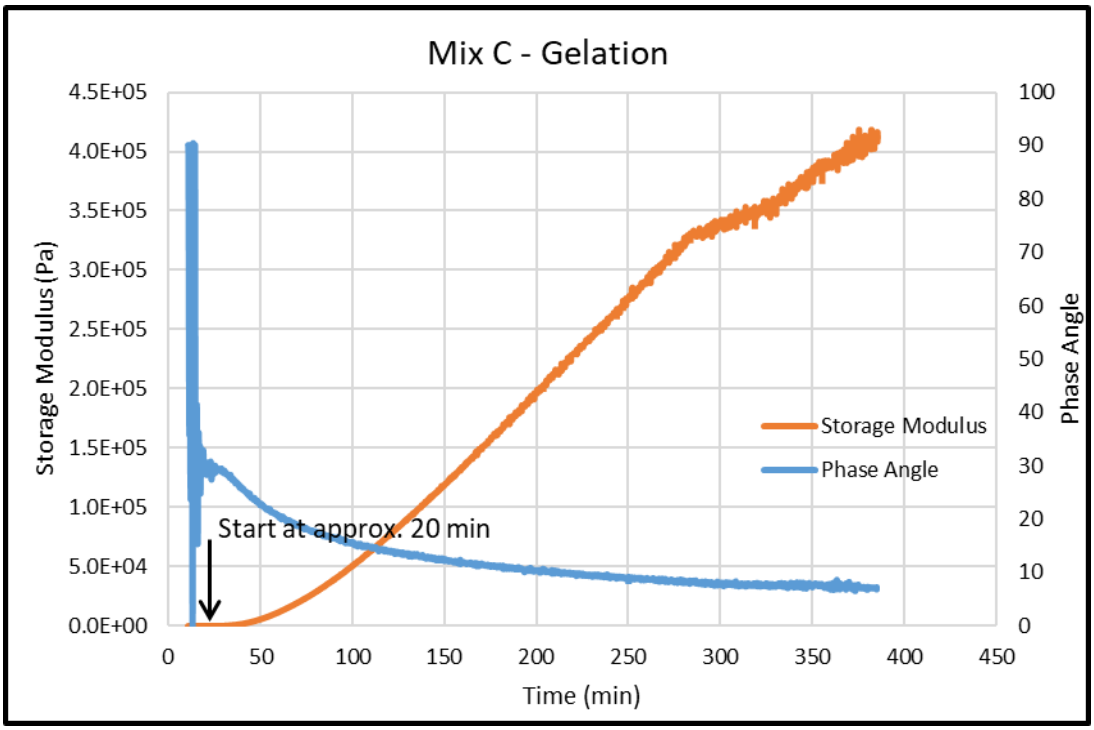

Figure 4-24: Mix C Gelation Assessment

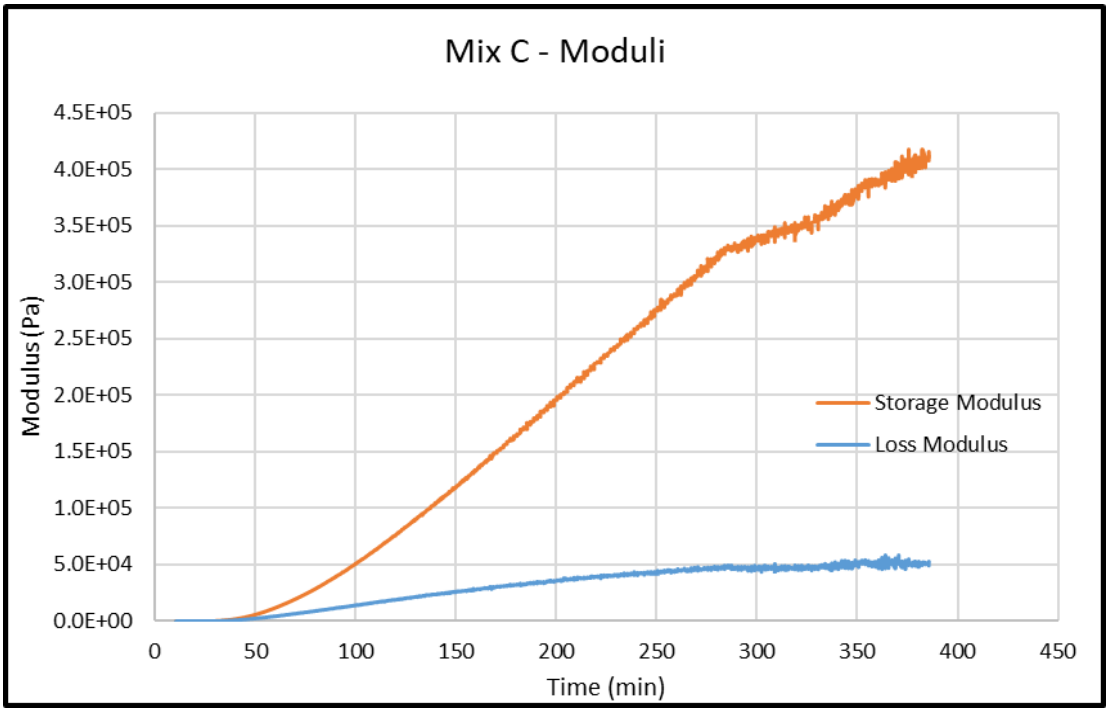

Figure 4-25: Mix C Moduli

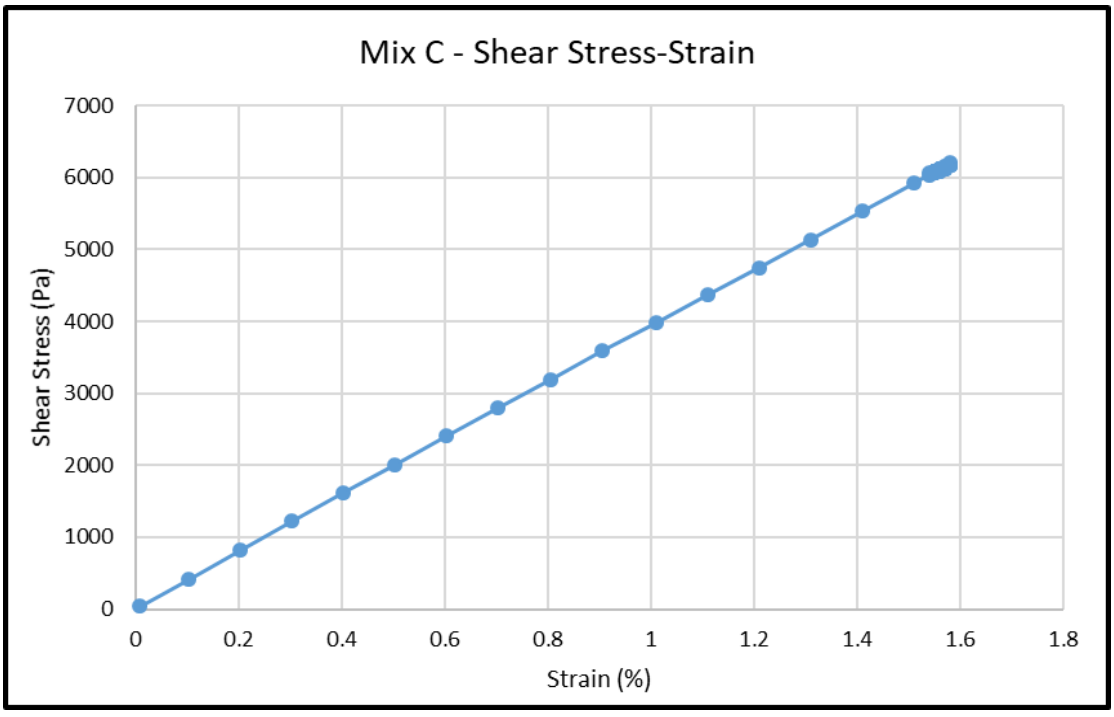

Figure 4-26: Mix C Post-Gelation Strength

The results for Mix AA are shown below.

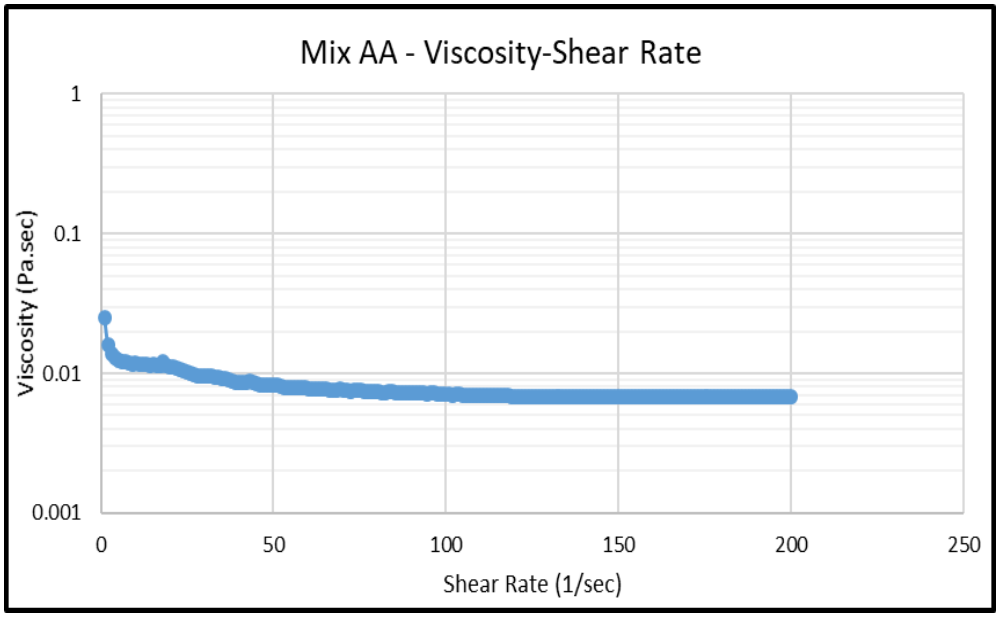

Figure 4-27: Mix AA Pre-Gelation Viscosity-Shear Rate

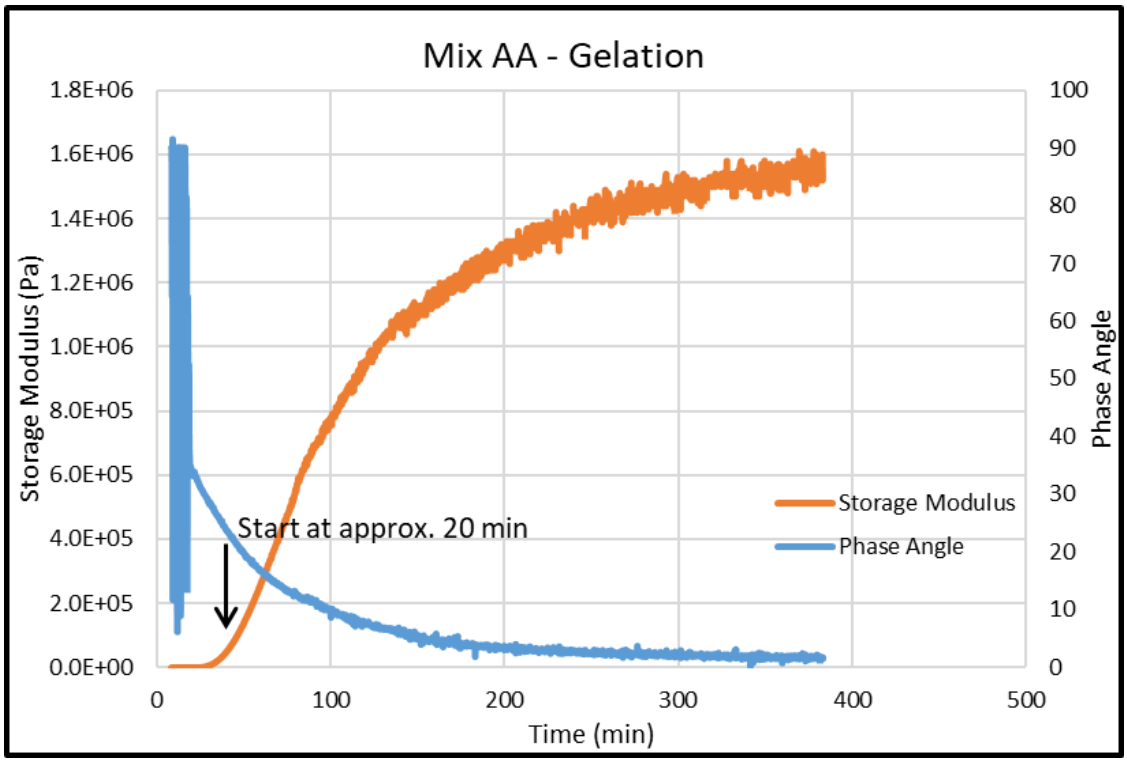

Figure 4-28: Mix AA Gelation Assessment

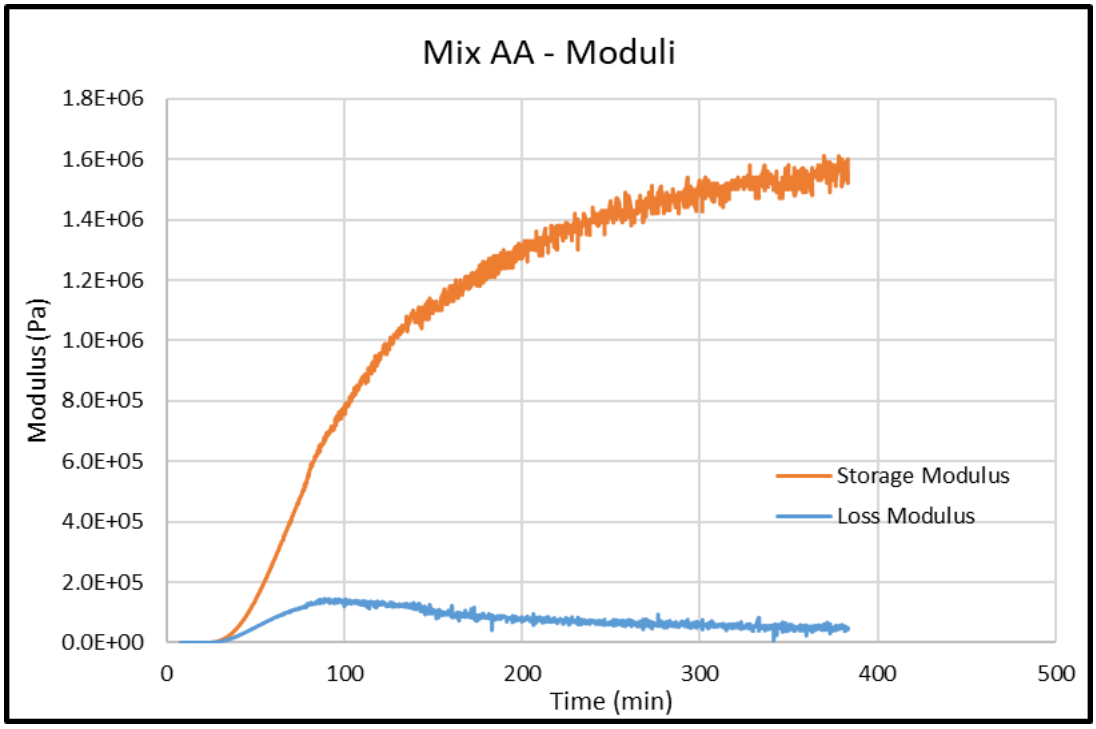

Figure 4-29: Mix AA Moduli

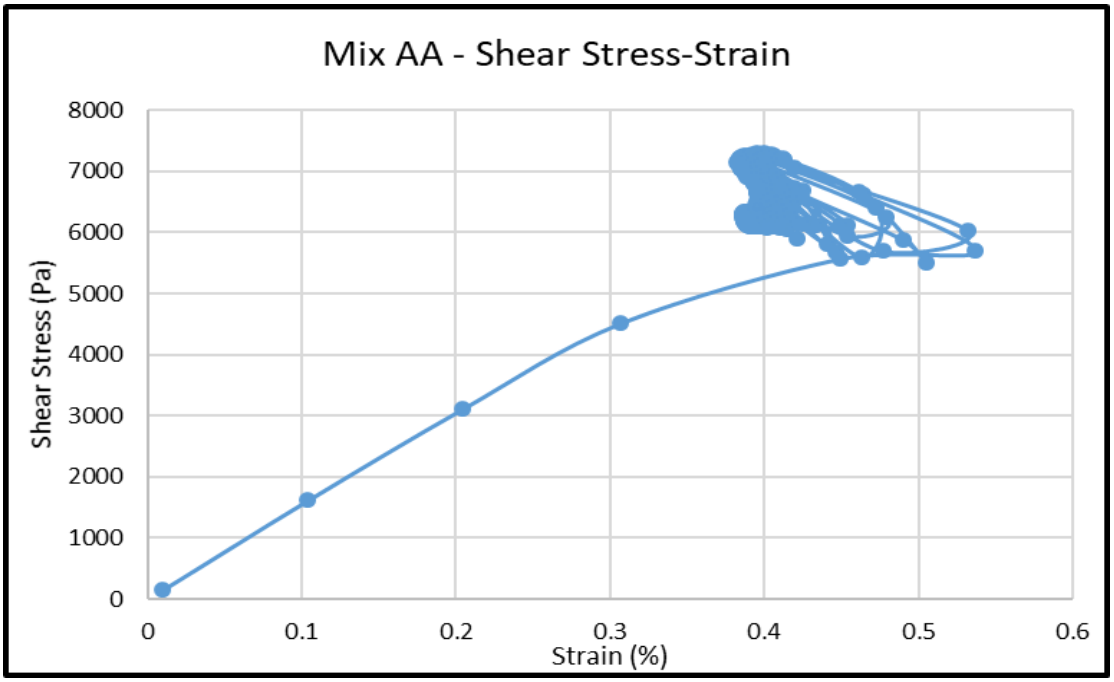

Figure 4-30: Mix AA Post-Gelation Strength

The results for Mix T1 are shown below.

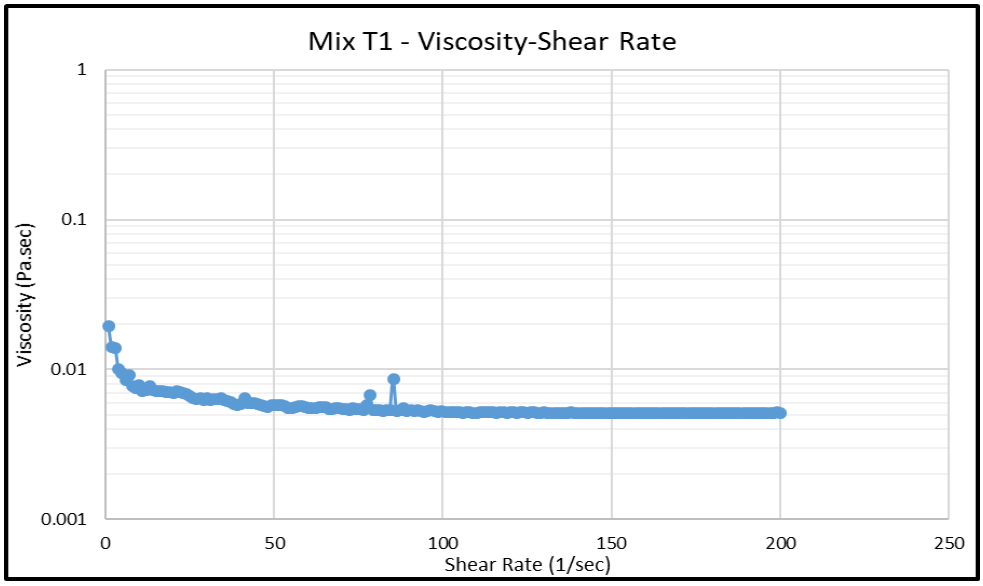

Figure 4-31: Mix T1 Pre-Gelation Viscosity-Shear Rate

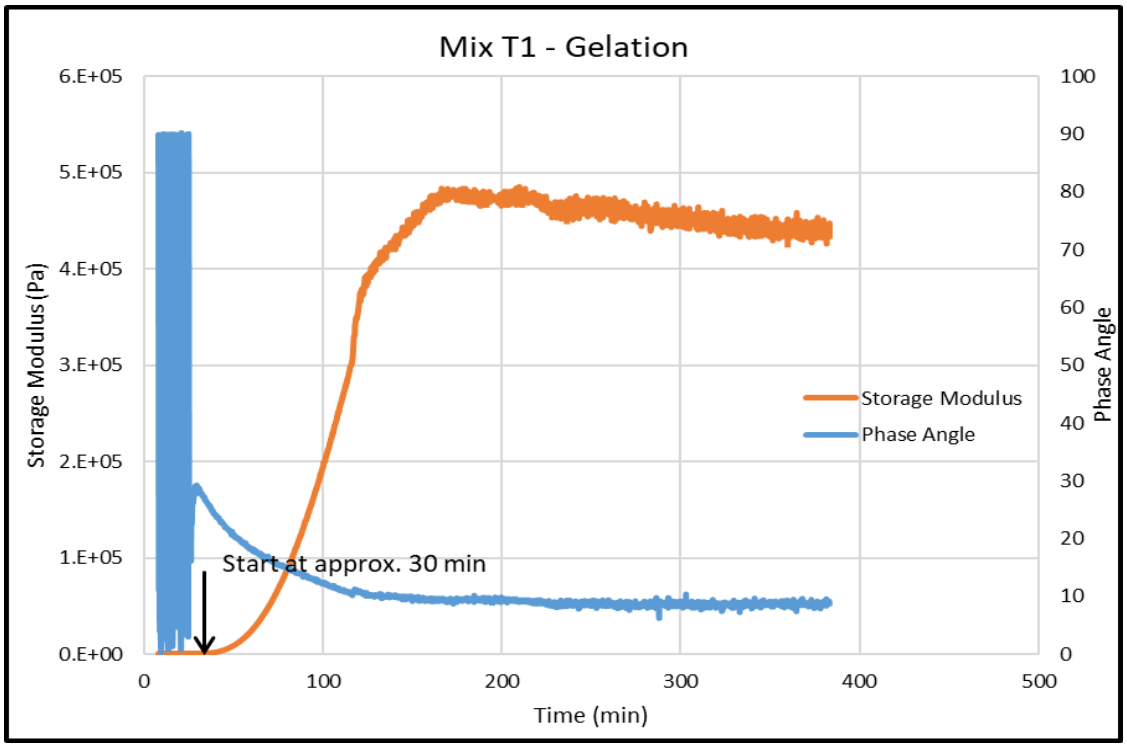

Figure 4-32: T1 Gelation Assessment

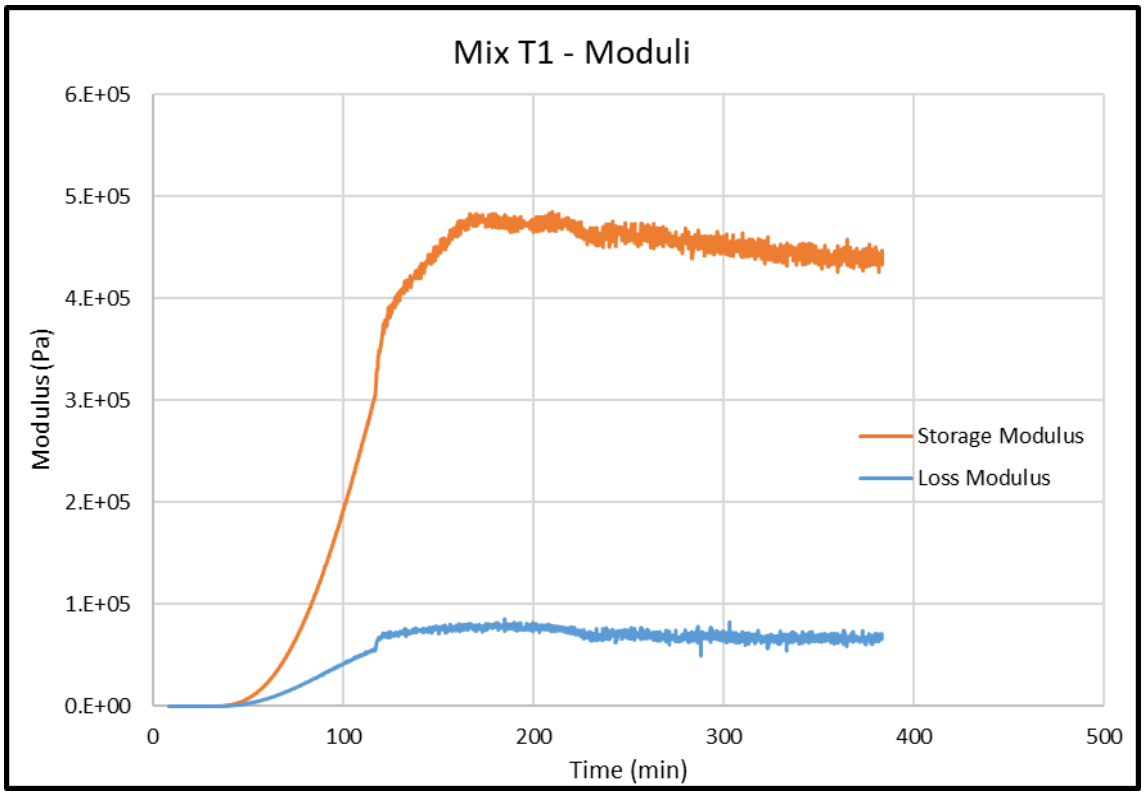

Figure 4-33: Mix T1 Moduli

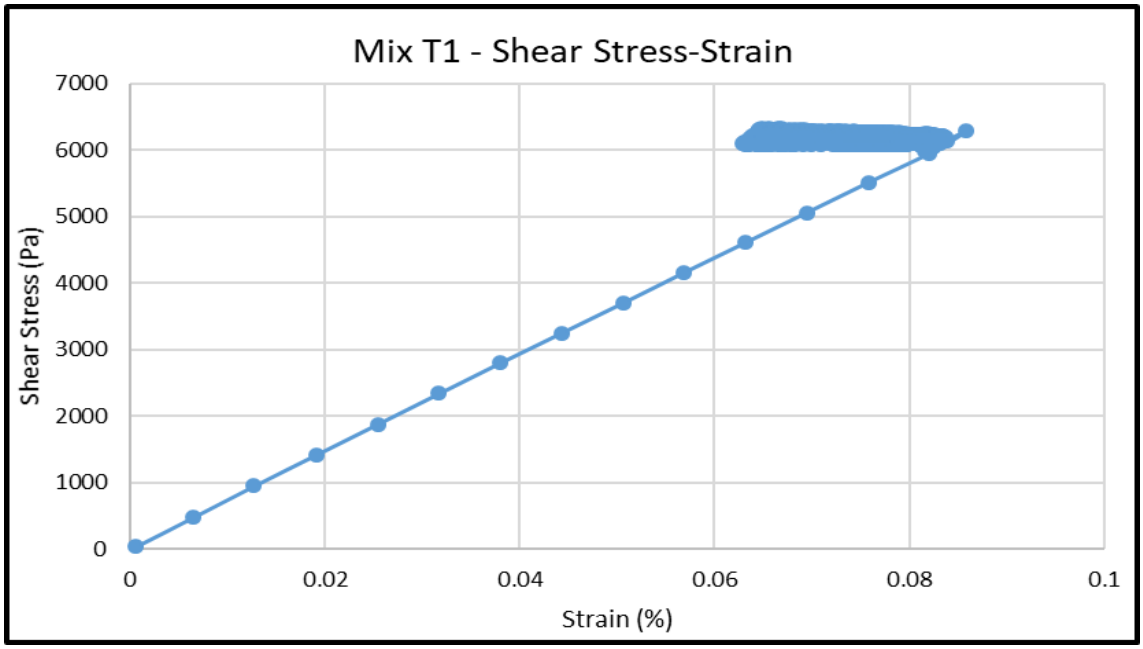

Figure 4-34: Mix T1 Post-Gelation Strength

The table below summarizes the results of the four tests run on the four different mixes:

Table 4-2: Rheology Testing with Hood Summary

Mix	A	C	AA	T1
Viscosity at High Shear Rate (Pa.s)	0.0047	0.0035	0.0068	0.0051
Gelation Start (min)	40	20	20	30
Storage Modulus (MPa)	1160	418	1610	485
Loss Modulus (MPa)	98.4	58.5	144	85.8

Mix A is again our base mix.

Mix AA is prepared by substituting some of the water in the mix with white vinegar. The mix is slightly more viscous, starts gelling in half the time, and attains a higher terminal storage and loss moduli.

Mix C is prepared by substituting a portion of the water in Mix AA with about double the amount of dibasic ester. The results show no change in gelation start time, however, a reduction in both moduli, and a low stiffness gel. This mix was dropped herein.

Mix T1 is prepared by lowering the amount of white vinegar in the mix, in an effort to increase permeation time (delay gelation start). This mix again showed lower moduli and more ductile performance as compared to mixes A and AA.

After the series of tests in this section and the previous section, Mix AA was deemed the most economical and effective mix. Mix AA was then chosen to be permeated through the series of 1D columns, and the results strength tested. Mix T1 was also used through some of the testing due to its delayed gelation time (meaning more grout can be permeated through the specimen).

The yield stress and yield strain from the last stage of testing are not included in the summary table as the strength exceeded the capacity of the rheometer for majority of the testing and therefore, no conclusions could be drawn from these results. The indicator to such a conclusion (capacity of the rheometer reached) is the fact that the tests were to be conducted up until 50% strain; a phenomenon never achieved in all the mixes.

The gel at hand is neither a true liquid nor a true solid; a visco-elastic material where some of the strain energy is dissipated mechanically. When a material is visco-elastic, this means it has a microstructure. A microstructure means that there are forces between the molecules or particles in the material. To break the microstructure, you need to apply a force larger than the ones holding it. When the applied force is smaller than the molecular or inter particle forces, then G' (storage modulus) is larger than G" (loss modulus); the material has some capacity to store energy and should be able to return, to

some extent, to its initial configuration before a mechanical force was applied. The material behaves as an elastic solid, although not an ideal one because some of the mechanical energy is dissipated. But when the applied force is higher, then the microstructure collapses and the mechanical energy applied to the material is dissipated through the changes to the material microstructure. G" becomes larger than G'; the material behaves more of a liquid than a solid.

In an effort not to destroy gel microstructure (only acquire small strain properties), a low amplitude shear strain is applied, and the storage and loss moduli measured. As can be seen in the "Rheology" section of this thesis, the small strain storage modulus of the material is much higher than the small strain loss modulus; this means that the low amplitude shear strain applied at each step is low enough not to alter gel microstructure.

Even with the last stage of shearing to obtain gel yield strength, we did not exceed the strength to break the microstructure. **Error! Reference source not found.** shows that s torage modulus is still higher than the loss modulus; meaning the microstructure in the gel is still unbroken. However, the visco-elastic behavior can be inferred due to the decrease in storage modulus with increasing strain and the increase in loss modulus. The increase in phase angle also corroborates this finding.

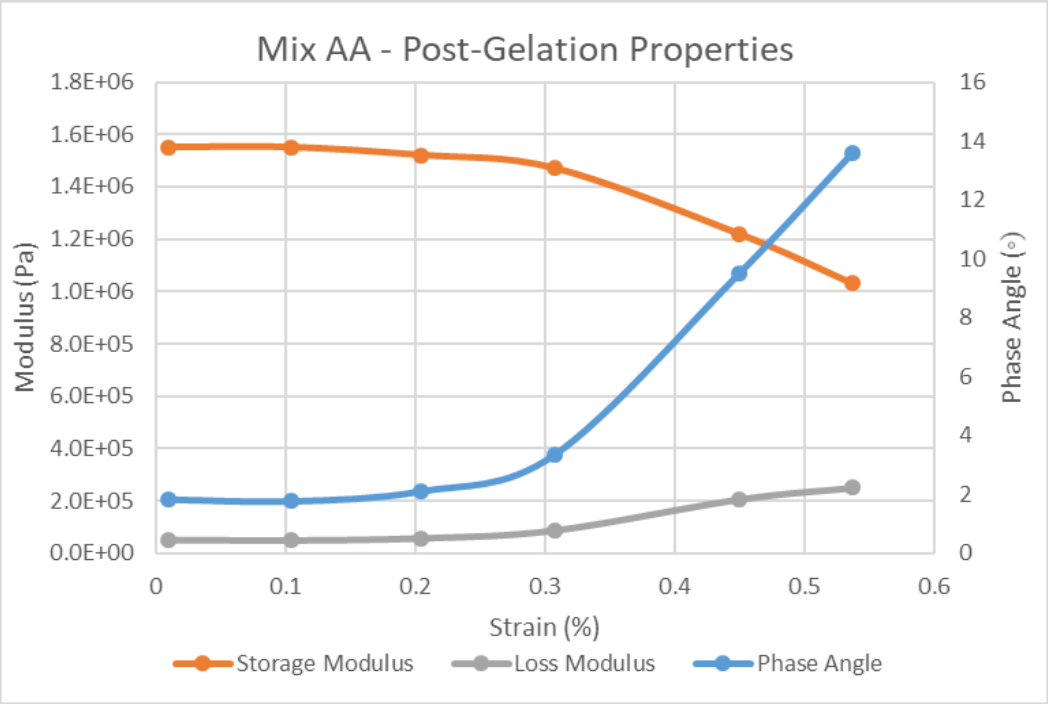

Figure 4-35: Mix AA Post-Gelation Properties

Comparing the results of both Mixes A and AA with and without the hood:

Table 4-3: Results Comparison with and without Hood

Hood	Off		On	
Mix	A	AA	A	AA
Viscosity at High Shear Rate (Pa.s)	0.0047	0.0068	0.0092	0.0234
Gelation Start (min)	40	20	45	15
Storage Modulus (MPa)	1160	1610	1730	1730
Loss Modulus (MPa)	98.4	144	143	179

The following conclusions are drawn:

- Viscosity of both mixes has increased when humidity is controlled, an indication of moisture migration when testing without the hood.
- An increase in both moduli is seen with the introduction of humidity control.
- Gelation start, post-gelation strengths and breakage strains are not altered.
- As seen in all of the moduli-time plots, gelation end is not as clear as in the "Testing without Hood" section, an indication that end of gelation is highly dependent on the humidity condition.

4.2 Syneresis Testing

Syneresis is the contraction of a gel accompanied by the separating out of liquid. A series of experiments were performed on the grouted masses and the grout itself to determine the extent of gel syneresis. Results from the various experiments will be sequentially presented in the sections to follow.

4.2.1 GEL SYNERESIS

At first, we started by testing Mixes A, AA, and C for gel syneresis. After careful preparation of the three mixes, three syringes of 60 ml capacity where filled with each sample. Additionally, about 100 ml of each sample was placed in a separate beaker. The idea was that the syringes allowed for volumetric readings of the water extraction process while the beakers were used for mass readings. Readings were taken over a period of about 500 hours when it was determined that volumetric readings are inadequate since the surfaces are not level and the human eye does not allow for the required precision. Additionally, this test also showed that a shear mixer is required when the mixes are set aside ready for permeation, this was due to the large variation in each of the three syringes; there was a one to two minute wait time to precisely fill the syringes to 60 ml, and the results as shown in **Error! Reference source not found.** are very different.

For gel syneresis, the following formula was used to obtain the loss whether by volume or by mass:

$$Syneresis = \frac{Original\ Volume/Mass - Reading\ Volume/Mass}{Original\ Volume/Mass}\ x\ 100$$

Mix A did not set even after 6 days and thus the use of this mix was discontinued.

Mix AA's results are shown below. For this mix, three additional syringes were tested for syneresis in an effort to reduce sample randomness, however it was determined that volumetric readings are ineffective in obtaining the level of precision required.

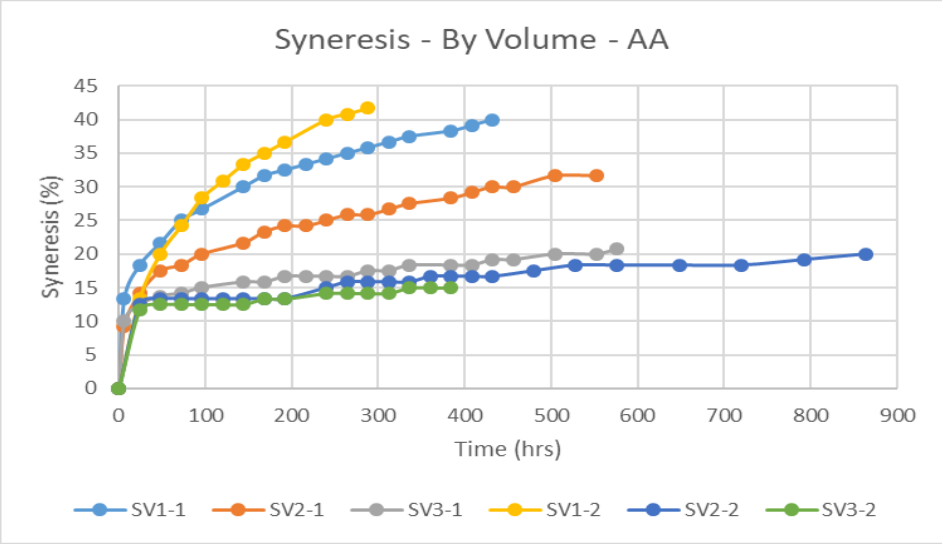

Figure 4-36: Mix AA Series 1 Volumetric Gel Syneresis

Mix C set but was not stable and its use discontinued further.

Results from the weight readings (beakers) are shown below:

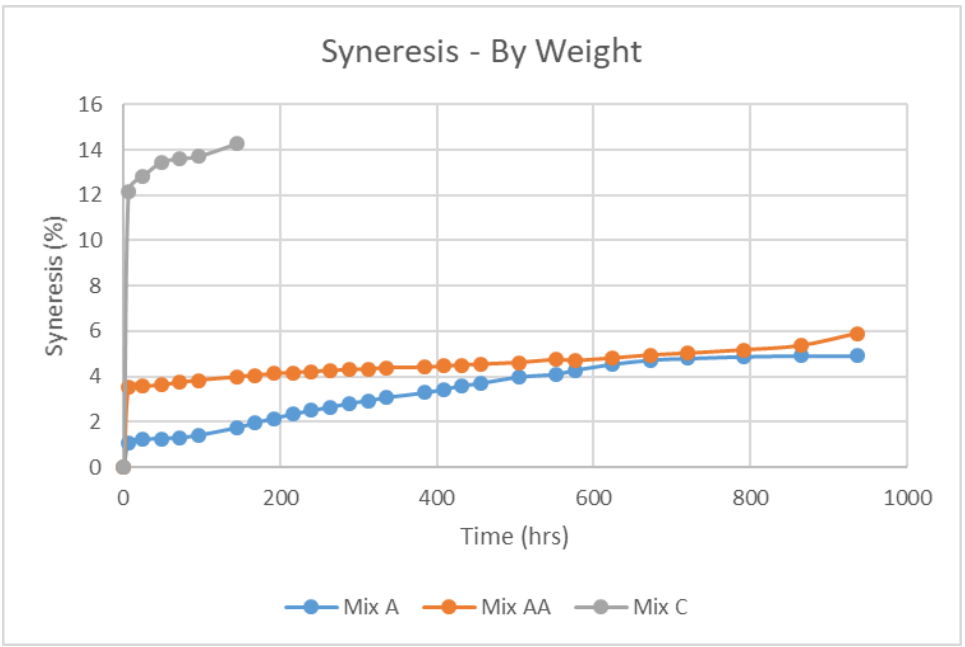

Figure 4-37: Mix A, AA, & C Series 1 Mass Gel Syneresis

As stated before, there is a large variation in the results due to the non-homogeneity of the mix, and the method used to obtain the results. The non-homogeneity problem is solved by constantly mixing the solution to prevent sedimentation. Additionally, the

surface area of grout in direct contact with air seems to dictate the results. This phenomenon will be addressed in a subsequent section.

The figure below shows the setup after 1 hour:

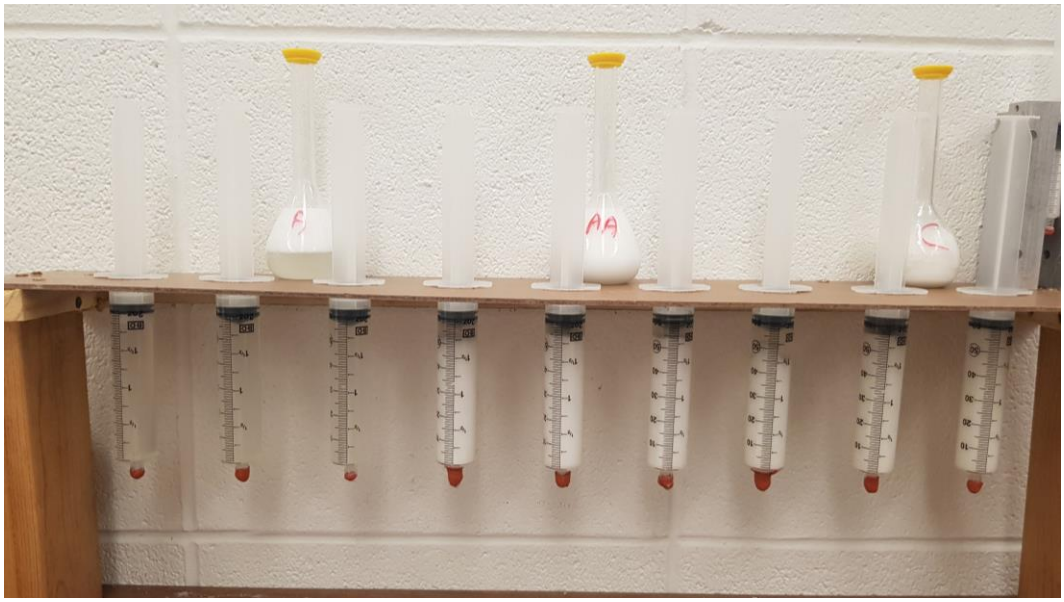

Figure 4-38: Gel Syneresis Series 1 Setup after 1 hour

The figure below shows the setup after 24 hours:

Figure 4-39: Gel Syneresis Series 1 Setup after 24 hours

The figure below shows the setup after 72 hours:

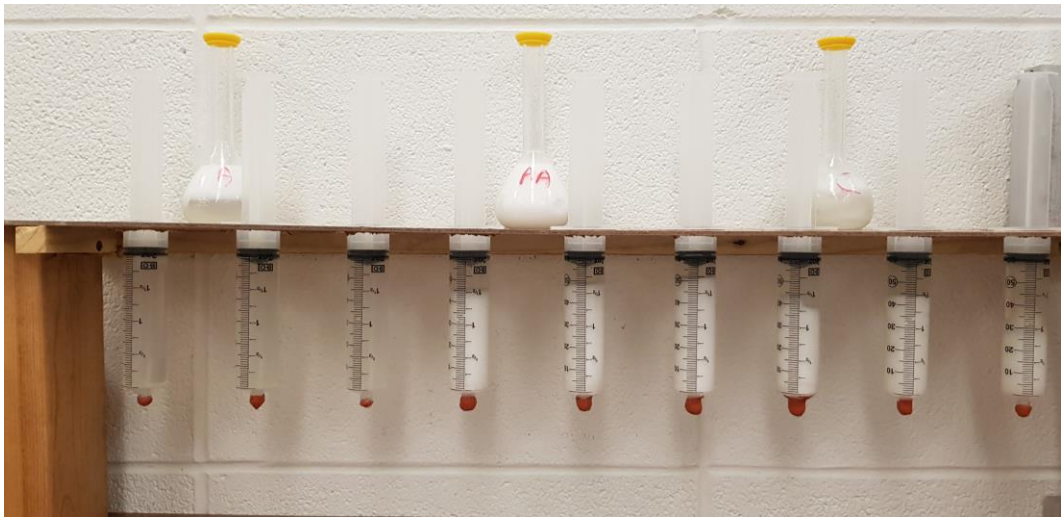

Figure 4-40: Gel Syneresis Series 1 Setup after 72 hours

A second series of syneresis tests was conducted; three syringes were prepared from a constantly stirred mix and the gel extracted carefully on day one. A larger beaker was also prepared. The three syringes were filled with Mix AA and a volumetric reading taken on day one, after which the gel was extracted and continuously weighed for 229 days. The results are shown below:

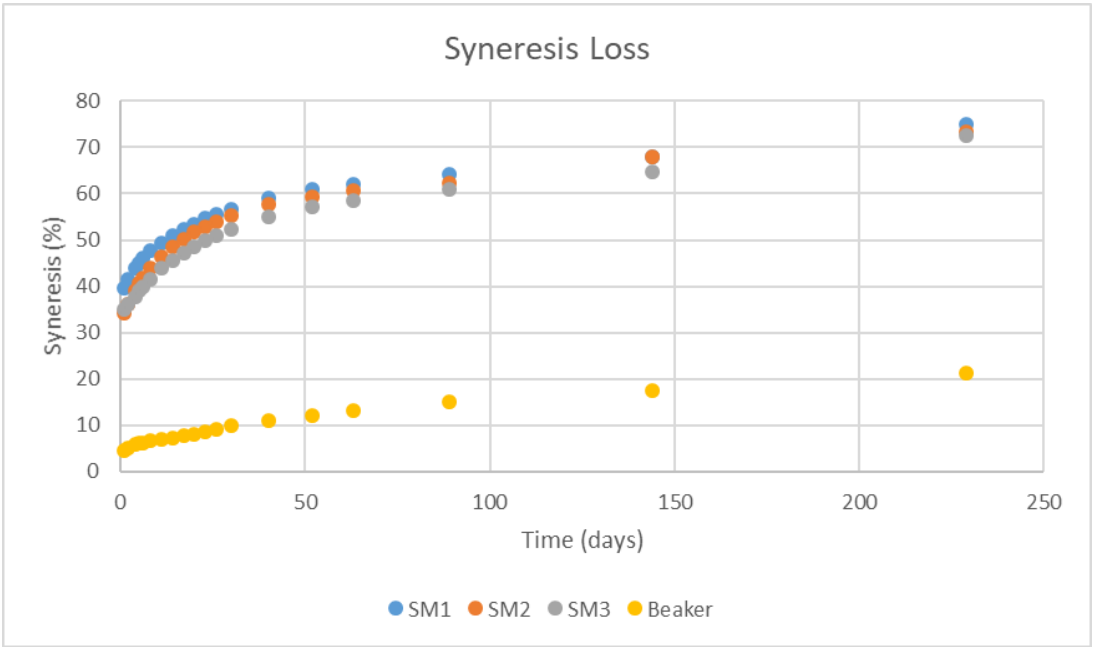

Figure 4-41: Gel Syneresis Series 2 Results

As expected, the variation in the results was greatly reduced, and we can see the difference in the results based on the method of syneresis testing. A change in mass of 35 to 40 percent is expected in the gel itself in the first 24 hours, and this rate decreases with time. A final change in mass of the gel of 70 to 75 percent is expected after about a year, and this finding concurs with the literature. However, if the gel was placed in a beaker, a lower amout of gel syneresis can be expected due to the fact that only a portion of the grout is in contact with the air around it. This in turn validates our hypothesis; surface area is an important parameter in determining the amout of syneresis to be expected. A figure of the setup is shown below:

Figure 4-42: Gel Syneresis Series 2 Setup

4.2.2 SYNERESIS IN GROUTED MASSES

In this section, three samples of different heights were prepared and tested continuously for volume and mass changes. The three samples were prepared as per the guidelines in the "Materials and Methodology" section above; however, an 8-inch sample was prepared and cut into 1, 2, and 4-inch specimens. The 8-inch sample was permeated with the maximum amount of grout it can take before the grout gels (about 7 pore volumes). Samples were then stored air-tight and tested continuously for about 250 days.

Additionally, nine other 6-inch samples were one-point tested at different intervals. All nine of the samples were also permeated with the maximum amount of grout they can take before gelation.

The table below provides a summary:

Table 4-4: Grouted Mass Syneresis Sample Properties

Sample Name	Age at Test
O1	3
O2	3
O3	3
O4	3
O5	3
O6	5
O7	6
O8	14
O9	14
S1	Continuous
S2	Continuous
S3	Continuous

The following plot shows the loss in mass due to water expulsion with time of the different specimens:

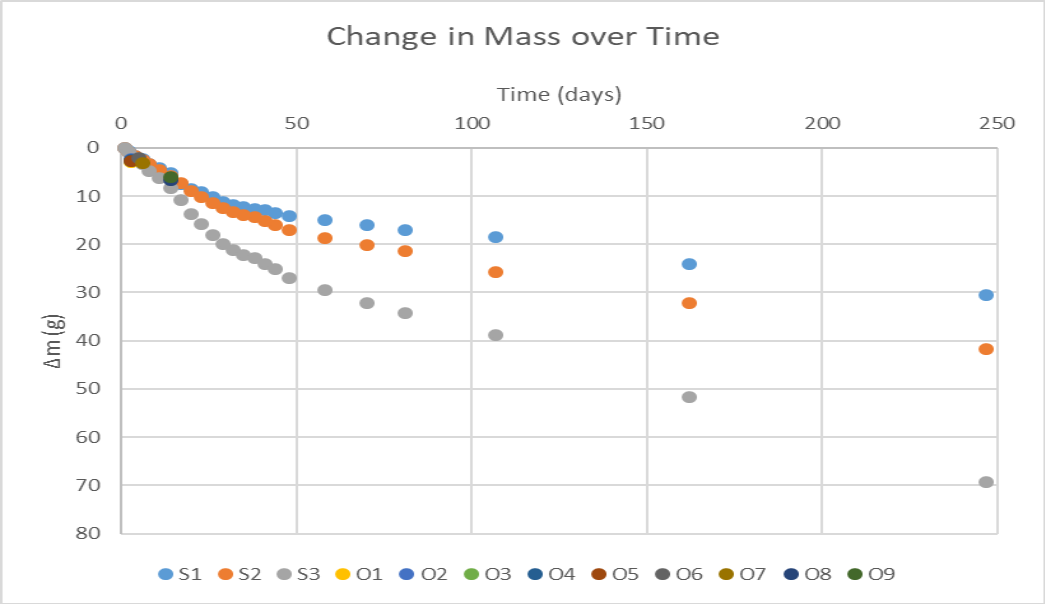

Figure 4-43: Grouted Mass Syneresis Change in Mass with Time

The following plot shows the change in volume of the three continuously monitored specimen over time:

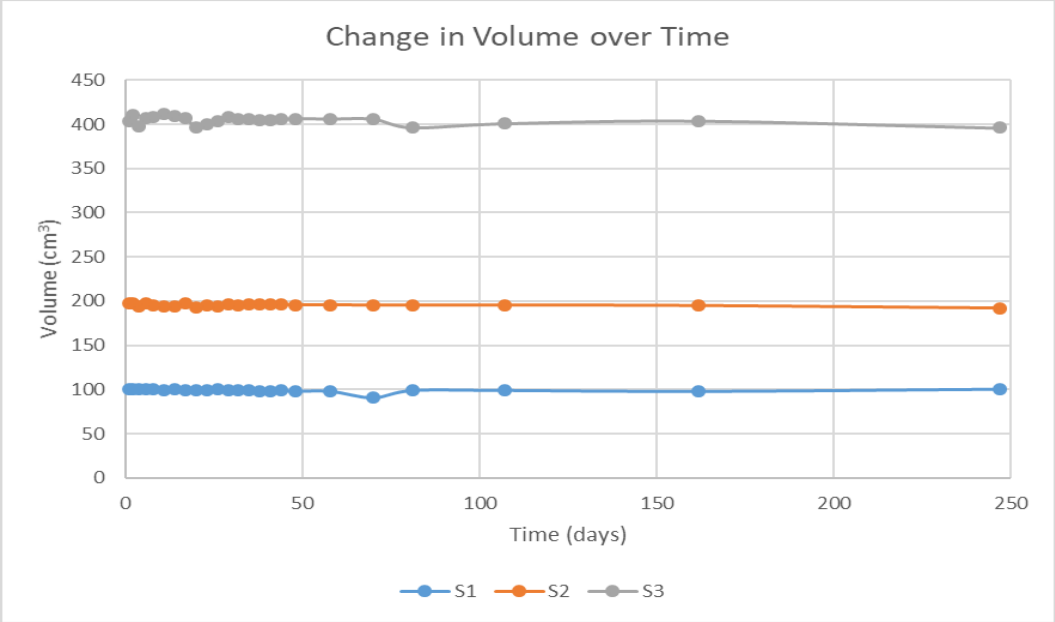

Figure 4-44: Grouted Mass Syneresis Change in Volume with Time

Error! Reference source not found. shows that there is no change in the volume of the s pecimen with the change in mass observed in **Error! Reference source not found.**. This can only mean the grout inside the voids is losing volume by drying, and thus a permeability increase is to be expected. Syneresis however does not change the volume of the grouted mass, the gel shrinks inside the specimen and water is lost internally.

For grouted mass syneresis, the data was normalized to both mass and surface area using the following two formulae, respectively:

$$\frac{\Delta m}{m_0} = \frac{m_{loss}}{m_0}\ x\ 100$$

$$\frac{\Delta \mathrm{m}}{\mathrm{SF}} = \frac{m_{loss}}{\pi dh + \frac{\pi d^2}{2}}$$

The results are shown in **Error! Reference source not found.** and **Error! Reference so urce not found.**, respectively.

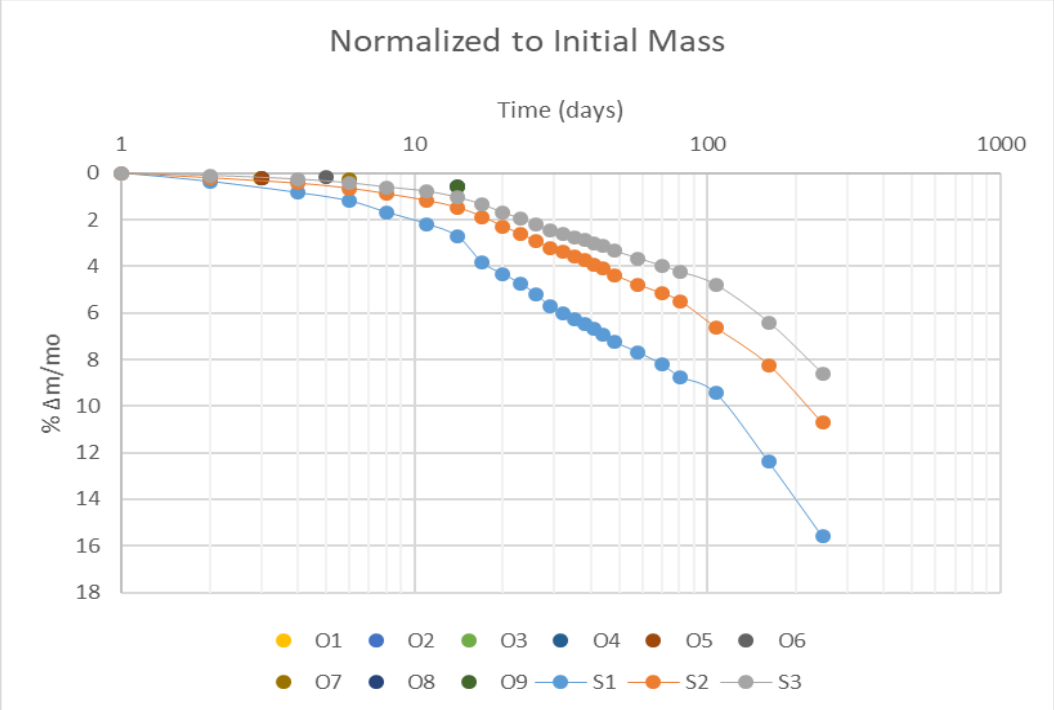

Figure 4-45: Grouted Mass Syneresis Results Normalized to Initial Mass of Specimens

As can be seen in **Error! Reference source not found.**, there is no unique relationship b etween the specimens' original mass and the mass lost. Thus, the syneresis process is not dependent on the mass of the grout itself.

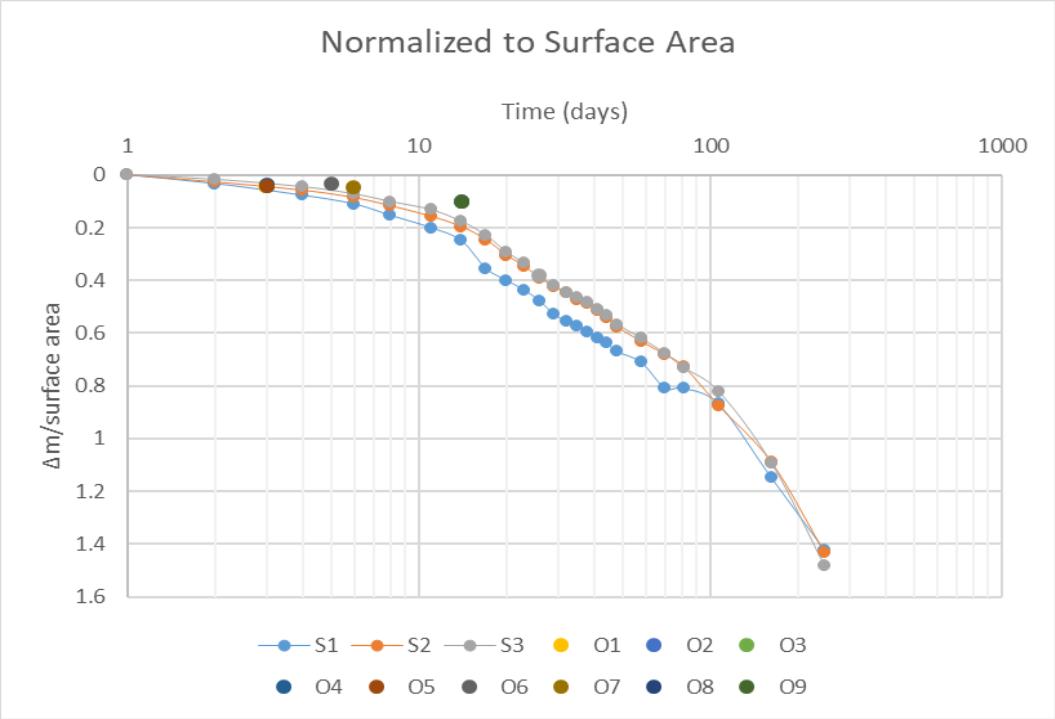

Figure 4-46: Grouted Mass Syneresis Results Normalized to Surface Area of Specimens

However, normalizing the data to the surface area of the specimens, we can see a unique relationship, as shown in **Error! Reference source not found.**. This corroborates our h ypothesis that the gel shrinks based on the contact area with the surrounding air. It is important to note that sample S1 had some problems when a chuck of the sample was lost on day 17 and thus validating the deviation from the curves of the two other samples.

A general syneresis curve is extracted using the data from S2 and S3 and is shown below in **Error! Reference source not found.**.

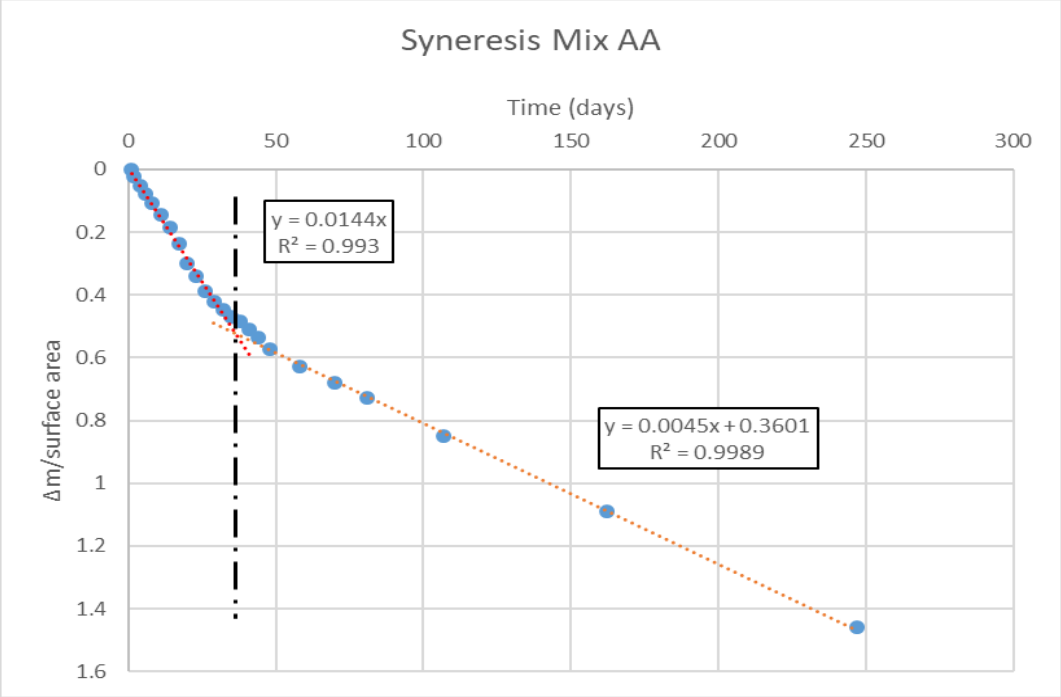

Figure 4-47: Grouted Mass Syneresis Generalized Curve for Mix AA

4.3 Strength of Grouted Masses

In this section, the results from strength testing of two grouts and various setups is shown.

4.3.1 PROOF OF GROUT SEDIMENTATION

The series of experiments were conducted to understand the extent of grout flow by gravity when the permeation phase ends before grout gelation. Two identical samples of one-foot were prepared as per the guidelines listed in the "Materials and Methodology" section. One pore volume of grout mix AA was permeated through both samples. It is also important to note that calculated sample pore volumes were comparable. The only difference between the two samples is the fact that one was stored vertically and the other horizontally. Both samples were extracted after one day and the results are shown below. Sample properties are shown in the table below:

Table 4-5: 12-inch Sample Properties

Parameter	Unit	Vertical Storage	Horizontal Storage
Void Ratio	-	0.69	0.67
Unit Weight	pcf	98	99
Relative Density	%	26.6	32.6
Volume of Voids	cm^3	519	511

For the vertically stored sample:

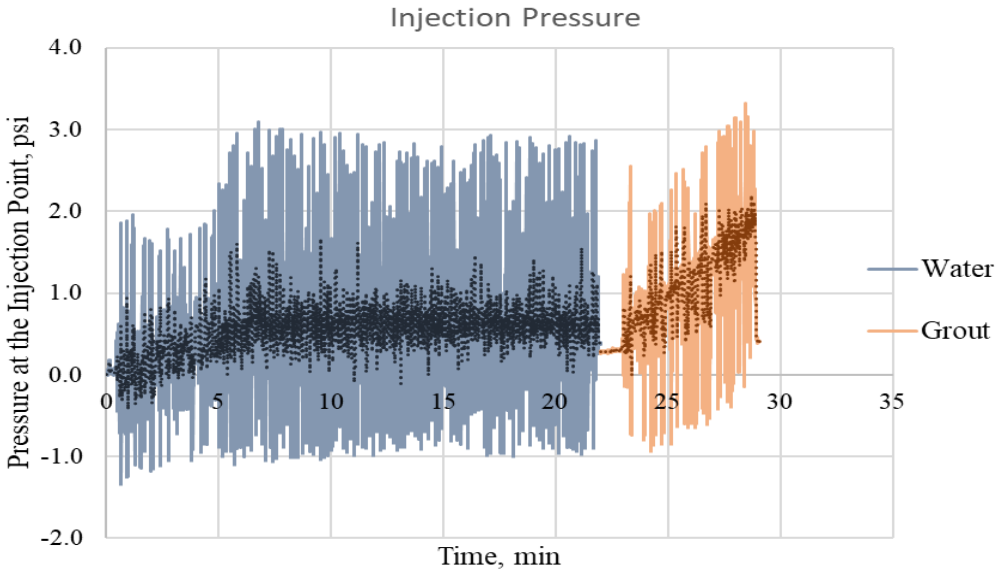

Figure 4-48: Vertically Stored 12-inch Sample Permeation Pore Pressure

A peristaltic displacement pump was used; this was the reason for the pulsation-like noise in the injection pressures as seen in **Error! Reference source not found.**Figure 4-48 a bove.

(a) (b)

Figure 4-49: Vertically Stored 12-inch Sample: (a) Setup (b) Sample Ungrouted Top

As seen in the Figure 4-49 (b) above, the grout was not intended to reach the top; 1PV of grout intake is implemented by ensuring the two samples and the bottom filter material only have the grout intake.

(a) (b)

Figure 4-50: Vertically Stored 12-inch Sample: (a) Samples Split upon Disassembling Permeation Cell (b) Upper Filter Material with No Grout Confirming One Pore Volume Permeation

The two samples split from each other upon handling in the extraction process indicating the top sample is very weak as seen in Figure 4-50.

.

Figure 4-51: Vertically Stored 12-inch Sample: Upper Sample Crumbles Upon Disassembling Permeation Cell

The top sample was not grouted as seen in Figure 4-51; the grout segregated and settled leaving the top sample almost with no grout. To find the grouted recovery rate, a uniform effort was used to scrape the un-grouted parts of the samples. We are left with:

(a) (b)

Figure 4-52: Vertically Stored 12-inch Sample: (a) Samples After Uniformly Scraping Weakly Grouted Sections (b) Reassembled 12-inch Sample

If reassembled, we can see that there is a distinct division of the grouted material:

Figure 4-53: Vertically Stored 12-inch Sample: Recovered Length

The recovered grouted sample is about 8.3” as shown in Figure 4-53.

For the horizontally stored sample:

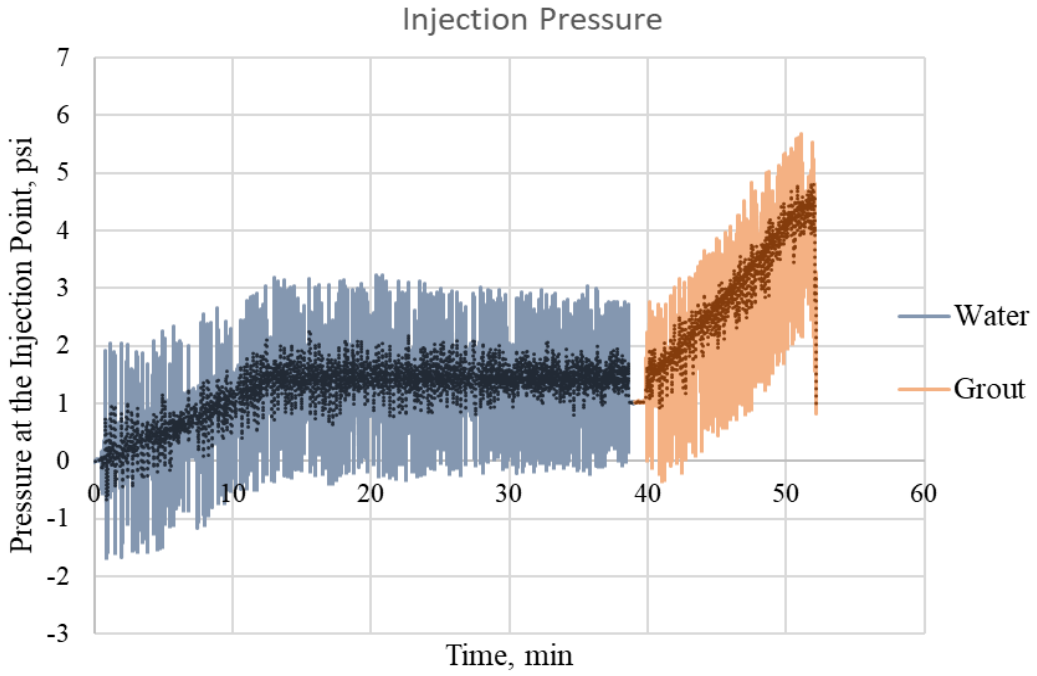

Figure 4-54: Horizontally Stored 12-inch Sample Permeation Pore Pressure

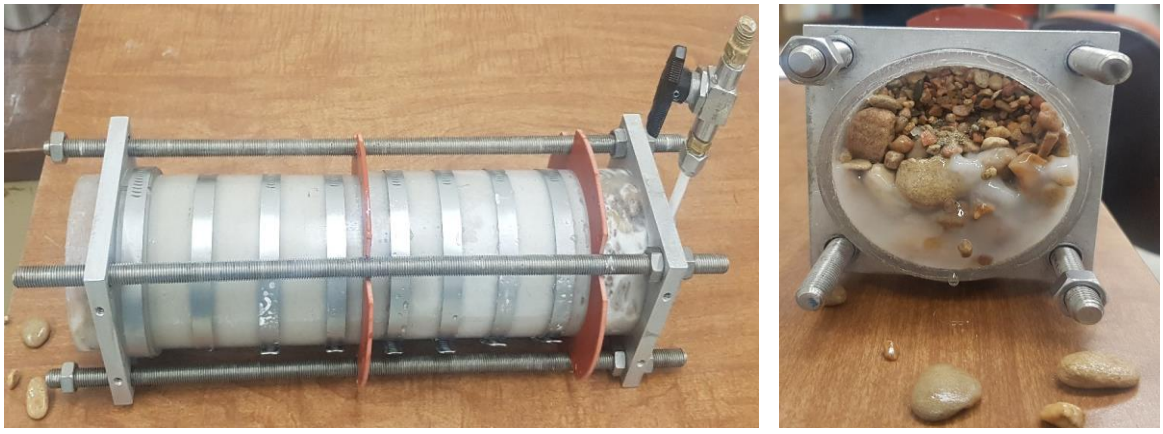

(a) (b)

Figure 4-55: Horizontally Stored 12-inch Sample: (a) Sample Setup (b) Upper Filter Material with Some Grout on the Bottom Showing Sedimentation Effect

It is clearly seen that storing the sample horizontally influenced where the grout settles (Figure 4-55). The grout has reached the top of the specimen, although permeation data indicate that the top 2" was not permeated with grout.

Figure 4-56: Horizontally Stored 12-inch Sample: Sample Crumbles Upon Disassembly

Sample is still weak and breaks upon handling towards extraction as seen in the picture above.

Figure 4-57: Horizontally Stored 12-inch Sample: Top Most Sample Has Little to No Grout on the Top

The part of the sample that was on the topside crumbles upon extraction. Again, the un-grouted parts of the sample are scraped to obtain:

Figure 4-58: Horizontally Stored 12-inch Sample: Recovered Length and Scraped Profile

Recovered sample is about 8.6” as per the figure above. Pocket penetrometer tests are done as an index to the strength profile with length for both samples.

Figure 4-59: Pocket Penetrometer Testing of 12-inch Samples

The results are shown in the figure below:

Figure 4-60: 12-inch Testing Series: Pocket Penetrometer Strength Profile with Height

4.3.2 TWO-FEET STRENGTH TESTING

With this information, a series of 2 ft tests were conducted to understand the strength variability of the mix with radius and orientation. Additionally, delaying the permeation such that the grouting process is stopped at the onset of gelation we believe will eliminate the sedimentation variable and allow us to compare the strength reduction due to sedimentation. The same one-dimensional setup was used; however, the horizontally stored samples are meant to show the extent of grout settling after the permeation has stopped and how this affects the strength of the grouted mass. Seven tests were performed in total, with the variation of three parameters; namely the number of pore volumes permeated through the sample, whether or not to delay this permeation such that permeation is stopped at the onset of gelation, and storage orientation. Table 4-6 below summarizes the testing program:

Table 4-6: 24-inch Testing Series Overview

Sample Name	Number of Permeated Pore Volumes	Delayed Permeation	Storage Orientation
V-1-N	1	No	Vertical
H-1-N	1	No	Horizontal
H-1-NI	1	No	Horizontal
V-1-Y	1	Yes	Vertical
H-1-Y	1	Yes	Horizontal
V-2	2	N/A*	Vertical
H-2	2	N/A	Horizontal

*The time required to permeated 2 volumes is similar to the gelation time.

To clarify, when a 2 ft sample is permeated with one pore volume for instance, the bottom-most 6-inch sample is permeated with 4 pore volumes, the sample above with 3 pore volumes, and as such the topmost sample with 1 pore volume. For the horizontally stored one pore volume permeated sample with delay, we noticed a considerable amount of strength change within the time where the grouting is stopped and the column is tipped over for storage (less than half a minute); and as such, H-1-YI is the sample where truly there is no time for the grout to sediment vertically since we pushed the last pump cycle of grout while the sample is tipped over to become horizontal. The reason for not pumping the grout while the sample is horizontal is the fact that we have one-dimensional flow (volume controlled) and the flow gradient does not depend on whether the grout is permeated horizontally or vertically, unless we stop the pumping and gravity takes its course of action. Additionally, pumping the grout horizontally creates problems of preferential grout flow over the top of the sand and thus messes up the results, since the sand will tend to settle some small amount and create a pipe where the grout will flow easily. The pictures and plots below will show the strength results of the 6-inch samples cut from the 2-ft sample and tested after one day in an unconfined compression test.

The ideal pressure curves shown in the sections to follow are constructed as follows:

$$Q = k\frac{\Delta h}{\Delta l}A$$

The flow rate is controlled by the displacement pump to be 100 mL/min, the length of the specimen is measured, the cross-sectional area of the specimen is measured and dictated by the diameter of the mold, and the change in pressure is read directly from the experimental pressure curves when the specimen is overflowing and the pump is turned off (difference between 1D flow pressure and hydrostatic pressure). The permeability of

the specimen is back calculated, and the intrinsic permeability of the soil computed as follows:

$$K = k\frac{\rho g}{\mu}$$

Given the dynamic viscosity of the fluid and its density, the intrinsic permeability of the media is calculated. Then the conductivity of the media given the new fluid (Grout mix), with different dynamic viscosity and density is calculated and used to calculate the new change in pressure when the grout is permeated. The following equations dictate the calculation process:

$$K_{water} = K_{grout} \Leftrightarrow k_{water}\frac{\rho_{water} g}{\mu_{water}} = k_{grout}\frac{\rho_{grout} g}{\mu_{grout}} \Leftrightarrow k_{grout} = k_{water}\frac{\mu_{grout}\rho_{water}}{\mu_{water}\rho_{grout}}$$

$$k_{water}\frac{\Delta h_{water}}{\Delta l} = k_{grout}\frac{\Delta h_{grout}}{\Delta l} \Leftrightarrow \Delta h_{grout} = \frac{k_{water}}{k_{grout}}\Delta h_{water}$$

Time is related to distance proportionally since the cross-sectional area of the specimen is constant. The following equation is used to relate time to the height permeated:

$$t_{fill} = \frac{Q}{V_v}$$

The flow rate is the constant 100mL/min, and the void ratio is that calculated as in Appendix A. Time required to fill the two gravel layers is directly obtained from the experimental pressure curves.

With all the required parameters now calculated, we assume all the headloss is occurring in the sand (negligible headloss in the gravel layers as compared to that in the sand layer) and construct the curve using the following equation:

$$P_h = \gamma_{fluid} h_{gravel} + \gamma_{fluid} h_{sand} + \Delta h_{sand/fluid} + \gamma_{fluid} h_{gravel}$$

Any deviation from the ideal pressure curves during permeation (an increase in pressure), can only in indicate filtration.

For the vertically stored, one-pore volume permeated sample with no delay:

Table 4-7: 24-inch Testing: V-1-N Sample Properties

Sample Properties V-1-N					
Sample Name	Void Ratio	Relative Density (%)	Number of Pore Volumes Permeated	Unit Weight (psf)	Strength (psi)
S1	0.66	35.98	4.46	125.39	149
S2	0.66	35.98	3.34	128.98	33
S3	0.66	35.98	2.23	127.15	20
S4	0.66	35.98	1.11	Sample Not Recovered	

Figure 4-61: 24-inch Testing: V-1-N Grouted Sample

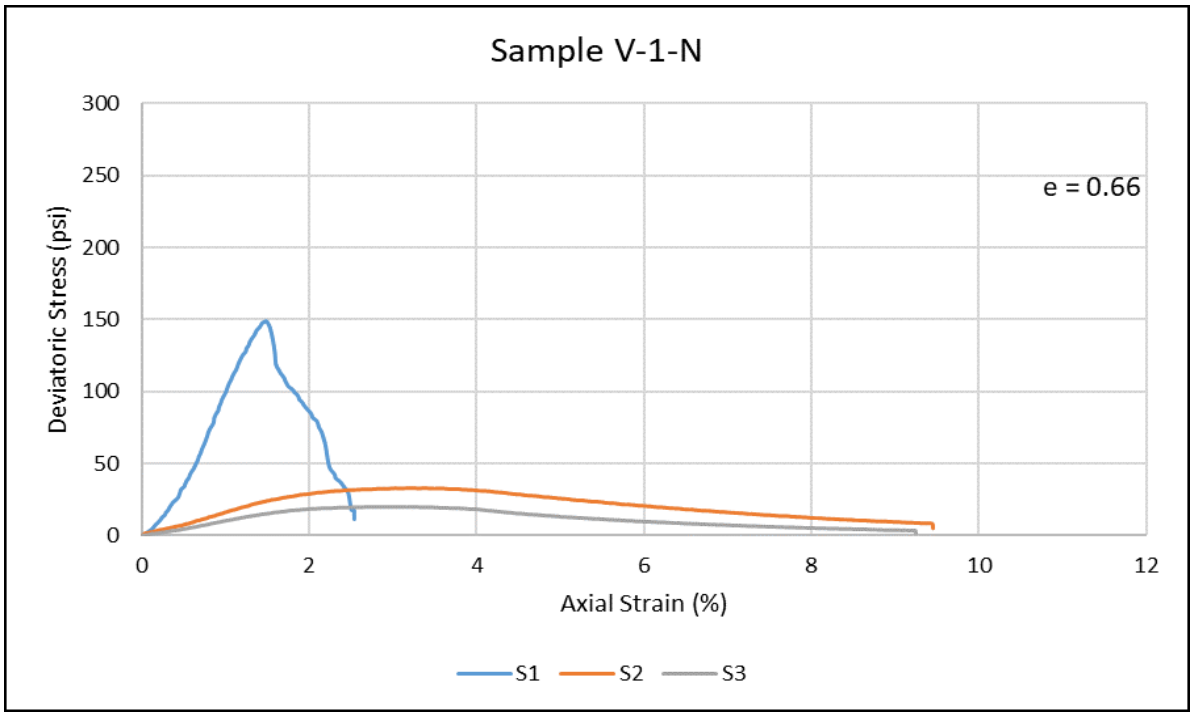

Figure 4-62: 24-inch Testing: V-1-N Strength of Samples

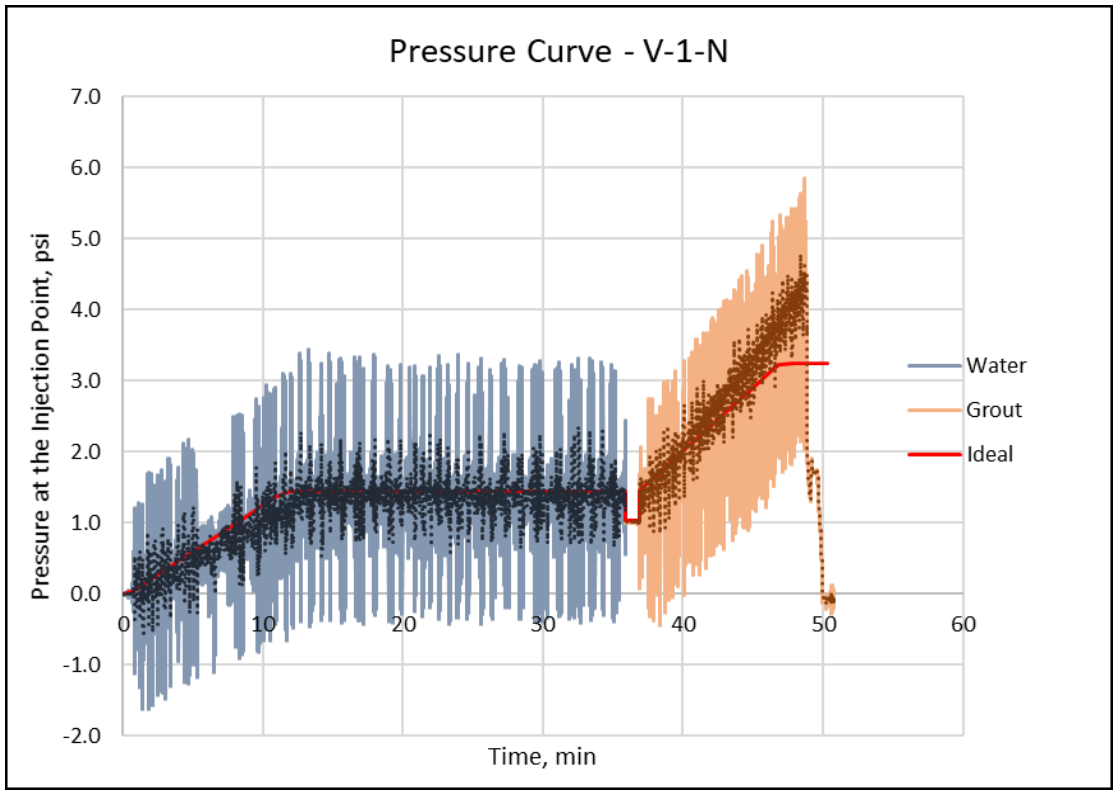

Figure 4-63: 24-inch Testing: V-1-N Injection Pressure Curve

For the horizontally stored, one-pore volume permeated sample with no delay:

Table 4-8: 24-inch Testing: H-1-N Sample Properties

Sample Properties H-1-N					
Sample Name	Void Ratio	Relative Density (%)	Number of Pore Volumes Permeated	Unit Weight (psf)	Strength (psi)
S1	0.66	34.79	4.35	128.35	154
S2	0.66	34.79	3.26	Sample Not Recovered	
S3	0.66	34.79	2.17	Sample Not Recovered	
S4	0.66	34.79	1.09	Sample Not Recovered	

Figure 4-64: 24-inch Testing: H-1-N Grouted Sample

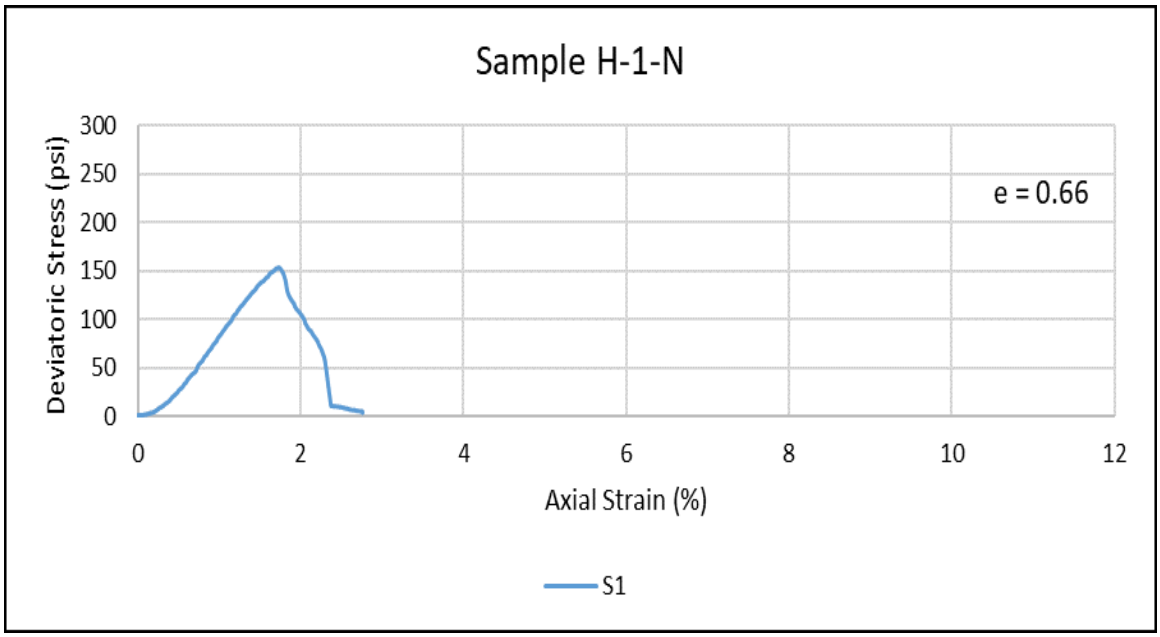

Figure 4-65: 24-inch Testing: H-1-N Strength of Samples

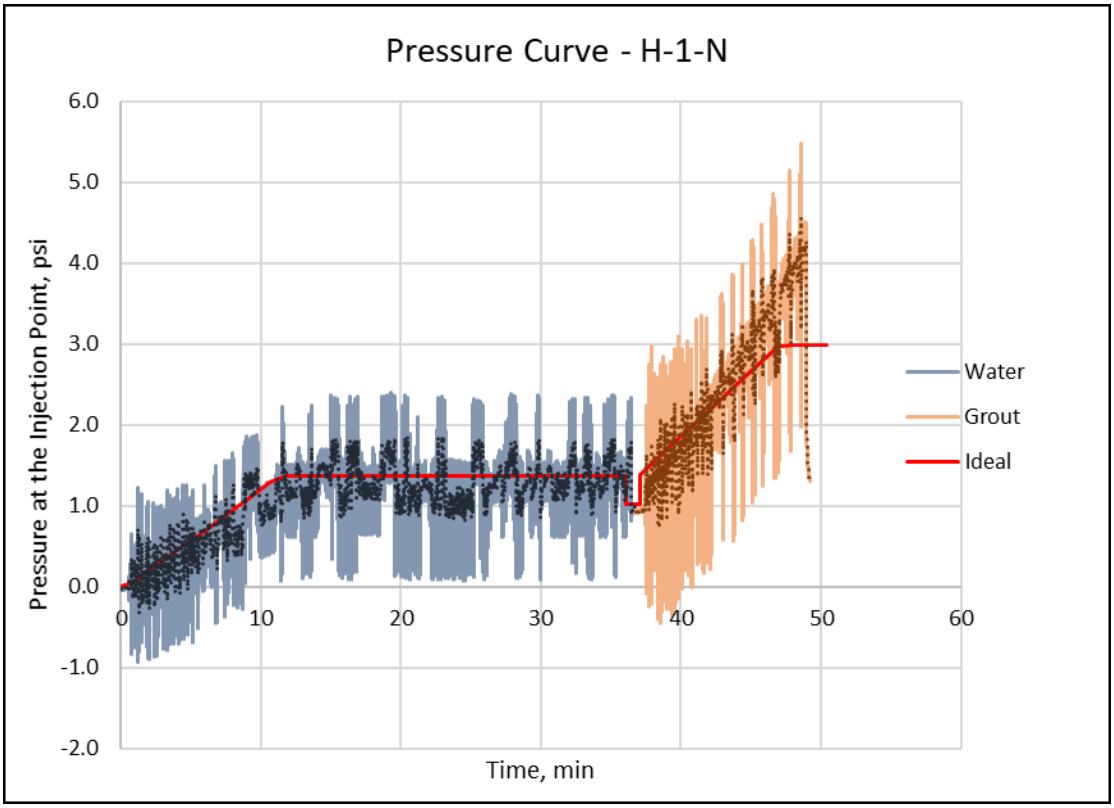

Figure 4-66: 24-inch Testing: H-1-N Injection Pressure Curve

For the immediately horizontally stored, one-pore volume permeated sample with no delay:

Table 4-9:24-inch Testing: H-1-NI Sample Properties

Sample Properties H-1-NI					
Sample Name	Void Ratio	Relative Density (%)	Number of Pore Volumes Permeated	Unit Weight (psf)	Strength (psi)
S1	0.65	34.79	4.59	124.03	150
S2	0.65	34.79	3.44	126.78	32
S3	0.65	34.79	2.29	Sample Not Recovered	
S4	0.65	34.79	1.15	Sample Not Recovered	

Figure 4-67: 24-inch Testing: H-1-NI Grouted Sample

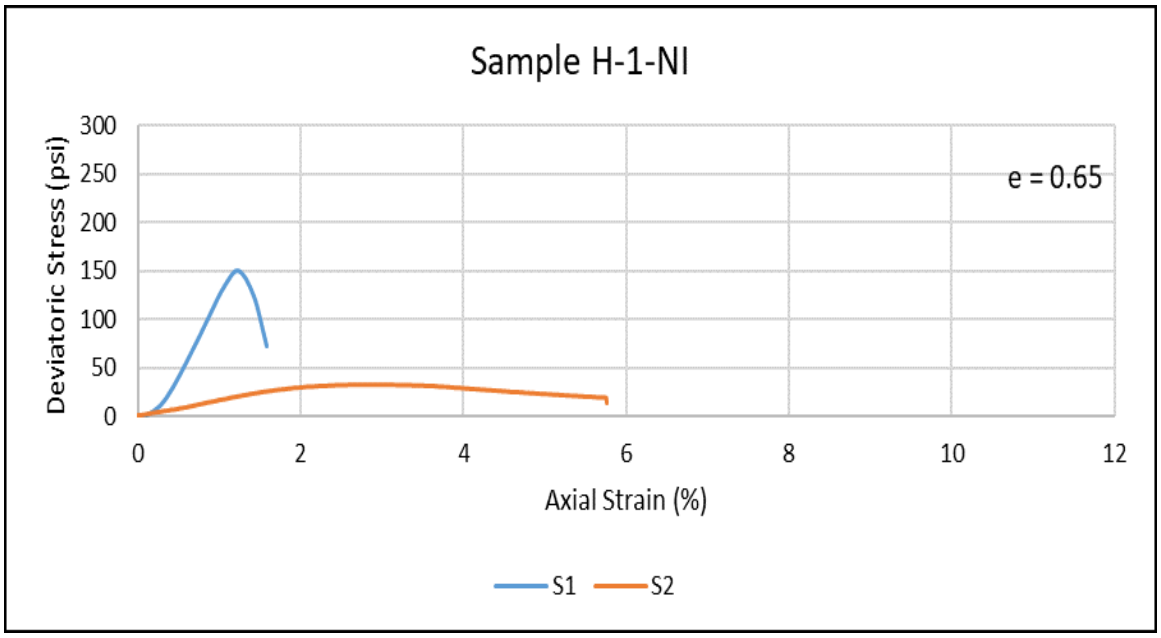

Figure 4-68: 24-inch Testing: H-1-N Strength of Samples

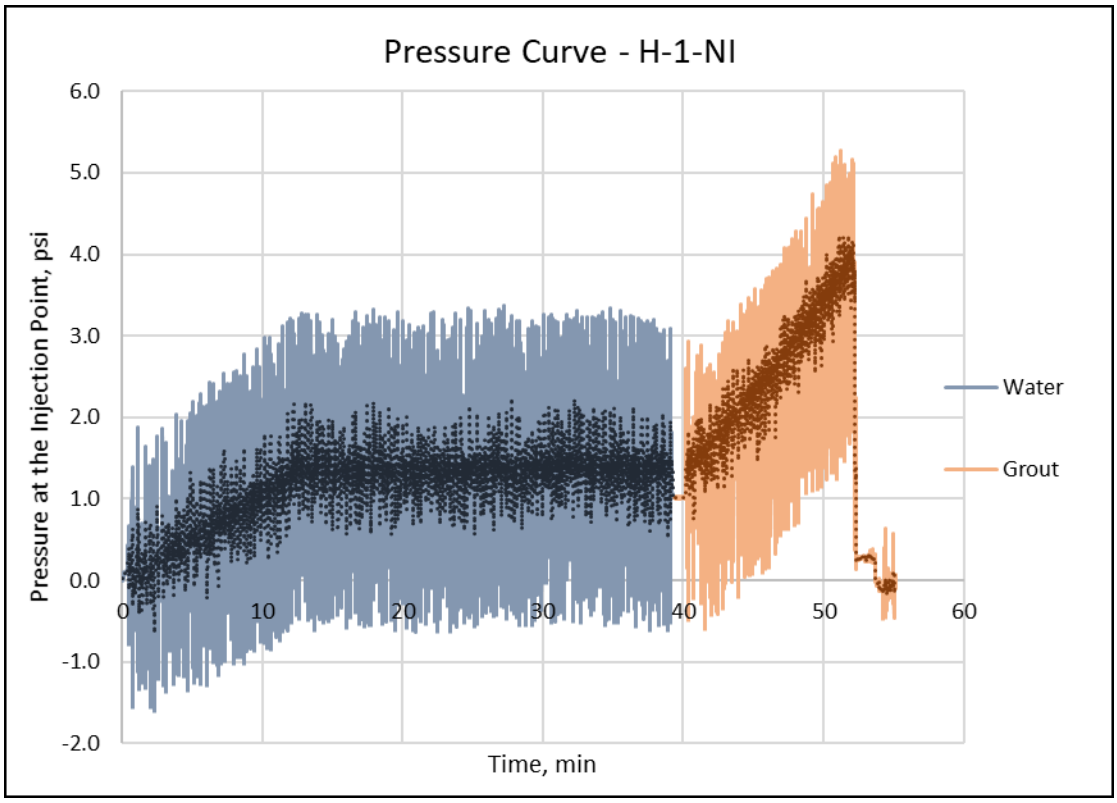

Figure 4-69: 24-inch Testing: H-1-NI Injection Pressure Curve

For the vertically stored, one-pore volume permeated sample with delay:

Table 4-10: 24-inch Testing: V-1-Y Sample Properties

Sample Properties V-1-Y					
Sample Name	Void Ratio	Relative Density (%)	Number of Pore Volumes Permeated	Unit Weight (psf)	Strength (psi)
S1	0.66	36.68	4.22	122.45	247
S2	0.66	36.68	3.17	128.18	53
S3	0.66	36.68	2.11	126.73	45
S4	0.66	36.68	1.06	126.79	34

Figure 4-70: 24-inch Testing: V-1-Y Grouted Sample

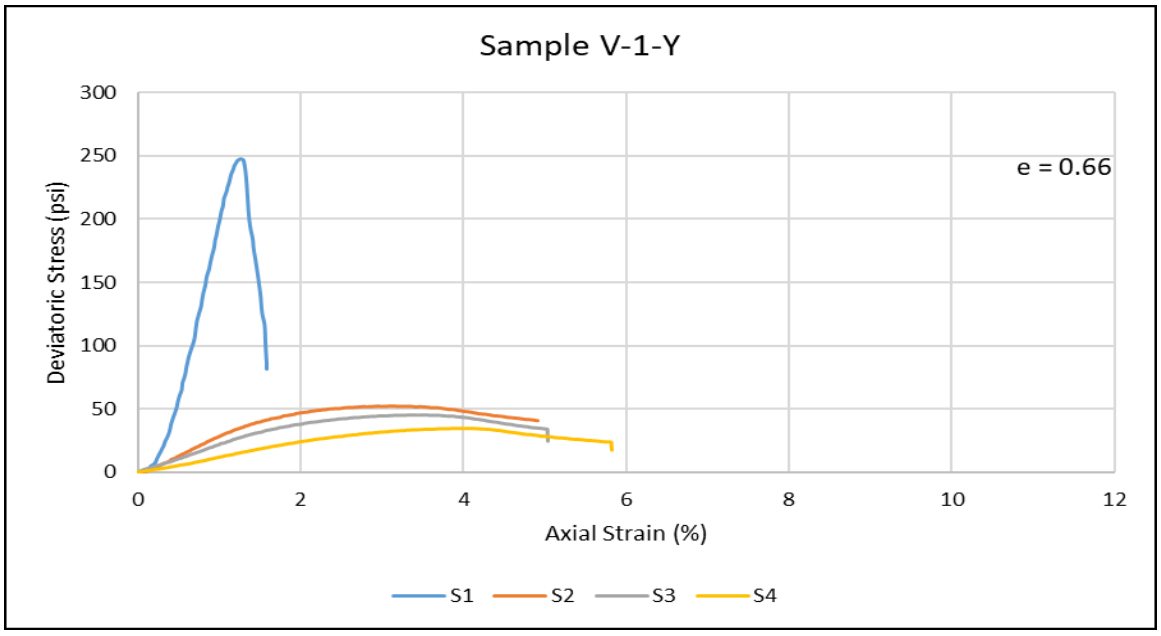

Figure 4-71: 24-inch Testing: V-1-Y Strength of Samples

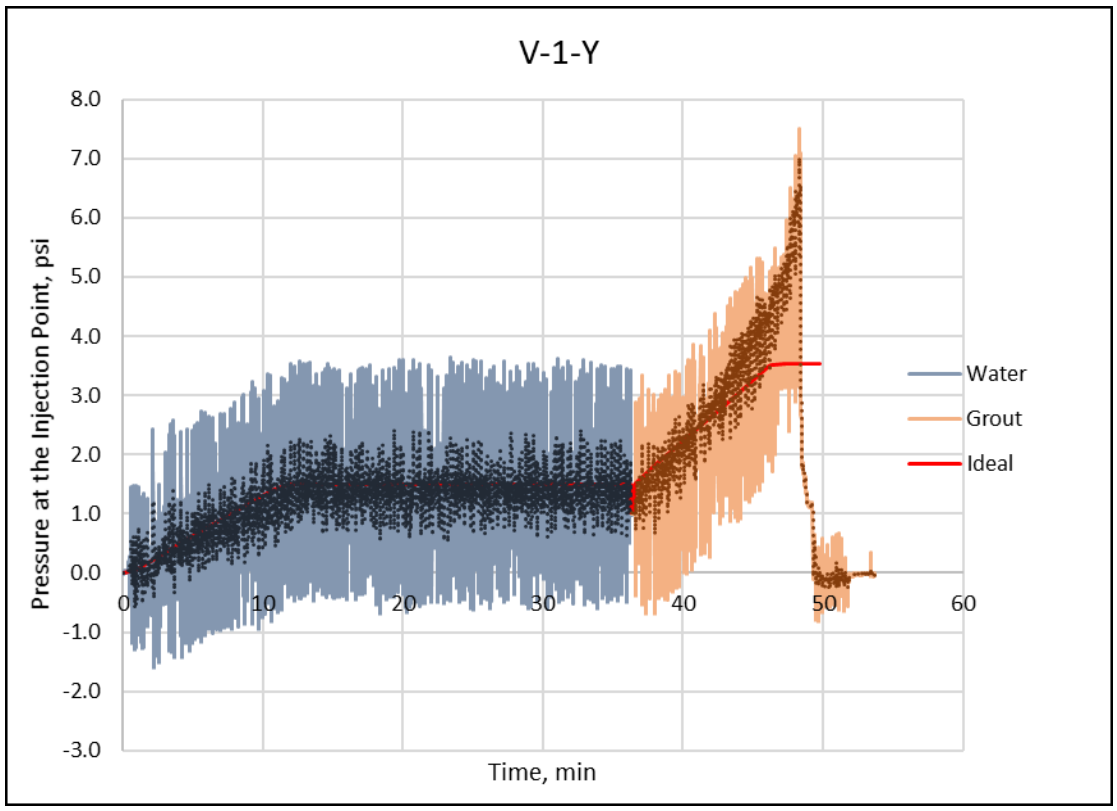

Figure 4-72: 24-inch Testing: V-1-Y Injection Pressure Curve

For the horizontally stored, one-pore volume permeated sample with delay:

Table 4-11: 24-inch Testing: H-1-Y Sample Properties

Sample Properties H-1-Y					
Sample Name	Void Ratio	Relative Density (%)	Number of Pore Volumes Permeated	Unit Weight (psf)	Strength (psi)
S1	0.65	38.11	4.16	126.80	231
S2	0.65	38.11	3.12	128.27	63
S3	0.65	38.11	2.08	128.32	47
S4	0.65	38.11	1.04	Sample Not Recovered	

Figure 4-73: 24-inch Testing: H-1-Y Grouted Sample

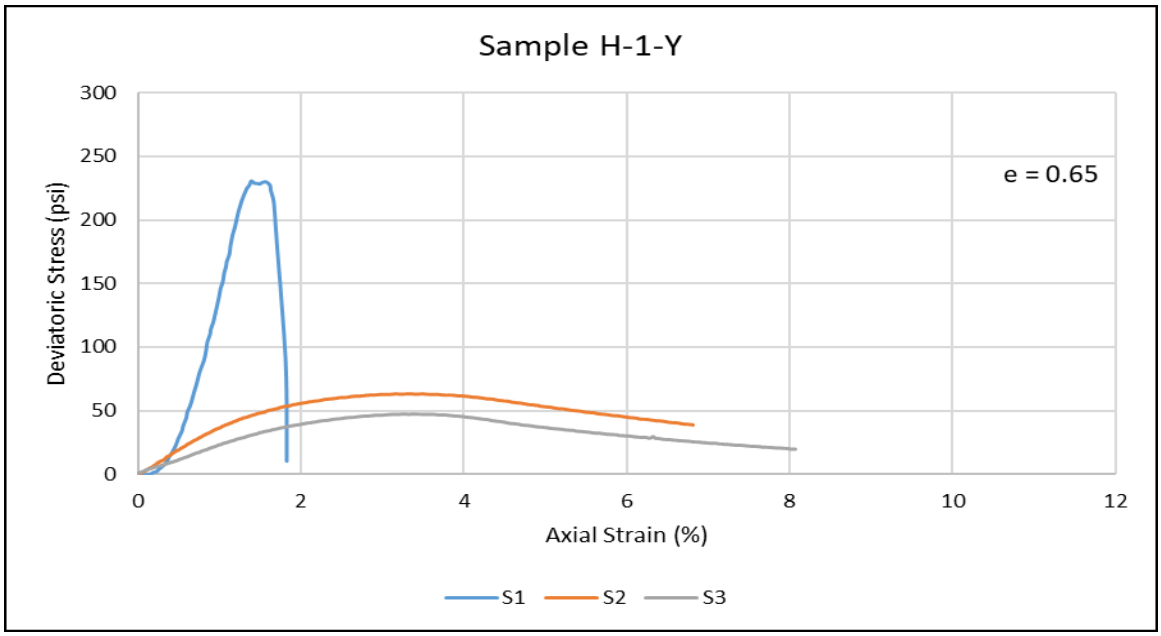

Figure 4-74: 24-inch Testing: H-1-Y Strength of Samples

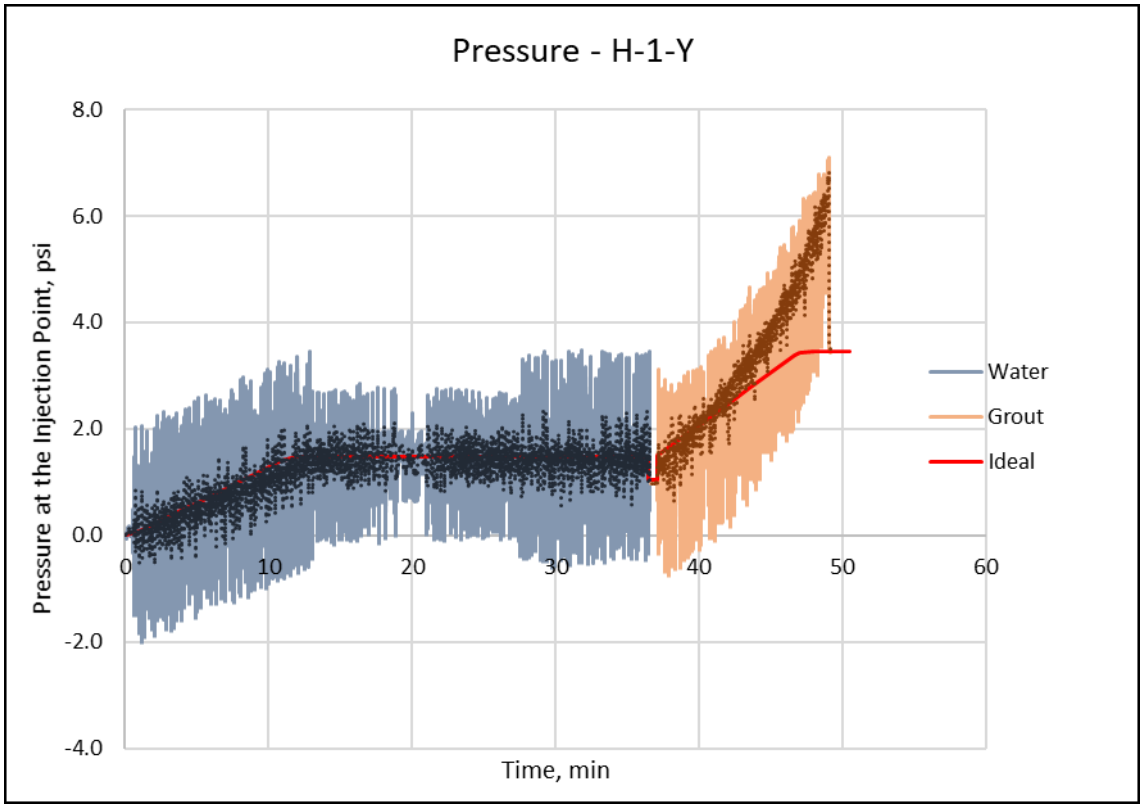

Figure 4-75: 24-inch Testing: H-1-Y Injection Pressure Curve

For the vertically stored, two-pore volume permeated sample:

Table 4-12: 24-inch Testing: V-2 Sample Properties

Sample Properties V-2					
Sample Name	Void Ratio	Relative Density (%)	Number of Pore Volumes Permeated	Unit Weight (psf)	Strength (psi)
S1	0.68	28.32	7.65	125.62	251
S2	0.68	28.32	5.73	126.35	103
S3	0.68	28.32	3.82	126.99	53
S4	0.68	28.32	1.91	125.84	49

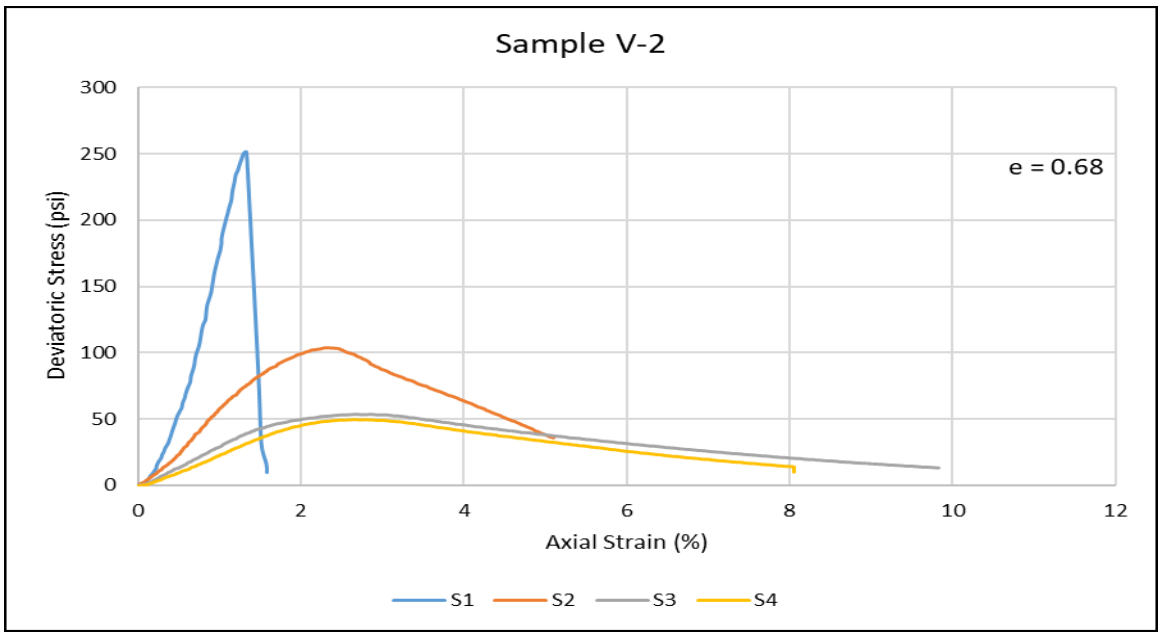

Figure 4-76: 24-inch Testing: V-2 Strength of Samples

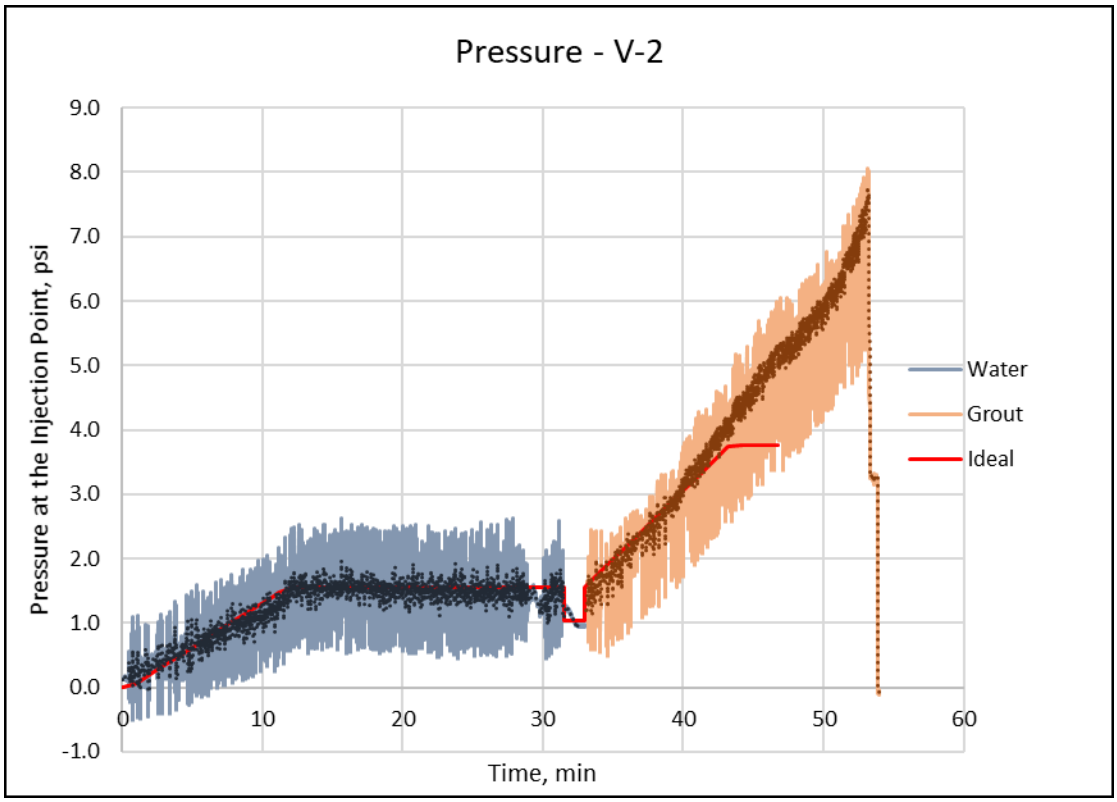

Figure 4-77: 24-inch Testing: V-2 Injection Pressure Curve

For the horizontally stored, two-pore volume permeated sample:

Table 4-13: 24-inch Testing: H-2 Sample Properties

Sample Properties H-2					
Sample Name	Void Ratio	Relative Density (%)	Number of Pore Volumes Permeated	Unit Weight (psf)	Strength (psi)
S1	0.67	33.79	8.04	124.61	244
S2	0.67	33.79	6.03	126.17	132
S3	0.67	33.79	4.02	125.82	49
S4	0.67	33.79	2.01	126.17	43

Figure 4-78: 24-inch Testing: H-2 Grouted Sample

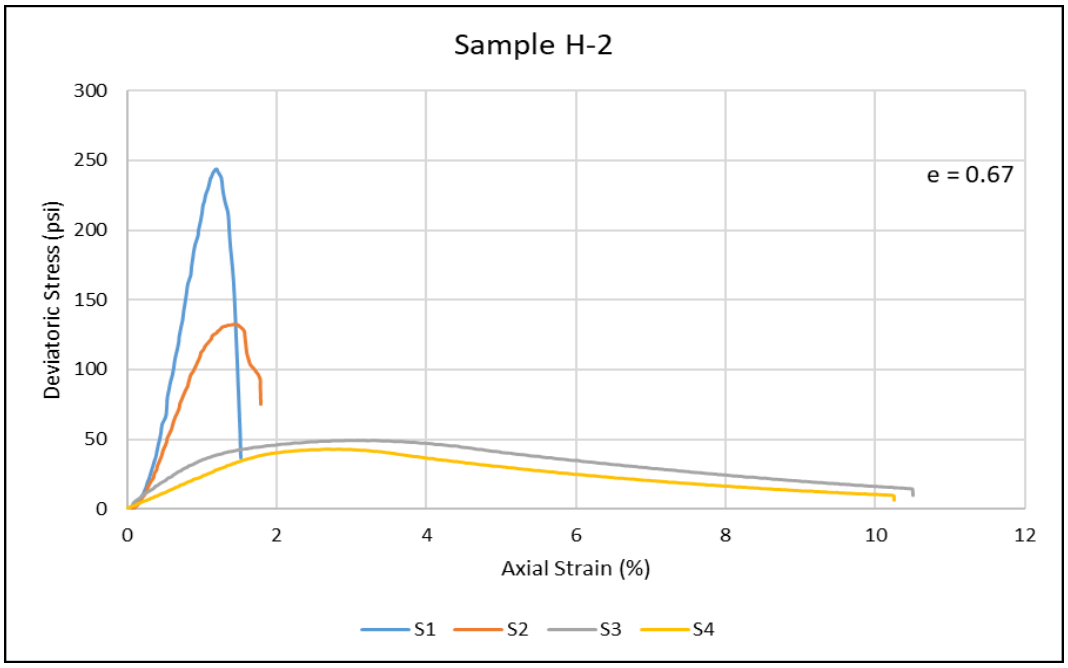

Figure 4-79: 24-inch Testing: H-2 Strength of Samples

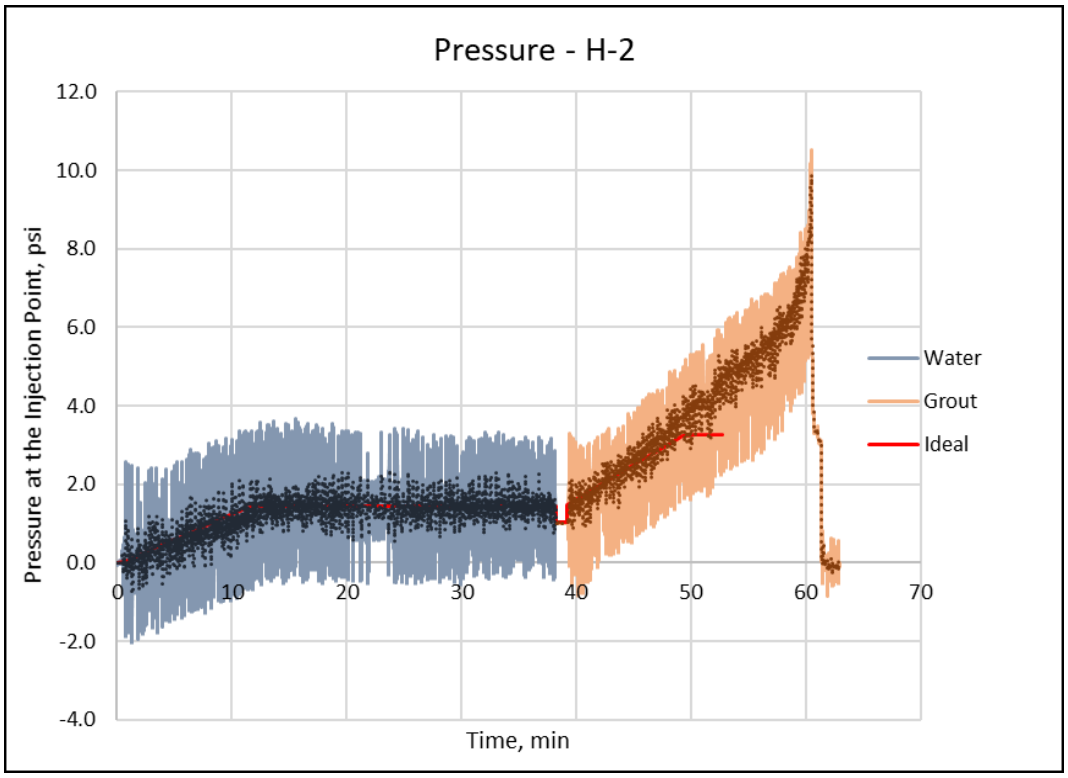

Figure 4-80: 24-inch Testing: H-2 Injection Pressure Curve

The profile of the samples was measured and plotted below for all the horizontally stored samples. H-2 is not shown since we obtained a full column.

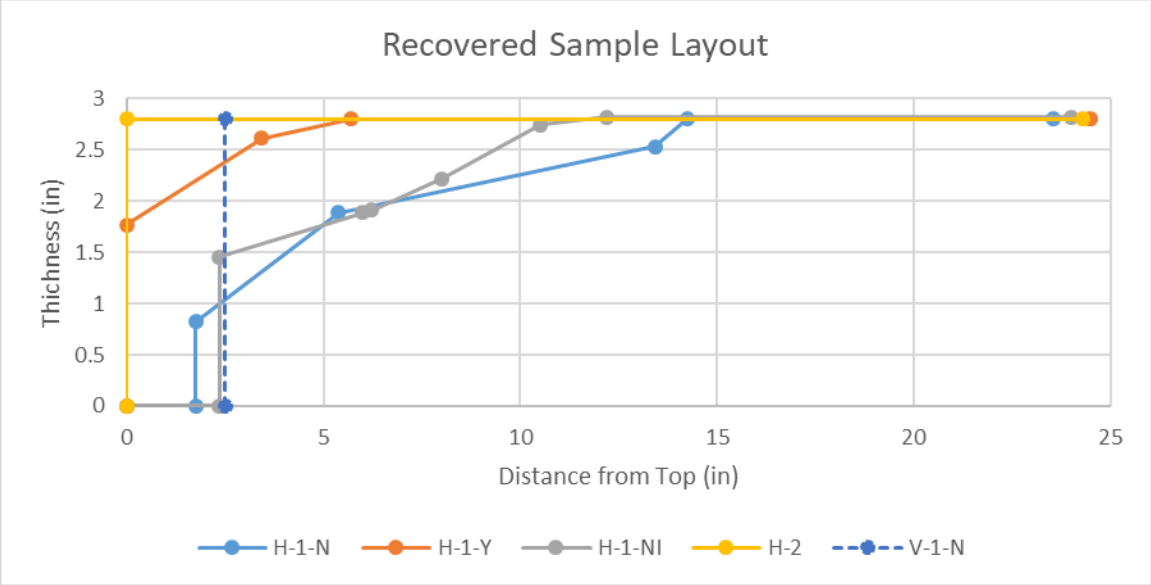

Figure 4-81: 24-inch Testing: Recovered Sample Layout

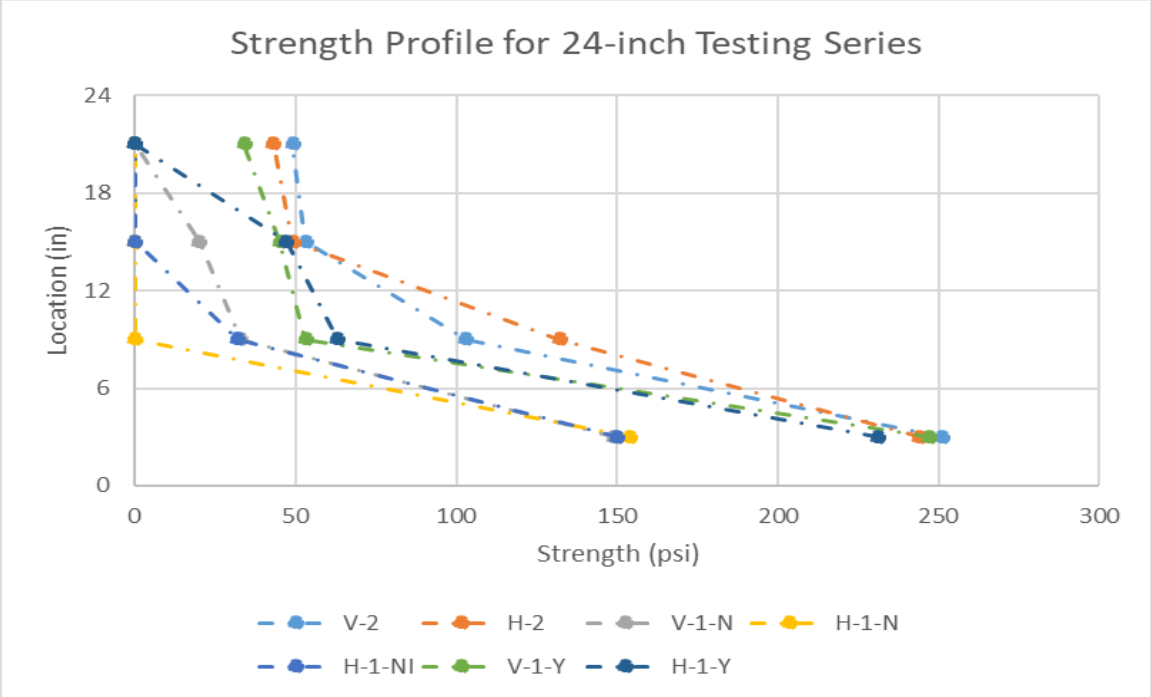

Figure 4-82: 24-inch Testing: Sample Strength Profile

Table 4-14: 24-inch Testing: Results Overview

Sample Name	Description	PV	Delayed	S1 (psi)	S2 (psi)	S3 (psi)	S4 (psi)	Recovered Length (in)
V-2	2PV Vertical Permeation/Vertical Storage	1.91	-	251	103	53	49	24
H-2	2PV Vertical Permeation/Horizontal Storage	2.01	-	244	132	49	43	24
V-1-N	1PV Vertical Permeation/Vertical Storage	1.11	No	149	33	20	NR	21.5
H-1-N	1PV Vertical Permeation/Horizontal Storage	1.09	No	154	NR	NR	NR	22.25
H-1-NI	1PV Vertical Permeation/Horizontal Immediate Storage	1.15	No	150	32	NR	NR	21.65
V-1-Y	1PV Vertical Permeation/Vertical Storage	1.06	Yes	247	53	45	34	24
H-1-Y	1PV Vertical Permeation/Horizontal Storage	1.04	Yes	231	63	47	NR	24

* NR: Sample Not Recovered

4.3.3 SIX-INCH STRENGTH TESTING

The two experiments above showed clearly the dependence of the grouted mass on the delay time. Again, what we mean by delay time is the time between the end of the grouting process and the onset of gelation. We acknowledge that the gelation process is not instantaneous, and that there will be some sedimentation during gelation, therefore a series of 6-inch samples were prepared and tested for strength (Unconfined compression) to understand the extent of its influence. Mix AA was also used in this experiment.

Figure 4-83: 6-inch Testing Series: Water Permeation

Figure 4-84: 6-inch Testing Series: Grout Permeation

Six samples were prepared as identically as possible (loose configuration) and permeated with different pore volumes of grout. The grouting stopped at the onset of gelation.

Sample properties and results are shown below:

Table 4-15: 6-inch Testing Series: Mix AA Delayed Permeation Sample Parameters

PARAMETER	UNIT	D-1	D-2	D-3	D-4	D-5	D-6
PERMEATED PORE VOLUME	#	1.24	2.49	2.86	3.75	5.23	6.44
VOID RATIO	-	0.69	0.70	0.64	0.65	0.65	0.66
RELATIVE DENSITY	%	23.83	21.13	41.53	40.23	39.47	35.01
INITIAL UNIT WEIGHT	pcf	97.70	97.27	100.65	100.42	100.30	99.54
FINAL UNIT WEIGHT	pcf	124.39	124.80	125.86	128.38	121.59	124.85
STRENGTH	psi	164	171	183	198	216	227
MODULUS	ksi	18.00	17.55	20.35	21.16	25.98	26.16

Another six samples were prepared as identically as possible (loose configuration) and permeated with different pore volumes of grout. The grouting started 30 seconds after mixing and stopped when the desired amount of pore volumes was permeated. Sample properties and results are shown below:

Table 4-16: 6-inch Testing Series: Mix AA Immediate Permeation Sample Parameters

PARAMETER	UNIT	I-1	I-2	I-3	I-4	I-5	I-6
PERMEATED PORE VOLUME	#	1.25	2.52	3.22	4.30	5.55	6.44
VOID RATIO	-	0.67	0.69	0.66	0.65	0.66	0.65
RELATIVE DENSITY	%	33.4	26.2	35.9	40.9	36.8	38.6
INITIAL UNIT WEIGHT	pcf	99.3	98.1	99.7	100.5	99.8	100.1
FINAL UNIT WEIGHT	pcf	126.33	125.82	124.09	124.44	121.78	123.31
STRENGTH	psi	5	53	90	146	202	221
MODULUS	ksi	0.27	3.36	6.88	17.56	24.21	21.37

Finally, a sample was prepared and permeated from start to finish (maximum permeation) to be used as the baseline case; the case where the grouted mass has the most strength.

Table 4-17: 6-inch Testing Series: Mix AA Maximum Permeation Sample Parameters

PARAMETER	PERMEATED PORE VOLUME	VOID RATIO	RELATIVE DENSITY	INITIAL UNIT WEIGHT	FINAL UNIT WEIGHT	STRENGTH	MODULUS
UNIT	#	-	%	pcf	pcf	psi	ksi
M	7.27	0.66	35.6	99.6	124.4	228	26.90

Once those results are plotted on a strength-pore volume plot as shown below, we see a direct relationship between both axes and for both permeation setups. The plot is shown below:

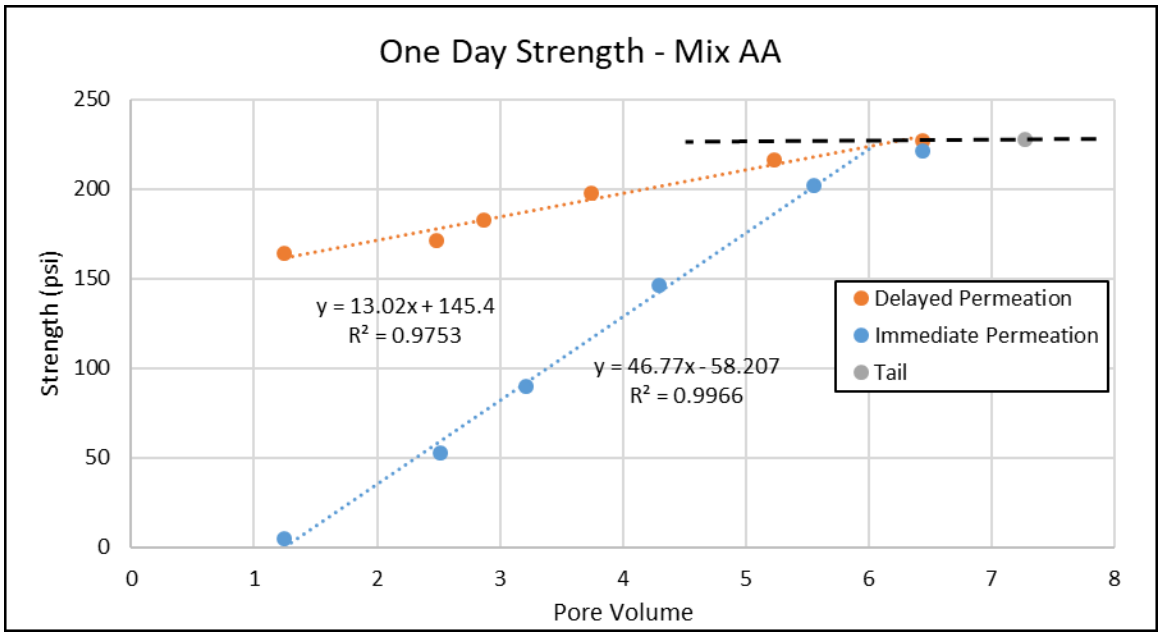

Figure 4-85:6-inch Testing Series: One Day Strength Curves for Mix AA

From the plot above, we conclude the following:

- As the number of pore volumes increases, the strength of the grouted mass increases whether permeated to the onset of gelation or not.
- There is a significant increase in strength of the grouted mass if the permeation is stopped on the onset of gelation, this increase being less effective at higher pore volumes (shorter delay time).
- Even when the sample is permeated to the onset of gelation, we see an increase in strength as the number of pore volumes increases; this may be attributed to filtration (gelation is not instantaneous as seen in the rheology section of this thesis).

Stress strain curves for the samples above are shown below:

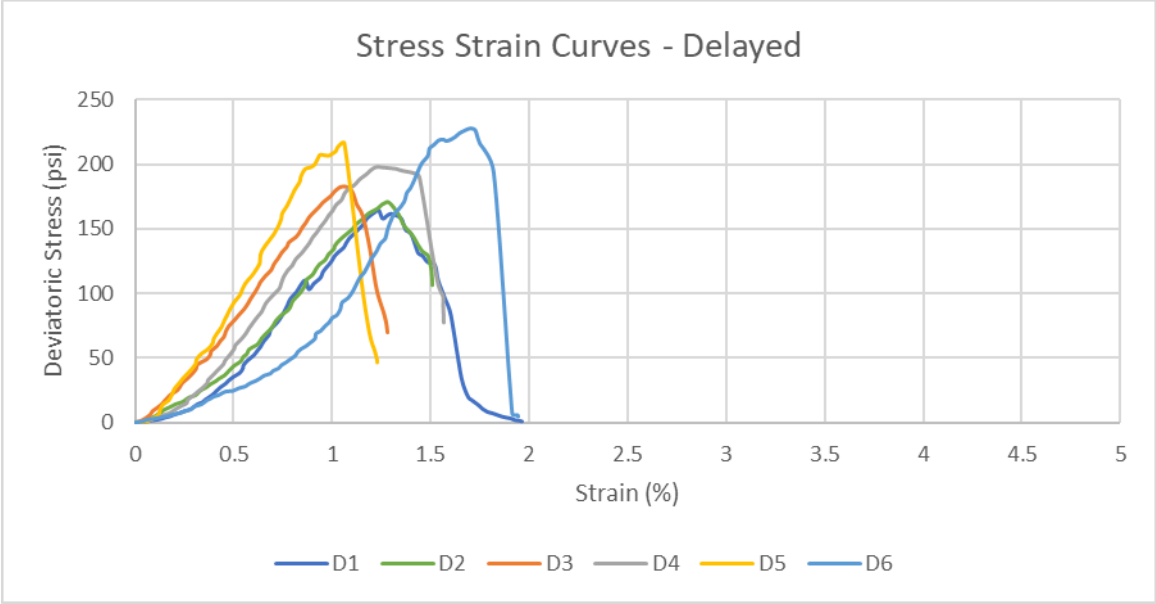

Figure 4-86: 6-inch Testing Series: Mix AA Delayed Permeation Stress Strain Curves

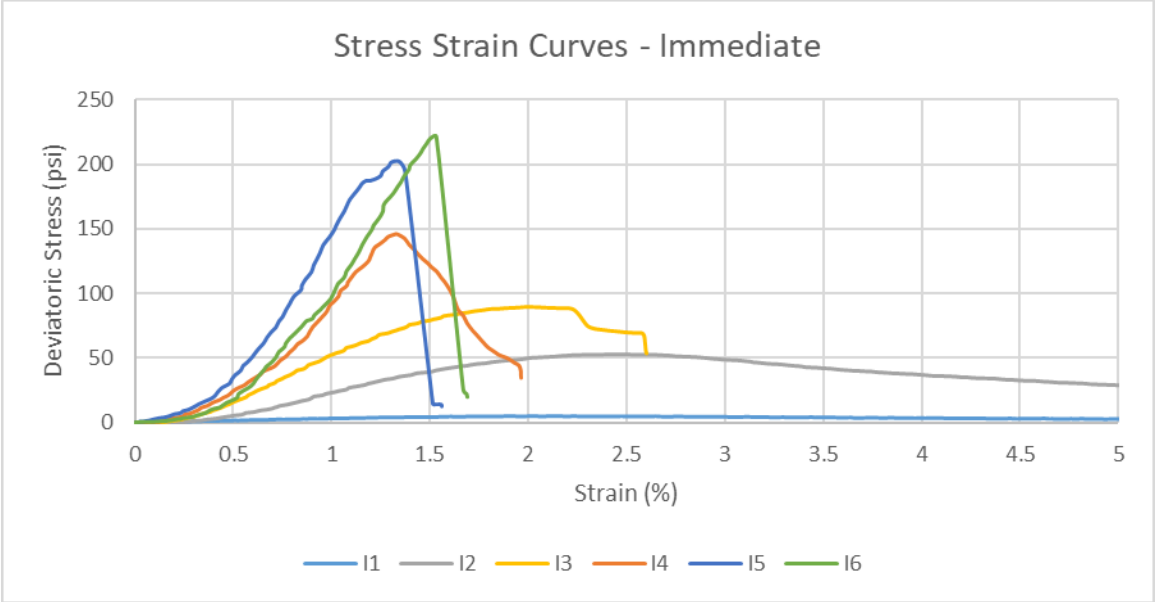

Figure 4-87: 6-inch Testing Series: Mix AA Immediate Permeation Stress Strain Curves

Delayed samples exhibit a much stiffer response than those immediately permeated samples. As the number of permeated pore volumes is higher, immediately permeated

samples exhibit a response similar to the delayed samples (stiffer response), since the time between the stopping the permeation to the onset of gelation is decreasing.

It is important to note that all delayed samples exhibit a stiff response as seen in and a vertical crack develops as the samples fail as shown in Figure 4-93 (a). However, immediately permeated samples with low numbers of pore volumes permeated exhibit the bulging failure as shown in Figure 4-92 (b). As the number of pore volumes increases in the immediately permeated samples, the strength of the samples increases, their response is stiffer, and they fail with the vertical crack as in the delay permeated samples.

(a) (b)

Figure 4-88: Sample Failure Mechanisms: (a) Vertical Crack Failure (b) Bulging Failure

Plotting modulus values for all specimen we obtain:

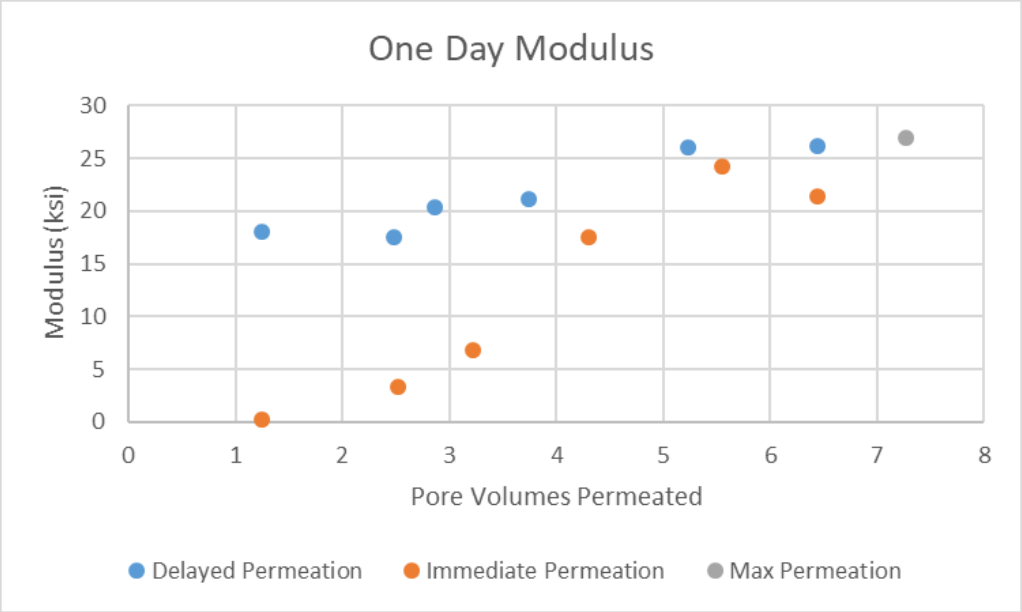

Figure 4-89: 6-inch Testing Series: Mix AA One Day Modulus

In a similar fashion, samples which are permeated after a delay exhibit higher moduli than those immediately permeated.

The same set of tests was performed using mix T1; this mix has lower vinegar concentration and thus a longer gelation time. Four samples were prepared as identically as possible (loose configuration) and permeated with different pore volumes of grout. The grouting stopped at the onset of gelation. Sample properties and results are shown below:

Table 4-18: 6-inch Testing Series: Mix T1 Delayed Permeation Sample Parameters

PARAMETER	UNIT	D-1	D-2	D-3	D-4
PERMEATED PORE VOLUME	#	1.41	2.33	5.02	6.99
VOID RATIO	-	0.63	0.64	0.65	0.70
RELATIVE DENSITY	%	48.0	44.5	39.9	22.9
INITIAL UNIT WEIGHT	pcf	101.8	101.2	100.4	97.6
FINAL UNIT WEIGHT	pcf	119.6	125.0	125.0	122.8
STRENGTH	psf	83	92	153	204
MODULUS	ksi	5.79	6.40	14.25	17.24

Another four samples were prepared as identically as possible (loose configuration) and permeated with different pore volumes of grout. The grouting started 30 seconds after mixing and stopped when the desired amount of pore volumes was permeated. Sample properties and results are shown below:

Table 4-19: 6-inch Testing Series: Mix T1 Immediate Permeation Sample Parameters

PARAMETER	UNIT	I-1	I-2	I-3	I-4
PERMEATED PORE VOLUME	#	1.17	3.10	5.56	7.51
VOID RATIO	-	0.64	0.68	0.64	0.68
RELATIVE DENSITY	%	43.4	29.5	42.8	30.3
INITIAL UNIT WEIGHT	pcf	101.0	98.6	100.9	98.8
FINAL UNIT WEIGHT	pcf	N/A	125.3	123.5	124.4
STRENGTH	psf	0	42	145	187
MODULUS	ksi	0.00	3.62	18.48	20.94

Finally, a sample was prepared and permeated from start to finish (maximum permeation) to be used as the baseline case; the case where the grouted mass has the most strength.

Table 4-20: 6-inch Testing Series: Mix T1 Maximum Permeation Sample Parameters

PARAMETER	PERMEATED PORE VOLUME	VOID RATIO	RELATIVE DENSITY	INITIAL UNIT WEIGHT	FINAL UNIT WEIGHT	STRENGTH	MODULUS
UNIT	#	-	%	pcf	pcf	psf	ksi
M	8.64	0.67	31.24	98.91	122.81	221	22.22

Once those results are plotted on a strength-pore volume plot as shown below, we see a direct relationship between both axes and for both permeation setups. The plot is shown below:

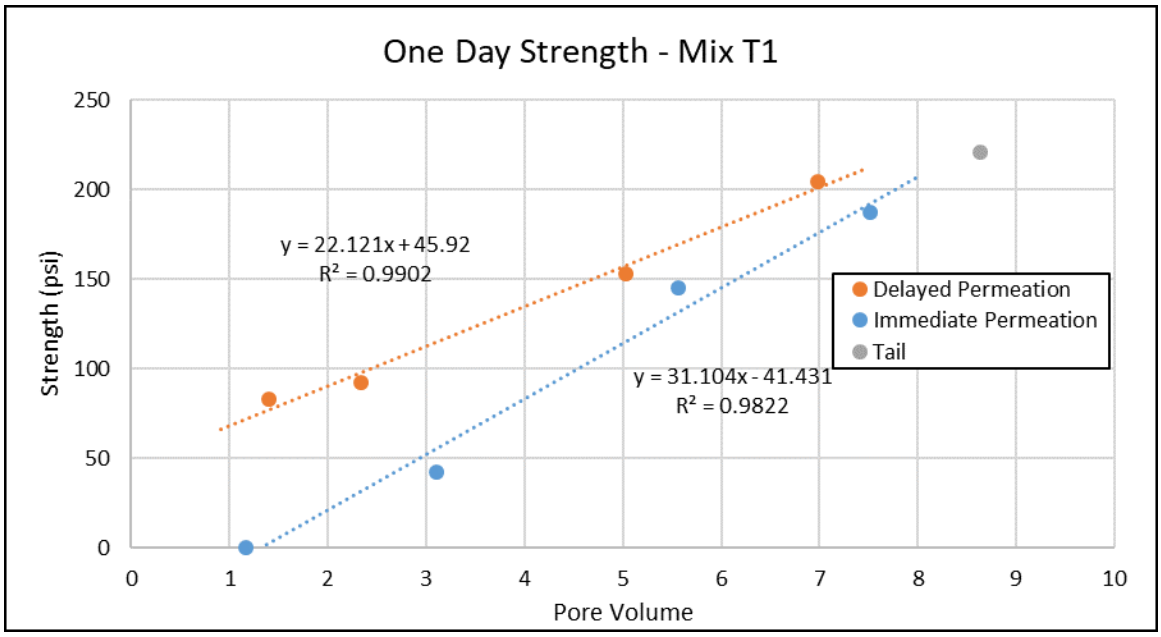

Figure 4-90: 6-inch Testing Series: One Day Strength Curves for Mix T1

From the plot above and comparing it with the results using Mix AA, we conclude the following:

- Both mixes are similar in the sense that there is a difference when the permeation is delayed to the onset of gelation; this difference is pronounced in mix AA, while it is minimal in mix T1.
- Mix T1 yields lower strength samples at low pore volumes in comparison with mix AA, however, maximum pore volume strength is similar to that using mix AA with the sample being slightly stiffer in mix AA.

Stress strain curves for the samples above are shown below:

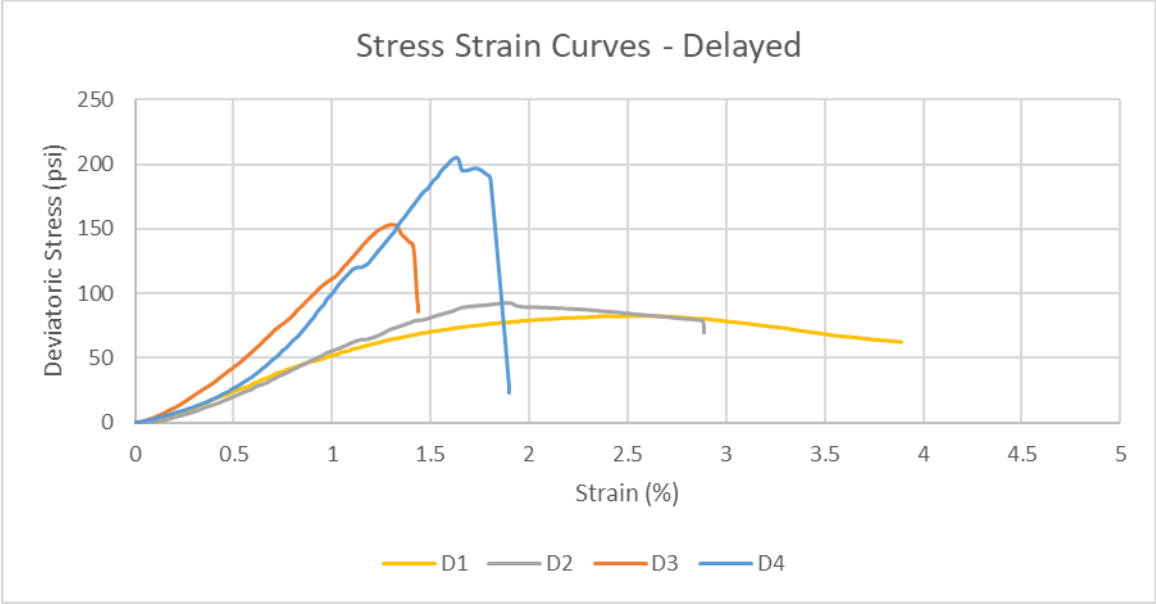

Figure 4-91: 6-inch Testing Series: Mix T1 Delayed Permeation Stress Strain Curves

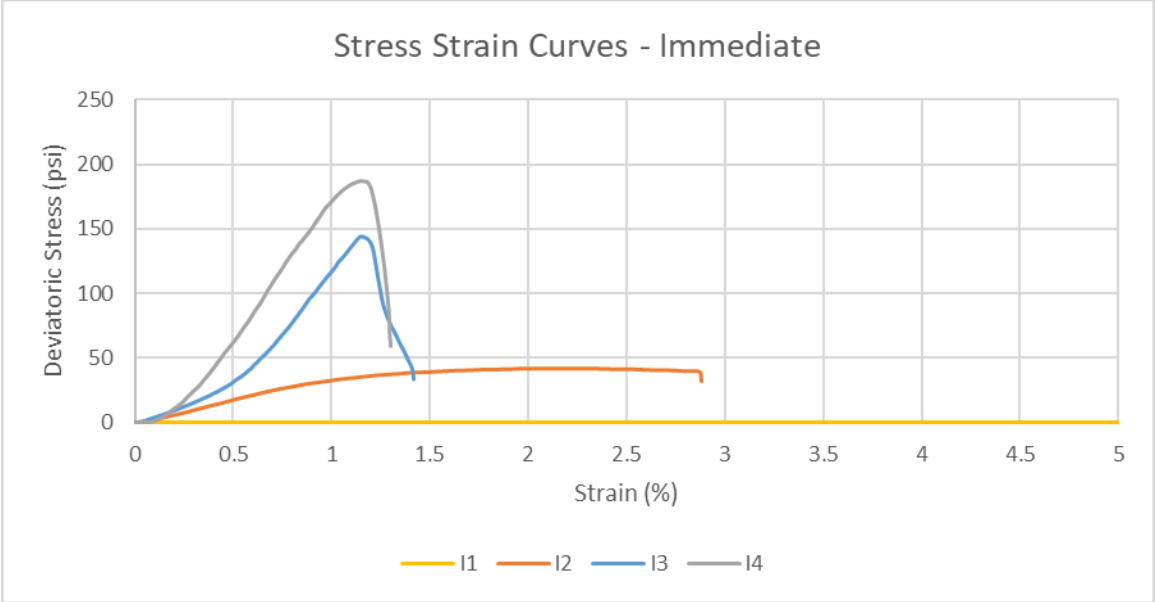

Figure 4-92: 6-inch Testing Series: Mix T1 Immediate Permeation Stress Strain Curves

Delayed samples exhibit a much stiffer response than those immediately permeated samples as seen with Mix AA. However, strengths and moduli of samples permeated with Mix T1 were lower than that exhibited by Mix AA.

Plotting modulus values for all specimen we obtain:

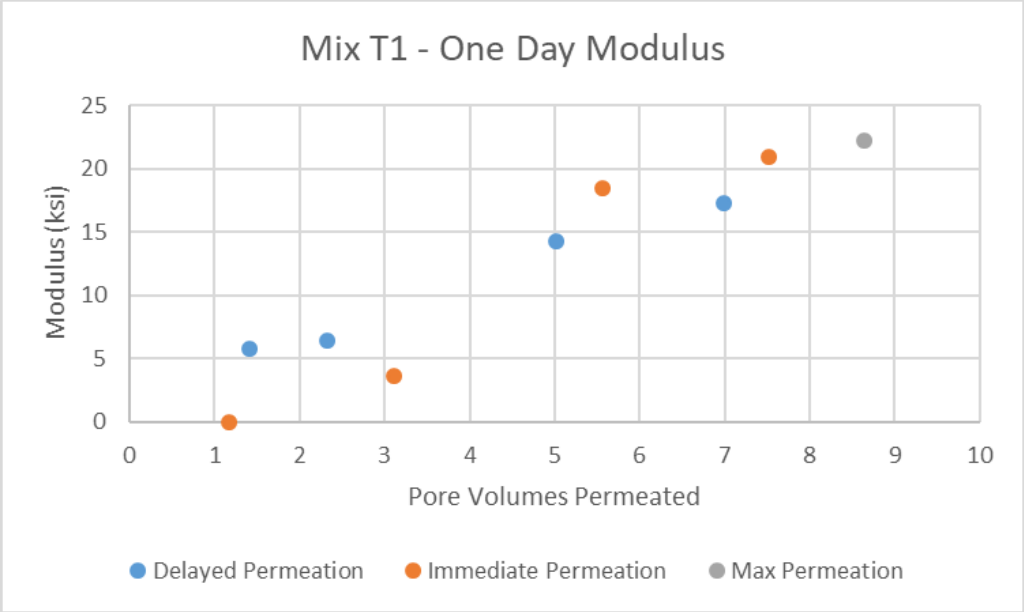

Figure 4-93: 6-inch Testing Series: Mix T1 One Day Modulus

CHAPTER 5. CONCLUSION

5.1 Summary of Performed Work

The field of chemical grouting has had many successes in altering engineering properties of soils over the years. Understanding the extent of improvement and its durability has been the topic of interest since its birth. However, the field is still highly reliant on pilot and laboratory testing due to the complexity and the high variability of its mechanisms.

The aim of this study is to create a grout able to effectively add cohesion to the ground and maintain its integrity with time. Sodium silicate solution precipitated with organic dibasic ester was used along with other components, to meet this target.

Rheological testing was performed on various candidate grouts to eliminate mixes with undesirable qualities. In this process, it was understood that humidity is an important parameter in quantifying grout properties. Mix AA was chosen as the most efficient and economical grout, due to its high strength and stiffness, during and post-gelation, as well as its low viscosity and desirable gelation start time. Testing also showed that the sodium silicate grouts are visco-elastic and have a microstructure, highlighted by the measurement of their complex modulus.

With the rheological data in mind, a series of strength and syneresis tests was initiated, with heavy reliance on Mix AA. After a series of pilot 6-inch, 12-inch, and 24-inch tests, it was quickly understood that components of the grout are settling when permeation times are long, and a shear mixer was introduced to deal with the problem. Mixing the grout thoroughly prior to injection is a very important aspect of the grouting process, in order to ensure uniform and controlled grouted-mass engineering properties. Preliminary testing also confirmed what rheological data about other mixes had concluded, and a new problem arose; grout settling when permeation stopped before the onset of gelation.

Two 12-inch setups were built, one stored vertically and the other horizontally, in order to visualize the sedimentation problem. Results showed that in fact components of the grout were moving throughout the specimen before gelation, and a full scale 24-inch testing series was designed. Pressure curves from preliminary tests as well as the pilot sedimentation test also showed a deviation in injection pressures from the ideal curve. Some sort of filtration; or clogging of some of the pores in the media, was present and was to be quantified. The 24-inch testing series consisted of 7 specimens, designed to show differences in grouted-mass strength due to injection radius, amount of grout injected, and delay in injecting this desired amount. Results indicated a high strength close to injection and a drastic decline in strength with increasing radius. Additionally,

grouted columns that were delay permeated were all recovered, while those immediately permeated lost the topmost first and even second specimens. The sedimentation process was also proved to be on the order of 1-2 minutes, due to the drastic difference in strength profile in the specimen that had the last pump cycle of grout horizontally pushed.

A further series of 6-inch testing was later devised, to characterize the effect of the delay in grout permeation and its effect on the strength of the grouted-mass. Numerous 6-inch specimen were permeated with numerous amounts of pore volumes of grout, with and without a delay in permeation. A linear trend was seen when the strength data was plotted against the number of permeated pore volumes; delayed samples acquired much high strength, with the difference being at its largest at the lowest pore volumes. A second set of 6-inch testing was performed using grout Mix T1 at a later stage; this grout being similar to Mix AA but having a delayed start of gelation. A similar trend was seen as that by Mix AA, and it can be concluded that the specimen acquires higher strength with higher number of pore volumes of grout injected, but delaying injection to finish at the onset of gelation is more effective in terms of acquiring the desired strength properties. It was further noted that about 7 pore volumes of Mix AA were required to obtain a 225 psi strength, and about 9 pore volumes with Mix T1. This result further corroborated and justified our labeling of Mix AA as being the most effective and economical mix devised.

Finally, gel syneresis testing showed that mass measurements are far more accurate than volumetric measurements. Results concluded that gel syneresis is in the order of 70% to 75% at about a year after mixing. These results corroborate results published by various authors throughout the literature. Again, the importance of mixing the grout prior to casting it in the desired form was seen; namely by the failure of obtaining consistent results in the preliminary program of gel syneresis testing. Grouted-mass syneresis testing however showed no change in volume over time as opposed to some of the literature out there, and it was concluded that the loss in mass due to water expulsion is related to the exposed surface area of the specimen rather than to its original mass.

5.2 Recommendations for Future Work

Sodium silicate-based grouts have been used and experimented with over a decade. Much of the work in understanding the mechanics of the process is undergone. However, a whole lot can be done in other areas to fully comprehend its progression. A lot of its applications is still dependent on rules-of-thumb and pilot testing. An effort to unify and standardize much of its applications is a must, and that can only be achieved through extensive testing and understanding of its complex processes.

In terms of the sodium silicate used in this thesis, testing can be extended to include:

- Formulating different mixes by adjusting different component proportions in the mixes.
- Adding or substituting some of the components in the mixes.
- Extending rheology testing to fully comprehend the visco-elastic microstructure characteristics of the various mixes.
- Understanding the mechanics behind the difference in testing specimens extracted from 6-inch permeations setups versus 12-inch or 24-inch setups.
- Testing specimens with larger and smaller diameters keeping the height to diameter ratio constant at 2.
- Testing specimens permeated under constant pressure rather than constant displacement.
- Producing standardized delay versus immediate permeation curves for the various mixes.
- Producing standardized syneresis curves for the various mixes.

A more comprehensive series of tests could include using different alkali silica ratioed sodium silicate, and inorganic hardeners and/or both organic and inorganic hardeners. Testing could also be done to understand the influence of temperature on setting rates and grouted-mass strength.

With such a vast amount of data at hand, methods can be developed to estimate the much required parameters in the design and analysis of grouting projects, with limited need to conduct pilot tests and/or laboratory testing.

CHAPTER 6. APPENDICES

6.1 Appendix A: Specimen Parameter Calculations

With the specimen height and mass measured, we can calculate the volume of the specimen as follows:

$$V = \frac{\pi}{4} D^2 h$$

Where h is the specimen measured height and D is the diameter of the split mold. The density of the specimen is then calculated as:

$$\rho = \frac{m}{V}$$

Where m is the measured mass of sand introduced into the split mold. Void ratio is also calculated as follows, given the specific gravity of the sand is 2.65 and the specimen is at zero saturation:

$$e = \frac{V - \frac{m}{G_s}}{\frac{m}{G_s}}$$

With the minimum and maximum void ratios, we can calculated the relative density of the specimen as follows:

$$D_r = \frac{e_{max} - e}{e_{max} - e_{min}} \; x \; 100$$

Volume of voids is also calculated as follows:

$$V_v = V - \frac{m}{G_s}$$

N.B.: The equations are used to calculate pre-grouting specimen properties. For post-grouting properties, the density of the specimen is calculated in the same fashion from the measured height and mass as shown above with a slight alteration where the actual diameter of the specimen is measured.

6.2 Appendix B: Unconfined Compression Test Analysis

Unconfined compression testing was performed on 6 inch cut and trimmed specimen. The load cell and LVDT were calibrated and manufacturer calibration factors evidenced. Given the data from the LVDT and load cell in volts, the following equation transforms the data into engineering numbers:

$$Engineering\ Number = \frac{(Output\ Voltage - Output\ Voltage\ at\ Zero)\ x\ Calibration\ Factor}{Excitation\ Voltage}$$

Load and displacement are the two engineering numbers aquired by the conversion of the output voltages from the load cell and LVDT, respectively.

The engineering strain is then calculated at each interval as:

$$\varepsilon = \frac{Displacement}{Original\ Height}\ x\ 100$$

The cross-sectional area of load application is calculated and corrected for change in height as follows:

$$A_c = \frac{\pi}{4} d^2 (1 - \frac{\epsilon}{100})$$

The deviatoric stress is then calculated as:

$$\Delta\sigma = \frac{Load}{A_c}$$

REFERENCES

- Baker, W. H. (1983). Design and control of chemical grouting. Washington, D.C.: U.S. Dept. of Transportation, Federal Highway Administration, Offices of Research and Development.
- Christopher, B. R., Atmatzidis, D. K., and Krizek, R. I. (1989), "Laboratory Testing of Chemically Grouted Sand," Geotechnical Testing Journal, GTJODJ, Vol.12, No.2
- Dano, C., Hicher, P.-Y., & Tailliez, S. (2004). Engineering Properties of Grouted Sands. Journal of Geotechnical and Geoenvironmental Engineering, 130(3), 328–338. doi: 10.1061/(asce)1090-0241(2004)130:3(328).
- Diefenthal, D.C., Borden, R.H., Baker, W.H., and Krizek, R.J. (1979) "Strength and Stiffness of Silicate Grouted Sand with Different Stress Histories" Geotechnical Testing Journal, GTJODJ, Vol. 2, No. 4, Dec. 1979, pp.200-205.
- Guyer, J. Paul. (2015), "An Introduction to Chemicals for Grouting of Soils," Continuing Education and Development, Inc. 9 Greyridge Farm Court Stony Point, NY 10980.
- Hurley, C. H. (n.d.) "Sodium Silicate Stabilization of Soils - A Review of the Literature".
- Karol, R. H. (2003). Chemical grouting and soil stabilization. New York, NY: Dekker.
- Krumrine, P., & Boyce, S. (1985). Profile Modification and Water Control with Silica Gel-Based Systems. SPE Oilfield and Geothermal Chemistry Symposium. doi: 10.2118/13578-ms
- Littlejohn, G. S. (1983), "Chemical Grouting," the South African Institution of Civil Engineers (Geotechnical Division), The University of Witwatersrand, Johannesburg.
- LittleJohn, G. S. (1985) "Chemical Grouting" Ground Engineering.
- Littlejohn, G. S., Concannon, M., and Wright, R. H. (1997) "Engineering properties of silicate-R100 ester chemical grout", Ground Engineering.
- May, J.H., Larson, R.J., Malone, P.G., Boa, J.A., and Bean, D.L. (1986), "Grouting Techniques in Bottom Sealong of Hazardous Waste Sites," Hazardous Waste Engineering Research Laboratory Office of Research and Development

U.S. Environmental Protection Agency Cincinnati, Ohio 45268 No. DW-96930581

- Ortiz, R.C. (2015), "Mechanical Behavior of Grouted Sands," Theses and Dissertations-Civil Engineering. Paper 26. hDp://uknowledge.uky.edu/ce_etds/26
- Powers, J.P., Corwin, A.B., Schmall, P.C., and Kaeck, W.E. (2007), "Construction Dewatering and Groundwater Control: New Methods and Applications Third Edition", John Wiley & Sons, Inc. ISBN: 978-0-471-47943-7
- PQ Corporation. (2004), Sodium and Potassium silicates. Brochure ENG.
- PQ Corporation. (2003), Soluble silicate in geotechnical grouting applications. Bulletin 52–53, USA.
- Schiffman, R. L., and Wilson, C. R. (1956), "Mechanical behavior of chemically treated soils, Oct. 1956". Fritz Laboratory Reports. Paper 1708.
- Tallard, G.R., Caron, C. (1977) "Chemical Grouts for Soils" Volume I Available Materials FHWA-RD-77-50. Offices of Research and Development Federal Highway Administration U.S. Department of Transportation Washington, D.C. 20590. FCP No. 35B1-072. DOR-FH-11-8826
- Vipulanandan, C., & Krizek, R. J. (1986). Mechanical Behavior of Chemically Grouted Sand. Journal of Geotechnical Engineering, 112(9), 869–887. doi: 10.1061/(asce)0733-9410(1986)112:9(869)
- Wang, Yi. (2017), "A study on chemical stabilization of Oil Sands Mature Fine Tailings" Electronics and Dissertation Repository. 4937.
- Warner, J. 1935-. (2004). Practical handbook of grouting: soil, rock, and structures. Hoboken, NJ: John Wiley & Sons.
- Xue, Bingfeng. (2018) "A Study on Chemical Grouting of Quartz Sand". Electronic Thesis and Dissertation Repository. 5376.